D O C T O R A A T S P R O E F S C H R I F T

Faculteit wetenschappen

A Renormalisation Group Study of One-Dimensional Contact Processes

Jef Hooyberghs

Promotor : Prof. dr. C. Vanderzande

2002

Dankwoord/Acknowledgements

Eerst en vooral wil ik mijn promotor Prof. Carlo Vanderzande bedanken voor de afgelopen vier jaren. Hij was steeds beschikbaar voor discussies en zijn kennis, ervaring en begeleiding waren bepalend voor mijn onderzoek en deze thesis. Daarnaast zou ik ook de andere leden van de theoretische-fysica groep willen bedanken voor raad en interessante gesprekken: Prof. Marc Bouten, Prof. Roger Serneels, Prof. Chris Van den Broeck, dr. Bart Van Rompaey, dr. Mauro Copelli, dr. Ioana Bena, dr. Frank Daerden, Peter Leoni en Bart Cleuren. Een bijzondere plaats wordt hierbij ingenomen door Peter Leoni, die nu bijna vier jaar met mij het kantoor deelt. Ik zou hem willen bedanken voor deze aangename periode, zijn hulp en de gesprekken over fysica en veel meer.

Verder wil ik ook de andere mensen van het LUC bedanken voor de verrijkende samenwerking en de gezellige sfeer, in het bijzonder Prof. Herman Janssen, Rik Lempens en Jan Mertens.

In het project over het veralgemeend contactproces heb ik het genoegen gehad om met dr. Enrico Carlon samen te werken. Ik wil hem bedanken voor deze zeer leerrijke ervaring en zijn gastvrijheid.

During the research on the quenched random contact process I benefited from the collaboration with Prof. Ferenc Iglói, whose knowledge of disordered systems was indispensable.

Tot slot wil ik mijn vrouw Kris bedanken voor haar steun en geduld tijdens de momenten dat mijn thesis voorrang kreeg.

Voor financiële steun ben ik dank verschuldigd aan het F.W.O. Vlaanderen.

Abstract

In the theory of stochastic many particle systems one models phenomena of non-equilibrium statistical mechanics by means of a Markov process. The master equation, describing the time evolution of such a process, can formally be interpreted as a Schrödinger equation in imaginary time. In this approach, the (non-Hermitian) generator of the process plays the role of the Hamiltonian. This mathematical equivalence permits the successful application to stochastic systems of a number of exact, approximative or numerical methods from quantum mechanics.

A particularly interesting type of stochastic systems is formed by the processes having a phase transition between an absorbing state and an active state. Examples of these systems can be found in physics, chemistry and even biology. The best known process of this kind is the contact process.

In this thesis real-space renormalisation group techniques, which were originally developed for quantum mechanical systems, are applied to study stochastic models on a one-dimensional lattice, more precisely the critical behaviour and the universality of absorbing state phase transitions.

First, the standard renormalisation group (SRG) is adapted to a stochastic context resulting in one of the few analytical techniques capable of producing approximations for systems that can not be solved exactly. The SRG is successfully applied to the contact process for which it characterises the stationary critical behaviour with a competitive accuracy.

Next a generalisation of the contact process to a model with several absorbing states is studied by means of the density matrix renormalisation group (DMRG) algorithm. The results for the cases with one and two absorbing states are consistent with what was known from simulations done by an other author. For the models with more than two absorbing states new results were found, which are supported by analytical considerations in a particular limit.

Finally the experience of the previous two projects is used in the investigation of the quenched random contact process. In this model the local interactions on a lattice site are time-invariant stochastic variables, independently drawn from a given distribution with a certain variance, which gives a measure for the disorder. Very little was known about the stationary behaviour of this model since its extremely slow dynamics makes simulations inefficient. The renormalisation techniques in this thesis, suffer less from this problem. First, for the case of small disorder the SRG indicates that the critical behaviour is changed by the presence of disorder and the cross-over exponent is consistent with the Harris criterion. For intermediate disorder a DMRG study reveals that the critical exponents are continuously varying with the amount of disorder. Finally, an SRG calculation, suitably adapted to

strong disorder, shows that in this case the phase transition is characterised by a fixed point at infinite randomness. In this limit the renormalisation is expected to be exact. It is the first time exact critical exponents are found for a phase transition out of an absorbing state. Moreover, the exponents are the same as those previously found in a class of disordered quantum chains, suggesting a new kind of universality for strongly disordered systems.

Samenvatting

In de theorie van stochastische veeldeeltjessystemen modelleert men fenomenen uit de niet-evenwichts statistische fysica met Markov processen. De mastervergelijking die dan de tijdsevolutie beschrijft kan formeel opgevat worden als een Schrödinger vergelijking in imaginaire tijd. In deze context speelt de (niet-Hermitische) generator de rol van de Hamiltoniaan. Met deze wiskundige equivalentie kan men met succes allerlei exacte, benaderende of numerieke technieken uit de kwantummechanica toepassen.

Een bijzonder interessante klasse van stochastische systemen wordt gevormd door processen die een fase-overgang hebben tussen een absorberende en een actieve toestand. Deze systemen komt men tegen in de fysica, chemie en zelfs in de biologie. Het best gekende voorbeeld is het contactproces.

In deze thesis worden "real-space" renormalisatie technieken, die oorspronkelijk werden ontwikkeld in de kwantummechanica, aangewend voor de studie van stochastische processen op één-dimensionale roosters. Meer in het bijzonder wordt er in deze context gekeken naar kritisch gedrag en universaliteit van fase-overgangen uit absorberende toestanden.

Eerst wordt de standard renormalisatiegroep (SRG) aangepast aan het stochastisch formalisme, wat één van de weinige analytische technieken oplevert die benaderingen kunnen maken voor niet-oplosbare systemen. Deze SRG wordt met succes toegepast op het contactproces en resulteert in een zeer nauwkeurige karakterisatie van het stationaire kritische gedrag.

Vervolgens wordt een veralgemening van het contactproces naar een model met meerdere absorberende toestanden bestudeerd met de dichtheidsmatrix renormalisatiegroep (DMRG). Dit levert resultaten op die voor de modellen met één en twee absorberende toestanden consistent zijn met eerder gevonden gegevens van simulaties door een andere auteur. Voor de gevallen met meer dan twee absorberende toestanden worden nieuwe resultaten gepresenteerd die gestaafd worden door analytische oplossingen in een bepaalde limiet.

Tot slot wordt de opgedane kennis van de twee vorige projecten gecombineerd in een onderzoek van het contactproces met bevroren wanorde. In dit model zijn de lokale interacties op een bepaald roosterpunt tijdsonafhankelijke stochastische veranderlijken, getrokken uit een verdeling met een bepaalde variantie, die een maat is voor de wanorde. Over het stationaire gedrag van dit systeem was zeer weinig geweten omdat de extreem trage dynamica het gebruik van simulaties bemoeilijkt. De renormalisatiemethodes in deze thesis, hebben minder last van dit probleem. Ten eerste wordt de SRG gebruikt voor het geval van kleine wanorde en blijkt dat het kritisch gedrag verandert door aanwezigheid van wanorde. De gevonden cross-over exponent is consistent met het Harris-criterium. Vervolgens toont een DMRG studie aan dat voor inter-

mediaire wanorde de kritische exponenten continu afhangen van de grootte van de wanorde. Tenslotte wordt de SRG aangepast voor grote wanorde en blijkt dat in dit regime de fase-overgang gekarakteriseerd wordt door een vast punt met oneindige wanorde. In deze limiet wordt de renormalisatie exact en er wordt voor de eerste keer een set van exacte exponenten bepaald voor een fase-overgang uit een absorberende toestand. Daarbij komt dat de gevonden exponenten identiek zijn aan reeds gekende waarden voor wanordelijke kwantumkettingen, wat een nieuw soort van universaliteit suggereert voor systemen met sterke wanorde.

Contents

Chapter 1

Introduction

In this chapter the research topic is presented. The type of models studied is described and the attraction of the topic as a research theme is outlined. Together with some examples the used formalism is introduced. The chapter concludes with a synopsis presenting the structure of the thesis.

1.1 Topic of Research

In principle all phenomena in nature can be described by fundamental physical laws like Newtons equations of motion or the Schrödinger equation. For realistic macroscopic systems however, this approach is seldom possible. The number of degrees of freedom is often too high and the interactions are too complicated. Instead approximative techniques are used which isolate the relevant degrees of freedom and define effective dynamics on them. These dynamics should reproduce the effect of the interactions between these relevant degrees of freedom, but also that of the interplay with the irrelevant ones. The latter are is interpreted as noise acting on the system in a stochastic way. One arrives at a stochastic model describing the system phenomenologically. These models can then be studied statistically. Any possible realisation of the relevant degrees of freedom, is called a configuration or a microstate of the system and is denoted by η. The state of the system is then fully determined by the probabilities $P_\eta(t)$ to find the system at time t in the configuration η, and the stochastic dynamics determine the time evolution of $P_\eta(t)$.

The best known case is represented by models for thermal equilibrium. One has a system containing the relevant degrees of freedom. This system is in thermal contact with a reservoir at a certain temperature, and the degrees of freedom of the reservoir are considered relevant only in the sense that they serve as an infinite heat capacity. The reservoir and the system together form

a unity, isolated from the rest of the world. The system is considered to have reached a state of thermal equilibrium with the reservoir: the expectation value of any macroscopic quantity is not varying in time. Hence, this theory is intrinsically time-invariant and the probability distribution of the system $P_\eta(t)$ is stationary. This is mathematically realised by the assumption that every configuration of the *compound* system has equal probability, leading to a probability distribution for the *relevant* system of the form $P_\eta \sim e^{-H(\eta)/k_B T}$; the Gibbs ensemble with k_B the Boltzmann factor, T the temperature of the reservoir and $H(\eta)$ the energy of a microstate η of the system. Once the energy functional of such a system is given, the stationary ensemble is known and permits the calculation of expectation values. Hence the study of this subject is in principle straightforward; it is embedded in a well defined framework called equilibrium statistical mechanics. Historically, it produced a theoretical foundation for the heuristic laws of thermodynamics. Although explicit calculations can be very hard, a lot of good approximative techniques and exact solutions have been developed, which have produced a lot of insight in phenomena of complex macroscopic systems.

One such particularly interesting type of phenomena is this of phase transitions. As an example take the melting of ice at atmospheric pressure. When the temperature is continuously increased beyond $0°C$, the macroscopic properties of the material change abruptly. At the transition temperature one finds a coexistence of the ice and water phase. When at $0°C$ heat is added, the fraction ice/water decreases but the two phases always remain clearly distinct from each other. This kind of phase transition is called first order or discontinuous. For a different scenario, take the liquid-gas transition of water at its critical point ($p_c = 221 \cdot 10^5 Pa$, $T_c = 374°C$). When at the pressure p_c the liquid is heated up to T_c, the physical properties approach in a continuous way those of the gas phase at T_c. At the critical point one observes only one phase. An intuitive explanation for this second order or continuous phase transition lies in the divergence of the correlation length. At the critical point of such a transition, the degrees of freedom become correlated over infinitely large length scales. Fluctuations in the system can be felt by all degrees of freedom, resulting in collective behaviour and the existence of only one possible phase. When approaching the critical point, the differences in thermodynamic quantities between the gas and the liquid phase go to zero continuously. But these quantities are singular in that point and are often found to have a power-law dependence on the distance away from the critical point. These powers, in general irrational numbers, characterise the phase transition and are called critical exponents. The collective behaviour of the degrees of freedom makes an analytical study of these exponents non-trivial

and the introduction of a new method, the renormalisation group, was needed to fully understand this complex situation. These renormalisation techniques also explained the experimentally found concept of universality. For systems with short-range interaction, the critical exponents do not depend on the details of the interactions between degrees of freedom. Only the dimensionalities and symmetries of the system are relevant and they classify the continuous phase transitions into universality classes. Phase transitions of completely different systems can have the same critical exponents. A remarkable example of this is given by the transitions at the Curie-point of an uniaxial ferromagnet and at the critical point of a simple fluid. For systems in thermal equilibrium, all these phenomena are now well understood [1].

Most systems in nature are however not in thermal equilibrium. One often encounters perturbed systems, away from equilibrium, for which the probabilities $P_\eta(t)$ are still evolving in time towards stationarity. But even when the stationary state is reached, it does not have to be Gibbsian: for example, a system in thermal contact with two reservoirs at a different temperature can not be described by the Gibbs measure. More generally, when the dynamics of a system do not obey detailed balance with respect to the Gibbs measure (cf subsection 2.3.3), the stationary state into which the system will relax is a priori not known and the system is intrinsically out of equilibrium. To describe these systems one needs a way to represent the microscopic dynamics. This clearly exceeds the framework of equilibrium statistical mechanics and at the moment no general formalism exists for this non-equilibrium behaviour. It is much harder to grasp and the notion of universality is not yet clarified. The subject of this thesis is situated in this context. One particular approach to non-equilibrium statistical mechanics is used: *Markov processes*. In this approach one type of systems is studied: *reaction-diffusion systems*. The goal is to gain insight into dynamical and stationary behaviour, more precisely into phase transitions and the universality of non-equilibrium systems. To this end several renormalisation techniques are applied. The usefulness of more or less known ones is explored and an attempt is made to develop new ones. The research is focused on the mathematical models, less on the link between the models and physical realisations.

1.2 Reaction-Diffusion Systems

The main concept of reaction diffusion systems is that particles diffuse and/or react in a medium. One could think of it as a chemical reaction process, but it is more general. A particle does not have to represent a real physical particle, it could stand for anything from an electronic excitation in some material to

a car in a traffic model. A system can involve any kind of reaction: death and birth of a particle, annihilation of two particles, reproduction of an existing particle,... but we will only consider processes local in space. As an example, annihilation of two particles can only take place if they are within a given distance from each other. In addition the particles will always be regarded as having a hard core: any point of the medium can contain at most one particle. Depending on the reactions and diffusion one allows in the model and on their relative rates, one gets a particular reaction-diffusion system. These systems can be used to model a wide variety of phenomena in physics, chemistry and biology [2], [3].

In order to model the stochastic dynamics, a Markov process is used on a discrete configuration space, hence the medium of the particles has to be lattice-like and the hard core property of the particles is relevant. A restriction is made to *one-dimensional* lattices. There are two reasons for this. First, reaction-diffusion models in a low dimensional medium often have interesting behaviour. Unlike in equilibrium, even one-dimensional systems can have phase transitions. It is even true that high dimensional media can become less interesting since mean-field approximations are exact (as noted later). Secondly, in this research there is no direct concern with the modelling of real physical systems, but with general non-equilibrium properties. This makes the choice of one-dimensional "toy models" obvious. Although this choice of medium is a limitation, a considerable amount of interesting phenomena involve low-dimensional media: chemical reactions in porous media or on polymers, steps on crystalline surfaces, catalysis, ... and some two-dimensional phenomena like surface growth can be mapped on one-dimensional models [4]. Recently also some experiments were developed to check theoretical predictions for one-dimensional lattice systems. One example can be offered.

In solid state physics, the phenomenon of an exciton is well known. When an electron in a semiconductor is excited (e.g. by a laser beam) into the conduction band it leaves a hole in the valence band. In some materials this particle-hole pair remains strongly correlated in space, acting as a pseudo particle: the exciton. It has a natural decay with a known lifetime. When the exciton disappears (the electron falls back to the valence band) a photon with a well-defined wavelength is emitted. This phenomenon is called luminescence. In some materials these excitons can perform random walks. Upon meeting, one or both of them can disappear, resulting in what is called respectively a coagulation or an annihilation reaction. In both reactions a photon with a wavelength different from that of the natural decay is emitted. By measuring the luminescence one can keep track of the number of excitons and the different reactions taking place [5]. A one-dimensional realisation of this

reaction-diffusion system can now be made by using a polymer as the medium for the excitons. Another way to reduce dimensionality is by producing a material in which the diffusion of the excitons is extremely asymmetric. When they can only jump in one direction, one gets an effectively one-dimensional system.

1.3 Techniques and Examples

If a study is to be conducted into this kind of one-dimensional non-equilibrium systems, it is necessary to have a means of modelling the dynamics. Consider the explicit example of the diffusion-annihilation process with one type of particle: the particles perform random walks on the lattice by randomly jumping to a neighbouring site (if it is vacant), and two neighbouring particles can annihilate, resulting in two empty sites. The oldest method to introduce such dynamics is the law of mass action. It defines the reaction rate of two reactants to be proportional to the product of their concentrations. It inherently assumes that all reactants are homogeneously distributed at any instant of time. Hence the dynamics are independent of the dimension of the medium and since the reactants are assumed to remain homogeneously spread, there is no need for an explicit representation for the diffusion process. If the particle density is denoted by ρ, the method implies

$$\frac{d\rho}{dt} \sim -\rho^2, \tag{1.1}$$

resulting in an asymptotic decay in time of the form $\rho(t) \sim t^{-1}$. For the one-dimensional case however, it is known from an exactly solvable model that $\rho(t) \sim t^{-1/2}$. This discrepancy is due to spatial fluctuations in the particle density. When annihilation processes take place, the remaining particles become anticorrelated. In a one-dimensional medium, the diffusion is not effective enough to counter this effect and the assumption of homogeneity no longer holds. This anticorrelation opposes the annihilation process, resulting in a slower decay than that predicted by the simple law (1.1). This was also experimentally verified in the measurement of the luminescence of annihilating excitons [5]. The law of mass action is a mean-field technique and is only valid when diffusive mixing of particles is strong enough. This can be the case in media of higher dimension where this mixing is more effective. For a reaction-diffusion process often an upper critical dimension for the medium exists, above which mean-field is correct [6]. For several models this dimension is equal to two, explaining why the law of mass action may be used successfully in, for example, three-dimensional chemical reactions. For one-dimensional

systems however, one clearly is in need of a more profound technique, being able to include stochastic spatial fluctuations. One way of achieving this is by assuming that ρ also depends in a continuous way on a space coordinate, and that time evolution is described by a partial differential equation with a noise term [2]. A different approach, which we will adapt, is the use of a continuous time Markov process to model the dynamics in a discrete configuration space.

Consider again a one-dimensional lattice, containing only one type of (hard core) particles. A microscopic configuration η of the system is defined by saying for any site of the lattice whether it is empty (ϕ) or occupied (A). A diffusion step of a particle or a reaction process of some particles can be represented by a transition between the configuration before and after the action. Any reaction-diffusion system is now defined by giving the possible transitions and their corresponding rates. These transition rates define the time evolution of the *state of the system*: the probability distribution $P_\eta(t)$ over the configurations at time t. The assumption will always be that the rates are time-independent. This implies that the time derivative of the state only depends on the state itself and not on the way the system reached it. Chapter 2 explains how this assumption, known as the Markov condition, can lead to a time evolution given by

$$\frac{d}{dt}\left|P(t)\right\rangle = -H\left|P(t)\right\rangle . \tag{1.2}$$

This is a continuous time Markov process where $|P(t)\rangle$ is the probability distribution written in vector form, and H is a (time-independent) linear operator defined by the transition rates of the system under investigation. Following this approach the mathematical problem one is faced with, is solving equation (1.2). Since in general there will be infinitely many interacting degrees of freedom, even the task to find a stationary solution is far from trivial. A traditional way to tackle the problem is by the use of computer simulations, but in the last decade great progress has been made in finding numerical, approximating analytical and even exact analytical solutions. The majority of these methods is based on the insight that the technical problems of a Markov process are very similar to those one encounters in quantum mechanics. This can be seen in the fact that equation (1.2) has the form of a Schrödinger equation in imaginary time. The operator H plays a similar role as the Hamiltonian of a quantum spin chain. It turned out that not only the elegant formalism of quantum mechanics can be used, but also several of its solution techniques are adaptable. The importance of this close relation was realised only in the 1990s since when the quantum toolbox has been used extensively. The following (non-exhaustive) list gives some examples of these recent developments.

- For a certain ratio of the transition rates, the diffusion-annihilation pro-

cess, defined above, can be mapped onto a free fermion system using a Jordan-Wigner transformation. This can be solved exactly with a Fourier-transform, resulting for example in the correct density decay $\rho \sim t^{-1/2}$ [7]. Although the general conditions are not known, there are more examples of systems that can be transformed into a free fermion model [8].

- In the asymmetric exclusion process (ASEP), the hard core particles perform biased random walks: the rate for jumping in one direction is bigger than for the other. The dynamics of this model can be solved exactly using the Bethe ansatz [9]. Moreover, when this diffusion is made fully asymmetric and one adds input of particles on one endpoint of the lattice, and output of particles on the other, boundary induced phase transitions can be found: the stationary behaviour in the bulk of the system can be in a different phase, depending on the rates of input and output. This stationary behaviour can also be solved exactly [10], [11].

- The density-matrix renormalisation group (DMRG) is a numerical technique originally developed for one-dimensional quantum spin chains of finite lengths [12][13]. It iteratively approximates an initially chosen part of the spectrum of the Hamiltonian. At each iteration step the system length is enlarged and the configuration space is truncated in an efficient way. The algorithm makes it possible to numerically study large systems with high accuracy. When the research for this thesis initiated, the first applications of the DMRG to stochastic systems were being made [14],[15].

- In branching and annihilating random walk (BARW) models, besides diffusion and annihilation, the particles can undergo a branching process $A \to (m+1)A$: a particle with m empty neighbouring sites can produce an offspring of m particles on these sites. Each choice of m gives a different BARW model. Depending on the chosen rates for the annihilation and branching reactions, the stationary state of these systems can be in the *active* or *inactive* phase. Let us assume we start of with a state having a non-zero particle density. When the branching rate is taken small (with respect to the annihilation rate), the particle density will keep decreasing in time and the stationary state of the system will be the empty lattice: the probability distribution has all its weight on the configuration representing the empty lattice[1]. Once this state

[1] When m is even, and the initial number of particles is odd, the absorbing state is not the empty lattice, but the system with one particle left.

is reached, no particles are left and the dynamics stops: the system is stuck in this inactive or *absorbing* state. If the branching rate is chosen large, this absorbing state is still stationary, but no longer attractive. When the initial particle density is non-zero, the system will relax into a stationary state where the particle density ρ^* is non-zero. (This is true, provided the system is infinitely large, otherwise the system will always get trapped in the absorbing state due to fluctuations.) In this state, the macroscopic quantity ρ^* is time-invariant, but on a microscopic level, reactions keep occurring: the system is active. The stationary density as a function of the branching rate is a continuous function, sketched in Fig. 1.1.

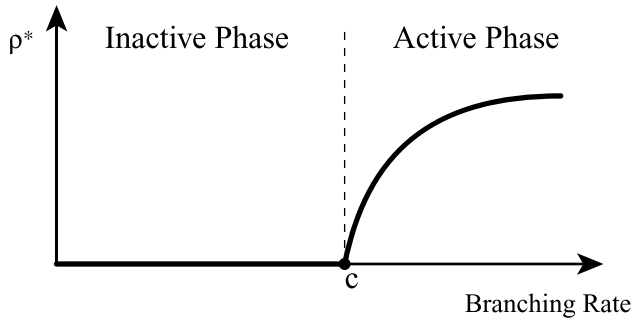

Figure 1.1: *Schematic phase diagram of a continuous phase transition out of an absorbing state: (attractive) stationary particle density ρ^* as a function of the branching rate.*

At some intermediate value c for the branching rate, the system is at the boundary of the active and inactive region. This is the critical point of a *continuous phase transition out of an absorbing state*, for which critical exponents can be introduced.

Using the relation with quantum mechanics, a field theoretic description for stochastic processes can be applied to construct a renormalisation approach [16], [17]. For a system having a continuous phase transition, one can then calculate critical exponents in an ε-expansion around the upper critical dimension. In the case of the BARW models this led to a classification of the critical behaviour based on the parity of m [18], [19]. For m odd the transition turned out to be in the universality class of directed percolation (DP). This class was already known from geometrical critical phenomena [20]. For m even, a new universality class was found. Since in this case the number of particles modulo two

is conserved, it was named the parity conserving (PC) class. There is still some disagreement about the requirements to be in this universality class. It is not clear whether or not a system can have this critical behaviour without having a quantity that is conserved modulo two.

These continuous phase transitions out of an absorbing state also form the main subject of this thesis. However, to study this phenomenon, not the BARW models but *the contact process* is used. Introduced as a simple model for the spreading of an epidemic [21], the contact process contains two competing elementary processes: self replication versus spontaneous death of an infection. If in the context of a many particle lattice model, an infected (healthy) entity is represented by a particle A (vacancy ϕ), the contact process with contamination rate λ, is defined by the transitions

$$\begin{array}{lcll} \phi & \rightarrow & A & \text{with rate } \frac{\lambda}{2} \times \text{(number of occupied neighbouring sites)} \\ A & \rightarrow & \phi & \text{with rate 1, independent of the neighbours.} \end{array} \tag{1.3}$$

With the particle density as the order parameter, and the empty lattice as the absorbing state, it is another example of a model with a continuous phase transition in the universality class of directed percolation. It was found that quite a few models with such an absorbing state have a transition belonging to this class. Although no model in the DP class has been solved exactly, this strong evidence of universality led to the so called DP conjecture [22],[23],[24]

DP Conjecture[2]**:** *In the absence of any special conservation laws and quenched disorder, continuous phase transitions between an active and a single absorbing state of many particle systems with local interactions and a scalar order parameter are of the directed percolation (DP) type.*

The contact process is the minimal model in this class and is sometimes called "the Ising model of the absorbing state phase transitions". It is an ideal system to test new techniques. In this thesis a new real-space renormalisation techniques is introduced and the known DMRG algorithm is applied. Although the actual research is about extended versions, the simple contact process played a central role as a non-trivial test case, and it will form the leading thread running through my thesis.

[2]The fact that BARW models with an even offspring belong to a different universality class, is consistent with this conjecture.

1.4 Synopsis

Chapter 2 introduces the quantum formalism which is nowadays common to describe stochastic processes on lattices. This formalism is applied to discuss the contact process and its scaling behaviour in the chapter thereafter. Chapter 4 develops the standard renormalisation for stochastic processes, which is first applied to an exactly solvable model and in the next chapter to the contact process and a generalised version with more absorbing states. The latter one is more profoundly studied by means of the DMRG in Chapter 6, where also the main idea of the numerical DMRG algorithm is explained. The last subject of the thesis is about the contact process with quenched random rates, which is covered in Chapter 7. To gain insight in this model several techniques are applied: the DMRG, the newly developed stochastic standard renormalisation and an adaptation of the latter one to systems with strong disorder.

Frequently used notations and abbreviations can be found in the first appendix.

Chapter 2

Quantum Hamiltonian Formalism

This technical chapter elaborates the claim made in Chapter 1 about the relation between a Markov process and quantum systems for one-dimensional lattice models.

In the first section the continuous time Markov process is defined in the form of a master equation. In the next section this is embedded in a vector formalism. First a basis-independent Dirac bra(c)ket notation is introduced, leading to a quantum-like formalism. Notions like the state of the system, the time evolution operator and expectation values are (re)defined in this context. Next we a specific representation is chosen and it is shown explicitly how to construct the operators needed in Markov processes. In the third section general properties of long time behaviour and stationary states are studied. Quantum techniques are used throughout the chapter, but subsection 2.3.4 gives a detailed example of how an expansion technique from quantum mechanics can be used in this stochastic context.

2.1 Master Equation

The choice to describe the time evolution of a stochastic system by a continuous time Markov process, leads to a formalism closely related to that of quantum mechanics. It was in the 1970s that this relation was discovered [25], [26], but it has been developed more extensively during the 1990s [27], [28], [29] when the interest in the stochastic dynamics of interacting particle systems increased. A very good overview of this development can be found in [30]. A more mathematical treatment of the subject is given in [31][32].

Throughout this thesis the models considered are all one-dimensional lat-

tice systems. In order to avoid complicated notations, we add in this chapter two further restrictions. (A generalisation removing these restrictions is straight forward.) First we consider the lattice to be of finite length, i.e. a chain of L sites. Secondly we assume that each site can be in only two possible states. These states are associated with the presence A or the absence ϕ of a particle. In this way the system can be in 2^L configurations. A configuration is denoted as η, and the set of all 2^L configurations as X. A randomly chosen element of X could look like the configuration in Fig. 2.1.

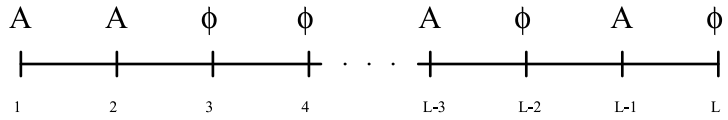

Figure 2.1: *A randomly chosen configuration* $\eta_0 \in X$

Suppose that at a given instant of time t_0, the system is in this configuration η_0. One now wants to introduce stochastic dynamics on this system. This could be realised by having the system jump in a stochastic way from one configuration to another. E.g. a particle at site 2 that jumps to site 3 is represented by a transition of the system from configuration η_0 to the corresponding configuration η with site 2 empty and site 3 occupied. This is easy to implement on a computer with a random number generator. Each time you set up the system in configuration η_0 and run your simulation, it will choose a random path wandering through the possible configurations. In statistical physics however, one is not interested in these particular realisations of the time evolution, but in the probabilities of finding them. These can then be used to calculate expectation values of physical quantities. That is why the state of the system is not defined as the configuration of the system, but as a probability distribution over all the configurations. Let us denote by $P_\eta(t)$ the probability of finding the system in configuration η at time t. The set of functions $P_\eta(t)$ is called the state of the system at any time t. It provides us with all statistical information needed about the system. Although the process is stochastic, the time evolution of $P_\eta(t)$, following from such a process, is now deterministic.

If you were to find the probabilities $P_\eta(t)$ using the computer simulation, you should run the program in principle infinitely many times. We replace it by an analytical approach making some assumptions on the form of stochasticity. We start by defining the basic rules of the dynamics: the transitions between different configurations. Let us denote the transition rate between configuration η and η' as $r_{\eta\to\eta'} \in \mathbb{R}^+$. These rates, which can be zero, are

used to define an exponential decay for every configuration η: the probability that η has not changed to some other η' is taken to decay exponentially in time with decay constant

$$\tau(\eta) = (\sum_{\eta' \in X/\{\eta\}} r_{\eta \to \eta'}) \tag{2.1}$$

or life time

$$\frac{1}{\tau(\eta)} = (\sum_{\eta' \in X/\{\eta\}} r_{\eta \to \eta'})^{-1}. \tag{2.2}$$

When configuration η decays, it will be to η' with probability

$$P_{\eta \to \eta'} = \frac{r_{\eta \to \eta'}}{\tau(\eta)}. \tag{2.3}$$

This means that the values of the rates set the time scale, while the ratios are the relative transition probabilities. Finally the rates $r_{\eta \to \eta'}$ are demanded to be independent on how the system got into η: the dynamics of these systems are history-independent, they form a Markov process. These assumptions lead to what is called the continuous time *master equation* for the probability distribution

$$\frac{d}{dt} P_\eta(t) = \sum_{\eta' \in X/\{\eta\}} \left[r_{\eta' \to \eta} P_{\eta'}(t) - r_{\eta \to \eta'} P_\eta(t) \right]. \tag{2.4}$$

The probability to find the system in configuration η increases by transitions from η' to η, represented by the positive terms in the rhs of the master equation, and decreases by transitions away from η, represented by the negative terms. It is easy to check that the dynamics following from (2.4) conserve probability:

$$\left\{ \begin{array}{l} P_\eta(t) \in \mathbb{R}^+ \\ \sum_{\eta \in X} P_\eta(t) = 1 \end{array} \right. \quad \Longrightarrow \quad \left\{ \begin{array}{l} P_\eta(t') \in \mathbb{R}^+ \\ \sum_{\eta \in X} P_\eta(t') = 1 \end{array} \right. \quad \forall t' \geq t. \tag{2.5}$$

This concludes the main idea of the formalism. We have the state of the system given by a probability distribution, and the time evolution of the state given by a linear differential equation in time. The analogy with quantum mechanics is obvious, although in that case the link between the state of the system and probabilities is different. In the study of stochastic systems, this formal analogy is used extensively. In the next section a vector representation for the master equation is developed. It will be the stochastic counterpart of the Schrödinger equation and it will make adaptation of quantum mechanical tools possible.

2.2 Vector Representation

2.2.1 Bra(c)ket notation

In this section the Dirac bra(c)ket notation is introduced to rewrite the master equation in vector form and to derive some general valid properties. After this subsection a specific vector representation will be chosen to give an explicit form to this formalism.

With each configuration η a linear independent vector $|\eta\rangle \in \mathbb{C}^{2^L}$ is chosen[1]. Together they form a basis of the vector space $\mathbb{C}^{2^L}$. On this space the standard inproduct is defined and the dual vectors $\langle\eta|$ form a basis of the dual space: $\langle\eta|\ \eta'\rangle = \delta_{\eta,\eta'}$. The state of the system, a normalised probability distribution is now defined as the vector

$$|P(t)\rangle = \sum_{\eta} P_\eta(t)\,|\eta\rangle\,. \tag{2.6}$$

(When not further specified, η in a sum runs over all η in X.) Next the master equation (2.4), defining time evolution for every probability $P_\eta(t)$, will be rewritten in one equivalent equation for the vector $|P(t)\rangle$. We introduce the matrix H, which is defined through its elements as

$$\begin{aligned} H_{\eta'\eta} &= \langle\eta'|\,H\,|\eta\rangle = -r_{\eta\to\eta'} \qquad \text{for } \eta \neq \eta' \\ H_{\eta\eta} &= \langle\eta|\,H\,|\eta\rangle = \sum_{\eta'\in X/\{\eta\}} r_{\eta\to\eta'}. \end{aligned} \tag{2.7}$$

The non-diagonal elements $H_{\eta'\eta}$ contain the negative transition rates for $\eta \to \eta'$, while the diagonal elements $H_{\eta\eta}$ contain the decay constant of the configuration η. Such an H, with negative non-diagonal elements and column elements adding up to zero, will be called a *stochastic matrix*. Using this form, the master equation (2.4) is equivalent with

$$\frac{d}{dt}\,|P(t)\rangle = -H\,|P(t)\rangle\,. \tag{2.8}$$

When a Markov process is written in this form, H is called the *infinitesimal generator*. This equation has the form of a quantum mechanical Schrödinger equation in imaginary time and H plays the same fundamental role as the Hamiltonian in quantum mechanics. It is this equivalence that makes adaptations of quantum techniques possible. Moreover, in the specific applications

[1] Only vectors that are $\in \mathbb{R}^{2^L}$ can have the meaning of a probability distribution, but sometimes one is forced to work with non-physical vectors (like the eigenvectors of a non-symmetric operator), which are $\in \mathbb{C}^{2^L}$. Therefore the more general case is considered here.

of Markov processes to many particle systems, one sometimes encounters generators identical to Hamiltonians of known quantum chains. That is why in this context H is called the *quantum Hamiltonian* or simply the Hamiltonian of the Markov process. We will use this term, but one has to be careful with its interpretation. As an example, the eigenvalues of H do not have the meaning of an energy. Eigenvalues can even be imaginary since in general H is non-hermitian. This also implies that left and right eigenvectors can not be related by simple transposition as in quantum mechanics (we will return to these points later). And as we will show next, expectation values are to be calculated in a way different from that in quantum mechanics. This arises from the fact that probabilities are given by the elements of $|P(t)\rangle$, and not by the square of the modulus of them.

An observable can be defined as a function $f : X \to \mathbb{R}$ associating a value with every configuration η. The expectation value of that observable is defined as $\sum_\eta f(\eta) P_\eta(t)$. This can be written in inproduct form if one first defines

$$F = \sum_\eta f(\eta) \, |\eta\rangle \langle\eta| \tag{2.9}$$

$$\langle s| = \sum_\eta \langle\eta| \, . \tag{2.10}$$

In matrix representation F is a diagonal matrix containing the function values of f on its corresponding diagonal elements, and $\langle s|$ is a row vector with each element equal to one. The expectation value of F (or f) can now be written as

$$\langle F\rangle = \langle s| \, F \, |P(t)\rangle \, . \tag{2.11}$$

The vector $\langle s|$ can also be used to express probability normalisation

$$\langle s| \, P(t)\rangle = \sum_\eta P_\eta(t) = 1 \tag{2.12}$$

and will be called the *normalisation vector*.

Next, using the time evolution operator e^{-Ht}, one can write down the formal solution of the master equation (2.8) once the initial conditions are given:

$$|P(t=0)\rangle = |P_0\rangle \tag{2.13}$$

$$|P(t)\rangle = e^{-Ht} \, |P_0\rangle \, . \tag{2.14}$$

Since this time evolution conserves probability, one has $\langle s| \, e^{-Ht} = \langle s|$ for every t. If one takes the derivative with respect to t, one gets

$$\langle s| \, H = 0, \tag{2.15}$$

which is nothing but a restatement of the fact that the elements in any column of H add up to zero, cf (2.7). This property can be used to derive an equation for the time evolution for expectation values. It is similar to the form known from quantum mechanics:

$$\begin{aligned} \frac{d}{dt}\langle F\rangle &= \frac{d}{dt}\langle s|\, F\, |P(t)\rangle \\ &= \frac{d}{dt}\langle s|\, Fe^{-Ht}\, |P_0\rangle \\ &= -\langle s|\, FH\, |P(t)\rangle \\ &= \langle [H,F]\rangle \end{aligned} \tag{2.16}$$

where $[H,F] = HF - FH$, the commutator between H and F.

2.2.2 Single-Site System

The Dirac bra(c)ket is a very useful tool to make general calculations in an elegant notational form, but in practical problems one is in need of a specific representation of the vectors. We now choose one representation and we will stick to it for the rest of the thesis. As a first example, we introduce the simplest case possible, a lattice consisting of one site: $L = 1$. When each site can be in two possible states (unoccupied or occupied by a particle), this system has $2^L = 2$ possible configurations $\eta_0 = \phi$ and $\eta_1 = A$, $X = \{A, \phi\}$. For a single site the following vector representation will be used for respectively an unoccupied and an occupied site

$$|\phi\rangle = \binom{1}{0} \qquad |A\rangle = \binom{0}{1} \tag{2.17}$$

and the dual vectors are just the transposed vectors. A probability distribution is then represented by the vector

$$|P(t)\rangle = P_\phi(t)\,|\phi\rangle + P_A(t)\,|A\rangle = \begin{pmatrix} P_\phi(t) \\ P_A(t) \end{pmatrix} = \begin{pmatrix} 1-\rho(t) \\ \rho(t) \end{pmatrix} \tag{2.18}$$

where, since $P_A(t)$ can be interpreted as the particle density ρ, we wrote $P_A(t) = \rho(t)$. The normalisation vector is

$$\langle s| = \begin{pmatrix} 1 & 1 \end{pmatrix}. \tag{2.19}$$

The quantum Hamiltonian for this system is:

$$H = \begin{bmatrix} r_{\phi\to A} & -r_{A\to\phi} \\ -r_{\phi\to A} & r_{A\to\phi} \end{bmatrix}. \tag{2.20}$$

And one can notice that indeed this matrix is in general not symmetric but always satisfies $\langle s|\, H = 0$.

Example 1 Let us calculate an expectation value for the single site system. Suppose one needs an expression for the average number of particles ρ in the system. The corresponding observable is

$$f: \begin{array}{lcl} |\phi\rangle & \to & 0 \\ |A\rangle & \to & 1 \end{array} \qquad \text{or} \qquad F = \begin{bmatrix} 0 & 0 \\ 0 & 1 \end{bmatrix}$$

From now on we will be using the following notations for single site operators

$$E^{00} = \begin{bmatrix} 1 & 0 \\ 0 & 0 \end{bmatrix}, E^{11} = \begin{bmatrix} 0 & 0 \\ 0 & 1 \end{bmatrix}, E^{01} = \begin{bmatrix} 0 & 1 \\ 0 & 0 \end{bmatrix}, E^{10} = \begin{bmatrix} 0 & 0 \\ 1 & 0 \end{bmatrix} \tag{2.21}$$

which is equivalent with $\left(E^{ab}\right)_{ij} = \delta_{a,i}\delta_{b,j}$. The average number of particles can now be written as the expectation value of E^{11}

$$\rho = \left\langle E^{11} \right\rangle = \langle s| E^{11} |P(t)\rangle = P_A(t)$$

2.2.3 Tensor Basis and Local Dynamics

In the previous subsection representations (2.17) were chosen for the basis vectors of the single-site space $\mathbb{C}^2$. A natural way to extend this to the case of a one-dimensional lattice of L sites is by using the tensor product $\otimes$. The configurations $|\eta\rangle$ of an L site lattice are represented by the basis vectors

$$\begin{array}{rcl} |\eta\rangle & = & |\eta_1\rangle \otimes |\eta_2\rangle \ldots \otimes |\eta_L\rangle \\ |\eta_i\rangle & \in & \{|A\rangle, |\phi\rangle\} = \left\{ \binom{0}{1}, \binom{1}{0} \right\} \end{array} \tag{2.22}$$

of the space $\mathbb{C}^{2^L}$. The basis of the dual space and the inproduct of $\mathbb{C}^{2^L}$ follow from the definition of the tensor product and the basis of the dual space and the inproduct of $\mathbb{C}^2$. As an example the vector $\langle s|$ (2.10) of the dual space can now be written as

$$\langle s| = \begin{pmatrix} 1 & 1 \end{pmatrix} \otimes \begin{pmatrix} 1 & 1 \end{pmatrix} \otimes \ldots \otimes \begin{pmatrix} 1 & 1 \end{pmatrix} \tag{2.23}$$

$$= \bigotimes_{i=1}^{L} \begin{pmatrix} 1 & 1 \end{pmatrix}. \tag{2.24}$$

This tensor basis is particularly interesting when working locally. As a first example consider the state of the system. In general this is a normalised (real-valued) linear combination of the basis vectors (2.6). But there is the special case where the occupation probability of a site is independent of every other site, in this case the state can be written as a product measure

$$|P(t)\rangle = \bigotimes_{i=1}^{L} \binom{1-\rho_i(t)}{\rho_i(t)} \tag{2.25}$$

of single-site states (2.18). Secondly, when representing operators on this vector space, one needs in general a 2^L by 2^L matrix. But one will often meet operators acting as the identity operator on every site except on a site n. As an example take the (diagonal) operator representing the observable counting the particles on site n. Such an operator can be written in local form as

$$\bigotimes_{i=1}^{n-1} \mathbf{1} \otimes E^{11} \bigotimes_{i=n+1}^{L} \mathbf{1} \doteq E_n^{11} \tag{2.26}$$

where $\mathbf{1}$ is the 2 by 2 identity matrix, and the tensor product of operators is defined in the standard way. From now on the short hand notation E_n^{ab} will be used for the 2 by 2 operator E^{ab} acting on site n. When acting on a configuration $|\eta\rangle$ this local operator E_n^{11} returns $|\eta\rangle$ when site n of configuration $|\eta\rangle$ is occupied and $0\,|\eta\rangle$ when site n is empty. Hence, the expectation value for the number of particles at site n can just as before be written as

$$\rho_n = \left\langle E_n^{11} \right\rangle = \langle s|\, E_n^{11}\, |P(t)\rangle\,. \tag{2.27}$$

This local notation can also be used to denote the Hamiltonian (2.7) of the system, provided the system has *local dynamics*. This means that transition rates $r_{\eta\to\eta'}$ are zero, except when η and η' only differ on "a few" neighbouring sites. The value of "a few" depends on the dynamics under consideration, for the models in this thesis it will often be 2: only 2-site processes are allowed. In a more physical picture, this means that a particle or vacancy can only interact with a neighbouring particle or vacancy (e.g. a particle can jump to an empty neighbouring site, but it can not jump to a next neighbouring site or further). Once these elementary local events are chosen, the dynamics are defined and the Hamiltonian can be constructed using local (2-site) operators. When the transition rates for these local events are the same for every site of the lattice, only a few transition rates define the complete dynamics of the system. As an example we now explicitly construct the Hamiltonian of the contact process.

Example 2 The Contact Process: Construction of the Hamiltonian

The dynamics of the contact process can be seen as a rudimentary form of a contamination process. A particle A is considered as a contaminated individual and a vacancy ϕ as a normal individual. The dynamics consist of two competing processes with rates independent of the place on the lattice. When a site next to a contaminated one is normal, it can become contaminated with rate $\lambda/2$. When a site is contaminated, it can become normal with rate 1. From now on local processes will be written in a table form like this:

$$\begin{array}{ccccc} A\phi \\ \phi A & \to & AA & & \text{rate } \frac{\lambda}{2} \\ A & \to & \phi & & \text{rate } 1 \end{array} \tag{2.28}$$

We will start by constructing the Hamiltonian for the 1-site process $A \to \phi$. Using the representation (2.17) the 1-site Hamiltonian takes on the form (2.20) leading to

$$h_i^1 = \begin{bmatrix} r_{\phi\to A} & -r_{A\to\phi} \\ -r_{\phi\to A} & r_{A\to\phi} \end{bmatrix} = \begin{bmatrix} 0 & -1 \\ 0 & 1 \end{bmatrix}$$

acting on every site i. Using notation (2.21) this can be written as

$$h_i^1 = -E_i^{01} + E_i^{11}$$

This is the form we will use. After some exercise writing down the Hamiltonian in this form is routine: every elementary event contributes to the Hamiltonian with two terms. A first term consists of the operator making the event (E^{01} transforms an A into a ϕ) multiplied by minus the rate, in this case 1. A second term is given by the corresponding diagonal operator multiplied by plus the rate. This term takes care of the probability normalisation (2.15).

Using the same trick, the 2-site Hamiltonian is constructed

$$\begin{aligned} h_i^2 = \quad & -\tfrac{\lambda}{2} E_i^{11} E_{i+1}^{10} + \tfrac{\lambda}{2} E_i^{11} E_{i+1}^{00} && (A\phi \to AA) \\ & -\tfrac{\lambda}{2} E_i^{10} E_{i+1}^{11} + \tfrac{\lambda}{2} E_i^{00} E_{i+1}^{11} && (\phi A \to AA) \end{aligned}$$

where e.g. $E_i^{11} E_{i+1}^{10}$ is the product of the two operators, which can also be written as $\bigotimes_{k=1}^{i-1} 1 \otimes E^{11} \otimes E^{10} \bigotimes_{k=i+2}^{L} 1$.

If we introduce periodic boundary conditions, and interpret the number of the sites as being modulo L, we can write the Hamiltonian of the contact process as

$$\begin{aligned} H = \sum_{i=1}^{L} \Big[& -1E_i^{01} + 1E_i^{11} - \frac{\lambda}{2} E_i^{11} E_{i+1}^{10} + \frac{\lambda}{2} E_i^{11} E_{i+1}^{00} \\ & - \frac{\lambda}{2} E_i^{10} E_{i+1}^{11} + \frac{\lambda}{2} E_i^{00} E_{i+1}^{11} \Big] \end{aligned} \tag{2.29}$$

To be precise, we should mention that in general the contamination term of the contact process is defined in a different way as in (2.28). This term is defined on a lattice of any dimension as: 'a normal site can become contaminated with a rate $\frac{\lambda}{q}$ times the number of contaminated neighbours', where q is the coordination number (number of neighbouring sites). On a one-dimensional lattice this means

$$\begin{array}{ll} A\phi A \to AAA & \text{rate } \lambda \\ A\phi\phi \to AA\phi & \text{rate } \frac{\lambda}{2} \\ \phi\phi A \to \phi AA & \text{rate } \frac{\lambda}{2} \end{array} \tag{2.30}$$

leading to a contamination term in the Hamiltonian of the form

$$\begin{aligned} h^3 = & -\lambda E_i^{11} E_{i+1}^{01} E_{i+2}^{11} + \lambda E_i^{11} E_{i+1}^{00} E_{i+2}^{11} \\ & - \frac{\lambda}{2} E_i^{11} E_{i+1}^{01} E_{i+2}^{00} + \frac{\lambda}{2} E_i^{11} E_{i+1}^{00} E_{i+2}^{00} \\ & - \frac{\lambda}{2} E_i^{00} E_{i+1}^{01} E_{i+2}^{11} + \frac{\lambda}{2} E_i^{00} E_{i+1}^{00} E_{i+2}^{11}. \end{aligned}$$

This looks like a 3-site operator, but one can split the first two terms as $-\frac{\lambda}{2}E_i^{11}E_{i+1}^{01}E_{i+2}^{11}-\frac{\lambda}{2}E_i^{11}E_{i+1}^{01}E_{i+2}^{11}+\frac{\lambda}{2}E_i^{11}E_{i+1}^{01}E_{i+2}^{00}+\frac{\lambda}{2}E_i^{11}E_{i+1}^{01}E_{i+2}^{00}$ and take them together with the four other terms to form

$$-\frac{\lambda}{2}E_i^{11}E_{i+1}^{01}(E_{i+2}^{00}+E_{i+2}^{11})+\frac{\lambda}{2}E_i^{11}E_{i+1}^{00}(E_{i+2}^{00}+E_{i+2}^{11})$$
$$-\frac{\lambda}{2}(E_i^{00}+E_i^{11})E_{i+1}^{01}E_{i+2}^{11}+\frac{\lambda}{2}(E_i^{00}+E_i^{11})E_{i+1}^{00}E_{i+2}^{11}.$$

The factors between brackets form identity operators. When collecting all the terms, one finds again (2.29), a sum of 2-site operators.

2.2.4 Mean-field

In the introduction it was mentioned that the law of mass action, where the reaction rate of two reactants is proportional to the product of their densities, represents a mean-field approach. This can be made clear in the quantum formalism of a Markov process. Consider the example of the contact process. If we want to construct a correct differential equation for the particle density at a site n, we can use (2.16):

$$\frac{d\rho_n(t)}{dt}=\frac{d}{dt}\left\langle E_n^{11}\right\rangle=\left\langle\left[H,E_n^{11}\right]\right\rangle.$$

Using the local character of the Hamiltonian of the contact process one can easily calculate the commutator, leading to

$$\frac{d}{dt}\left\langle E_n^{11}\right\rangle=-\left\langle E_n^{11}\right\rangle+\frac{\lambda}{2}\left\langle\left(1-E_n^{11}\right)\left(E_{n-1}^{11}+E_{n+1}^{11}\right)\right\rangle. \tag{2.31}$$

Note that this equation of motion for the local particle density, involves correlations of two operators at different sites. In turn, the equation of motion for correlations of two operators will couple to correlations of three operators, and so on. When this is not the case, the equations of motion are said to close and they can be studied by a Fourier transformation, see e.g. [33]. In general however, they do not decouple and can not be solved exactly. One way of finding an approximating solution is by neglecting the correlations, which is the essence of the mean-field assumption. If we impose translational invariance and replace $\left\langle E_n^{11}E_{n+1}^{11}\right\rangle$ by $\left\langle E_n^{11}\right\rangle^2$ we get the following non-linear differential equation for the contact process

$$\frac{d}{dt}\left\langle E_n^{11}\right\rangle=-\left\langle E_n^{11}\right\rangle+\lambda\left\langle E_n^{11}\right\rangle\left(1-\left\langle E_n^{11}\right\rangle\right) \tag{2.32}$$

which is nothing but the law of mass action

$$\frac{d\rho}{dt} = -\rho + \lambda\rho(1-\rho). \tag{2.33}$$

In a more sophisticated type of mean-field theory, one does not assume translational invariance. In this approach (2.31) is first rewritten as

$$\frac{d}{dt}\left\langle E_n^{11}\right\rangle = \frac{\lambda}{2}\left\langle E_{n-1}^{11} + E_{n-1}^{11} - 2E_n^{11}\right\rangle + (\lambda - 1)\left\langle E_n^{11}\right\rangle + \frac{\lambda}{2}\left\langle \left(E_{n-1}^{11} + E_{n+1}^{11}\right) E_n^{11}\right\rangle .$$

In this form one then neglects again the correlations, and to study macroscopic properties the continuum limit is taken for the space coordinates, leading to a partial differential equation of the form

$$\frac{\partial\rho(\mathbf{r},t)}{\partial t} = D\cdot\nabla^2\rho(\mathbf{r},t) + a\cdot\rho(\mathbf{r},t) + b\cdot\rho^2(\mathbf{r},t). \tag{2.34}$$

In mathematical literature this kind of equations is called a reaction-diffusion equation. This form can be used to find mean-field values for correlation lengths.

Finally, a correct continuum description of the contact process is given by [34]

$$\frac{\partial\rho(\mathbf{r},t)}{\partial t} = D\cdot\nabla^2\rho + a\cdot\rho + b\cdot\rho^2 + \eta(\mathbf{r},t), \tag{2.35}$$

in which η is a Gaussian noise with a correlator

$$\left\langle \eta(\mathbf{r},t)\eta(\mathbf{r}',t')\right\rangle \sim \rho(\mathbf{r},t)\delta(\mathbf{r}-\mathbf{r}')\delta(t-t'). \tag{2.36}$$

Notice that the density itself enters in the correlator since it is required that the empty lattice is a stationary state of the process: this form of noise implies that if at time t the system contains no particles $\rho(\mathbf{r},t) = 0$, it will remain empty at all later times. If the factor $\rho(\mathbf{r},t)$ was absent in the correlator, a fluctuation would be able to create particles from the vacuum.

This continuum description forms an alternative to the Markov approach used throughout this thesis. The question whether, for a medium of a given dimension, the extra noise term in an equation like (2.35) changes the critical behaviour or not, can form a criterion to find the upper critical dimension of a model.

2.3 Late-time behaviour

2.3.1 Spectrum of H

Looking at the master equation (2.8) it is clear that the time evolution of a vector is most simple when it is an eigenvector of H. Let us denote these eigenvectors and the corresponding eigenvalues of the Hamiltonian as $|\psi_0\rangle, |\psi_1\rangle, \ldots$

and $E_0, E_1, \ldots$. Just like in quantum mechanics it is convenient to write the time evolution of a state $|P(t)\rangle$ in this basis, by inserting the identity operator[2]

$$\mathbf{1} = \sum_i |\psi_i\rangle \langle\psi_i| \tag{2.37}$$

leading to

$$\begin{aligned} |P(t)\rangle &= e^{-Ht} |P_0\rangle \\ &= \sum_i e^{-E_i t} \langle\psi_i |P_0\rangle |\psi_i\rangle . \end{aligned} \tag{2.38}$$

Remark 3 Before going further with this notation, several remarks are at place here. First of all, in general the eigenvectors $|\psi_i\rangle$ cannot be normalised. As we will show later on, the form of a stochastic Hamiltonian H implies that every eigenvector with a non-zero eigenvalue has a zero stochastic norm $\langle s |\psi\rangle = 0$, making it impossible to interpret the vector as a probability distribution of the system. The eigenvectors of H can be used as a basis to represent a probability distribution, but have themselves no such physical meaning. One encounters the same problem in quantum mechanics for some Hamiltonians.

But since the Hamiltonian of a stochastic system is in general non-symmetric, it has some properties not found in quantum mechanics:

Eigenvectors belonging to different eigenvalues can be non-orthogonal. In quantum mechanics one can put the right eigenvectors in a matrix which is orthogonal (unitary) and hence the inverse of this matrix is the transposed. Left and right eigenvectors, needed for the basis transformation (2.38), are consequently related by transposition. In the stochastic case, left eigenvectors have to be calculated separately by solving the eigenvector equation, or by calculating the inverse of the matrix of right eigenvectors, the dual basis. When we write $\langle\psi_i|$ in the context of eigenvectors, we will always assume this to be the left eigenvector associated with the right one $|\psi_i\rangle$ (and not simply the transposed of it). We take them to be dual: $\langle\psi_i |\psi_j\rangle = \delta_{i,j}$.

Eigenvalues of H can be complex numbers. We return to this point after the remark.

In general it can happen that the multiplicity of an eigenvalue is bigger than the dimension of the corresponding eigenspace. In this case H cannot be transformed into a diagonal form, but only into a Jordan form. This means that in the time evolution of (2.38) the corresponding term gets an extra prefactor, being a polynomial function in time. But since the real part of every eigenvalue E_i is positive (as we will see further), this extra factor does not change the late-time behaviour of the system. Hence we will no more consider this case in future.

To get a better idea of what (2.38) implies, the form of the spectrum of H is essential. First, H has a known left eigenvector with eigenvalue zero :

[2]The interpretation of $|\psi_i\rangle$ is given in the remark on this page.

$\langle s| H = 0$ (2.15), so H must have a right eigenvector with eigenvalue zero. Denote this eigenvalue $E_0 = 0$. Secondly, a theorem by Gershgorin [35] puts some limitations on the spectrum of matrices having the form of H (2.7). Define first

$$r = \max_i(H_{ii}) \ \in \mathbb{R}^+. \tag{2.39}$$

(Remember that the diagonal element H_{ii} is the decay rate of configuration η_i.) Then, the theorem of Gershgorin implies that all eigenvalues E_i of H are in the complex plane and $|E_i - r| \leq r$, cf Figure 2.2. This ensures the

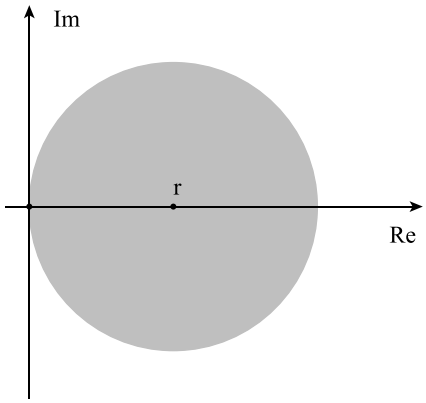

Figure 2.2: *Spectrum of H lies on the disk with centre r and radius r.*

following important properties about the spectrum of the Hamiltonian H of any Markov process

$$\begin{aligned} &E_0 = 0 \ \text{ is an eigenvalue of } H \\ &\forall \text{ eigenvalue } E_i \text{ of } H: \quad \begin{array}{l} \mathrm{Re}(E_i) \geq 0 \\ \mathrm{Im}(E_i) > 0 \Longrightarrow \mathrm{Re}(E_i) > 0. \end{array} \end{aligned} \tag{2.40}$$

We will always order the eigenvalues by increasing real part $\mathrm{Re}(E_0) \leq \mathrm{Re}(E_1) \leq \ldots$, and we will call an eigenvector with eigenvalue zero, a *ground state* of the Hamiltonian. When talking about the low lying spectrum, this is always with respect to the real part.

2.3.2 Decay to a Stationary State

Any ground state of the Hamiltonian has two important properties. First, it can be normalised to be a probability distribution while an eigenvector with

a non-zero eigenvalue cannot be normalised:

$$\left.\begin{array}{c} H\left|\psi_i\right\rangle = E_i\left|\psi_i\right\rangle \\ \left\langle s\right| H = 0 \end{array}\right\} \Longrightarrow 0 = \left\langle s\right| H\left|\psi_i\right\rangle = E_i\left\langle s\right.\left|\psi_i\right\rangle . \tag{2.41}$$

For $E_i \neq 0$, we have $\left\langle s\right.\left|\psi_i\right\rangle = 0$. When the eigenvalue is zero, e.g. $E_0 = 0$, the vector can be normalised:$\left|\psi_0\right\rangle \rightarrow \left|\psi_0\right\rangle / \left\langle s\right.\left|\psi_0\right\rangle$ and it is a well defined state of the system. In the latter case, we will always assume normalisation constants to be taken into the vectors $\left\langle s\right.\left|\psi_0\right\rangle = 1$. Secondly a ground state is an invariant probability distribution under time evolution:

$$\frac{d}{dt}\left|\psi_0\right\rangle = -H\left|\psi_0\right\rangle = 0. \tag{2.42}$$

That is why a ground state is called a *stationary state* of the system. Any expectation value in this state, is a constant in time.

When comparing the time evolution in the form (2.38) with the time evolution in quantum mechanics, the big difference is the absence of the imaginary i in the exponential. Since (2.40) implies that the real part of a non-zero eigenvalue is always strictly positive, one can see that the probability of being in a non-stationary state, decays exponentially in time. From whatever state you start, the system will always end up in a stationary distribution $\left|P^*\right\rangle$.

$$\lim_{t\to\infty} e^{-Ht}\left|P_0\right\rangle = \left|P^*\right\rangle . \tag{2.43}$$

As a consequence, these ground states play a very prominent role in stochastic processes. It was very simple to show the existence of a ground state, but calculating such a distribution explicitly is often very hard or impossible. Even for the determination of the number of (linearly independent) stationary states there is no general scheme known. Uniqueness of the stationary state is however an important matter, since for a system with more ground states the initial distribution is relevant: it determines the linear combination of ground states the system will evolve into. This becomes clear on the level of the time evolution operator where one can write the infinite-time limit as a projection operator ($T^* = (T^*)^2$)

$$\lim_{t\to\infty} e^{-Ht} = T^*. \tag{2.44}$$

When a system has only one stationary state $\left|\psi_0\right\rangle$, this operator can trivially be written as

$$T^* = \left|\psi_0\right\rangle\left\langle s\right| . \tag{2.45}$$

For the case of $n > 1$ ground states this needs some extension. Denote $\left|\psi_{0_i}\right\rangle$ the right and $\left\langle\psi_{0_i}\right|$ the left ground states. Since for any $\left\langle\psi_{0_i}\right|$

$$\frac{d}{dt}\left\langle\psi_{0_i}\right| e^{-Ht} = -\left\langle\psi_{0_i}\right| He^{-Ht} = 0 \tag{2.46}$$

one can write

$$\langle \psi_{0_i} | = \lim_{t\to\infty} \langle \psi_{0_i} | e^{-Ht}. \tag{2.47}$$

The vectors $|\psi_{0_i}\rangle$ span the space of stationary states. If they are normalised this leads to the following identity for any initial state $|P_0\rangle$

$$\lim_{t\to\infty} e^{-Ht} |P_0\rangle = \sum_{i=1}^{n} |\psi_{0_i}\rangle \langle \psi_{0_i}| \lim_{t\to\infty} e^{-Ht} |P_0\rangle = \sum_{i=1}^{n} |\psi_{0_i}\rangle \langle \psi_{0_i}| P_0\rangle . \tag{2.48}$$

The general form of the projection operator is now

$$T^* = \sum_{i=1}^{n} |\psi_{0_i}\rangle \langle \psi_{0_i}| \tag{2.49}$$

and $\langle \psi_{0_i}| P_0\rangle$ is the probability that an initial state $|P_0\rangle$ evolves into the stationary state $|\psi_{0_i}\rangle$. Since for every initial state $|P_0\rangle$: $\sum_i \langle \psi_{0_i}| P_0\rangle = 1$, one gets the identity

$$\sum_i \langle \psi_{0_i}| = \langle s| . \tag{2.50}$$

Conservation laws and physical arguments can often be very useful to get insight in stationary states. As a simple example, random walks of hard core particles on a lattice of L sites, conserve the number of particles. Hence this stochastic process has at least L+1 stationary states, one for each number of particles. If one now adds a death process $A \to \phi$, only one stationary state will remain, the state with probability one for the configuration without particles.

After a study of the stationary states, one can ask the question how the system evolves into these states. For a finite system the answer is clear. The time evolution (2.38) and the spectrum (2.40) tell us that the decay in time is exponentially fast, and for long times this decay is dominated by the eigenvalue $E_{\min}$ with the smallest non-zero real part. The late-time behaviour for a process with initial state $|P_0\rangle$, evolving into a stationary state $|P^*\rangle = T^* |P_0\rangle$, can then be written as

$$|P(t)\rangle = |P^*\rangle + e^{-E_{\min} t} \langle \psi_{\min}| P_0\rangle |\psi_{\min}\rangle \tag{2.51}$$

provided $\langle \psi_{\min}| P_0\rangle$ is not accidentally zero. Since ground states have eigenvalue zero, the real part of $E_{\min}$ is often written as Γ_0, the lowest "energy" gap, and the relaxation time of this process as $\tau = \dfrac{1}{\Gamma_0}$. For a system with infinitely many degrees of freedom, the reasoning becomes more delicate. It can happen that the low lying spectrum of H becomes continuous. The gap

Γ_0 becomes zero and the relaxation can become slower than exponential. In critical systems one often encounters algebraic decay. The lowest gap Γ_0, is an important quantity in the study of dynamics of infinite systems. But one has to be careful. The fact that Γ_0 becomes zero in the infinite-volume limit, does not mean that the relaxation will be non-exponential. It can happen that $\Gamma_0 \to 0$, but that the rest of the low spectrum does not become dense. This simply means that in the infinite-volume limit the number of ground states increases, and there still remains a finite gap with the first excited state.

2.3.3 Detailed Balance

Sometimes it is important to construct a Markov process such that an a priori known state is stationary. This is needed for example if one wants to study dynamics of systems evolving into equilibrium (Gibbs state) or if one wants to perform Monte Carlo simulations of equilibrium systems. One way of realising this, is by imposing the condition of detailed balance on the dynamics. A Markov process with transition rates $r_{\eta\to\eta'}$ is called to be in detailed balance with respect to a state $|P\rangle = \sum_\eta P_\eta |\eta\rangle$ if

$$\frac{r_{\eta\to\eta'}}{r_{\eta'\to\eta}} = \frac{P_{\eta'}}{P_\eta}. \tag{2.52}$$

This implies that the *probability current* from η to η' is zero:

$$J_{\eta\to\eta'} = r_{\eta\to\eta'}P_\eta - r_{\eta'\to\eta}P_{\eta'} = 0. \tag{2.53}$$

The master equation 2.4 immediately implies that $|P\rangle$ is a stationary state of the system.

Consider the case of an equilibrium system with

$$P_\eta = e^{-\beta E(\eta)} \tag{2.54}$$

where E is the energy functional on the configuration space and β is proportional to the inverse temperature. The condition of detailed balance then reads

$$\frac{r_{\eta\to\eta'}}{r_{\eta'\to\eta}} = e^{-\beta\Delta E} \tag{2.55}$$

with $\Delta E = E(\eta') - E(\eta)$ the energy barrier between the two configurations. This can then easily be used to implement a Monte Carlo simulation of an equilibrium system or to study the decay of a system to equilibrium. A famous example of the latter case are the Glauber dynamics for the Ising system [33].

The presence of detailed balance, i.e. this absence of all probability currents $J_{\eta\to\eta'}$ in a stationary state, is a rather strong condition. For a system

having such a state one can derive several properties making an analytical study more easy [30]. For example, it can be shown that the Hamiltonian H can be mapped on a symmetric operator by a diagonal transformation, implying e.g. that all eigenvalues of H are real. However, in general (as for the models studied further in this thesis) only the weaker relation $\sum_{\eta' \in X/\{\eta\}} J_{\eta \to \eta'} = 0$ holds for any stationary state and such properties can not be derived.

2.3.4 Infinite-Rate Expansion

The infinite-rate expansion or the separation of time scales is a well known technique which in the context of the quantum formalism can easily be derived from a Schwinger-Dyson expansion, a typical quantum tool. Consider a multiparticle system with some processes occurring much faster than all the others. This is described by a Markov process where some transition rates are much bigger than the others. Transitions associated with the fast processes have a very big decay constant and they are occurring all the time. Transitions associated with the slow processes are occurring only now and then. Hence the dynamics of the system take place on two highly separated time scales. One can now look at the system on a time scale associated with the slow processes and determine the effective dynamics. This is done by approximating the time evolution operator by the slow processes, perturbed by the fast processes. In the extreme limit of the large rates going to infinity, the method is exact and can be derived in the following way.

Write the Hamiltonian of the system as

$$H = H_0 + \lambda H_1 \tag{2.56}$$

where H_0 is the Hamiltonian of the slow processes, λH_1 that of the fast processes and λ the large rate. One can use the Schwinger-Dyson expansion, known from quantum mechanics, to write

$$\begin{aligned} e^{-(H_0+\lambda H_1)t} \;=\; & \Big[1 - \int_0^t d\tau_1 e^{-\lambda H_1 \tau_1} H_0 e^{\lambda H_1 \tau_1} \\ & + \int_0^t d\tau_1 \int_{\tau_1}^t d\tau_2 e^{-\lambda H_1 \tau_1} H_0 e^{-\lambda H_1 (\tau_2 - \tau_1)} H_0 e^{\lambda H_1 \tau_2} \\ & - \int_0^t d\tau_1 \int_{\tau_1}^t d\tau_2 \int_{\tau_2}^t d\tau_3 e^{-\lambda H_1 \tau_1} H_0 e^{-\lambda H_1 (\tau_2 - \tau_1)} H_0 e^{\lambda H_1 (\tau_3 - \tau_2)} H_0 e^{\lambda H_1 \tau_3} \\ & + \ldots \Big] e^{-\lambda H_1 t} \end{aligned} \tag{2.57}$$

where all factors are time ordered: $0 \leq \tau_1 \leq \tau_2 \leq \ldots \leq t$. In this form the limit $\lambda \longrightarrow \infty$ is taken. Denote

$$T^* = \lim_{\lambda \to \infty} e^{-\lambda H_1 t} = \lim_{t \to \infty} e^{-H_1 t} \tag{2.58}$$

the projection operator on the ground states of H_1, as in (2.44). The expansion (2.57) becomes

$$\begin{aligned}\lim_{\lambda\to\infty} e^{-(H_0+\lambda H_1)t} &= T^* - \int_0^t d\tau_1 T^* H_0 T^* + \int_0^t d\tau_1 \int_{\tau_1}^t d\tau_2 T^* H_0 T^* H_0 T^* \\ &\quad - \int_0^t d\tau_1 \int_{\tau_1}^t d\tau_2 \int_{\tau_2}^t d\tau_3 T^* H_0 T^* H_0 T^* H_0 T^* + \ldots \\ &= \left[1 - t\,(T^* H_0 T^*) + \frac{t^2}{2!}\,(T^* H_0 T^*)^2 \right. \\ &\quad \left. - \frac{t^3}{3!}\,(T^* H_0 T^*)^3 + \ldots\right] T^* \end{aligned} \tag{2.59}$$

resulting in a time evolution given by

$$\lim_{\lambda\to\infty} e^{-(H_0+\lambda H_1)t} = e^{-\tilde{H}_0 t} T^* \tag{2.60}$$

$$\tilde{H}_0 = T^* H_0 T^*. \tag{2.61}$$

This means that any initial state $|P_0\rangle$ is by T^* first projected onto the space spanned by the ground states of H_1. Then the effective dynamics given by $\tilde{H}_0$ take place on this limited space. The form of $\tilde{H}_0$ can be understood intuitively. In between every rare event of H_0 a lot of events of λH_1 take place: the system evolves very quickly into a ground state of H_1, represented by the projection operator T^*.

If the ground states of H_1 can be found exactly, it is simple to determine $\tilde{H}_0$. When the original operator H is an Hamiltonian of a stochastic process with local interactions, so will be $\tilde{H}_0$ and sometimes these effective dynamics turn out to be simpler than the original ones.

Chapter 3

Contact Process and Scaling

The contact process will keep returning in this thesis as the archetype of a model with a continuous phase transition out of an absorbing state. In this chapter it will be used to introduce the notion of critical exponents and the concept of scaling. But first the contact process will serve as a case-study to apply the mean-field approach and the quantum formalism in order to get some insight in the behaviour of the model.

3.1 Contact Process

3.1.1 Mean-field

Although we know that quantitative results of a mean-field approximation for one-dimensional systems can not be trusted, the use of the simple law of mass action (see section 1.3) can be instructive to get a first view on a systems behaviour. Therefore we will start with the application of it to the contact process. Let us first briefly review how this process is defined. The medium of the model is a lattice and each lattice site is either empty ϕ or occupied A. The dynamics can be interpreted as the spreading of an epidemic when an infected entity is identified with A and a healthy one with ϕ. As mentioned before (cf example 2, subsection 2.2.3), the contact process on a one-dimensional lattice is then defined by the transition rates

$$\begin{array}{lcll} \phi A \\ A\phi & \rightarrow & AA & \text{with rate } \frac{\lambda}{2} \\ A & \rightarrow & \phi & \text{with rate } 1 \end{array} \tag{3.1}$$

where λ is called the contamination or the branching rate. Now we can translate these reactions by the law of mass action (cf subsection 3.1.1) into the

differential equation $\frac{d\rho}{dt} = \lambda.\rho(1-\rho) - \rho$ where ρ is the particle density. This can be rewritten as

$$\frac{d\rho}{dt} = (\lambda - 1)\rho - \lambda\rho^2. \tag{3.2}$$

In the area of population dynamics, relation (3.2) is known as the Verhulst or the logistic equation [36]. In Fig 3.1 the time-derivative of ρ is sketched as a function of ρ for small and big λ. Depending on the contamination rate, one encounters two regimes. When $\lambda < 1$ the time derivative of ρ is negative,

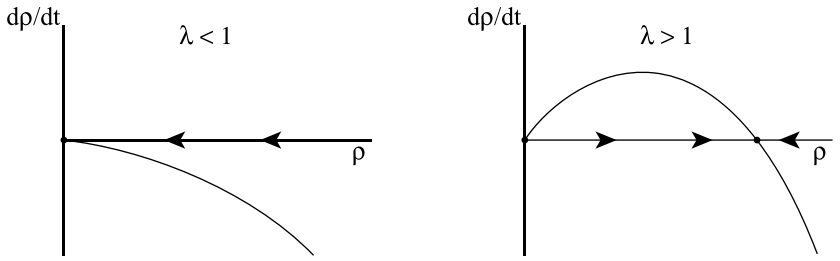

Figure 3.1: *The time-derivative of the particle density, according to the law of mass action, in the contact process with contamination rate λ. The flow of ρ in time is indicated by arrows and stationary values are represented by a dot.*

independent of the value of ρ. The only stationary value is an attractive one and given by $\rho^* = 0$. For $\lambda > 1$ this is still a stationary value, but it is no longer attractive. When the initial particle density is non-zero, the system will end up in a state with $\rho^* = \frac{\lambda-1}{\lambda}$. The (attractive) stationary particle density as a function of λ looks like the sketch in Fig. 1.1. For the time evolution, equation (3.2) gives an exponential decay

$$\rho(t) - \rho^* \sim e^{-|1-\lambda|t} \tag{3.3}$$

for $\lambda \neq 1$ and in the $t \to \infty$ limit. At the critical point $\lambda = 1$ the solution is algebraic

$$\rho(t) \sim t^{-1}. \tag{3.4}$$

The qualitative picture of this approximation is consistent with what is known about the contact process when described by a continuous time Markov process. It possesses an absorbing state: the empty lattice with $\rho = 0$. If this is reached, no escape is possible since all reactions are halted. This state is however only attractive when the contamination rate is smaller than a critical value λ_c. For $\lambda > \lambda_c$ the system has (in the case of an infinitely large system)

a second, attractive stationary state with $\rho > 0$. When the system is non-critical, the particle density approaches its stationary value exponentially fast, while for $\lambda = \lambda_c$ the decay is algebraic.

The quantitative part of this mean-field result is however not correct. As we will see later, for the one-dimensional lattice the mean-field value of $\lambda_c = 1$ is an underestimate. This can be understood intuitively. The process $A\phi, \phi A \to AA$ creates correlations between the particles, while the process $A \to \phi$ is independent of the neighbours and as a consequence can only destroy and not create (anti)correlations. When λ is close to λ_c one can expect the particles in the system to be correlated, and this makes (especially in low dimensional media) the contamination process less effective, resulting in a bigger λ_c. The mean-field theory exhibits the same lack of accuracy for critical exponents which can be defined around the continuous phase transition at $\lambda = \lambda_c$. For the contact process these mean-field exponents become exact only for a spatial dimension larger than the upper critical dimension $d_c = 4$ [37].

Later we will turn to better approximative techniques, but first we will give a few mathematically exact results that are known about the contact process.

3.1.2 Some Exact Properties

In Chapter 2 we chose the single-site representations $|A\rangle = \binom{0}{1}$, $|\phi\rangle = \binom{1}{0}$ and showed how for a system with local interactions the quantum Hamiltonian can easily be written as a sum of local operators. In example 2 we constructed the Hamiltonian for the contact process, which for periodic boundary conditions and with lattice site numbering modulo L, the system size, can be written as

$$H = \sum_{i=1}^{L} h_i^1 + h_i^2 \tag{3.5}$$

with

$$h_i^1 = \bigotimes_{k=1}^{i-1} \mathbf{1} \left[\otimes h^1 \otimes\right] \bigotimes_{k=i+1}^{L} \mathbf{1} \tag{3.6}$$

$$h_i^2 = \bigotimes_{k=1}^{i-1} \mathbf{1} \left[\otimes h^2 \otimes\right] \bigotimes_{k=i+2}^{L} \mathbf{1} \tag{3.7}$$

and

$$h^1 = -E^{01} + E^{11} \tag{3.8}$$

$$h^2 = -\frac{\lambda}{2} E^{11} \otimes E^{10} + \frac{\lambda}{2} E^{11} \otimes E^{00} - \frac{\lambda}{2} E^{10} \otimes E^{11} + \frac{\lambda}{2} E^{00} \otimes E^{11} \tag{3.9}$$

the one- and two-site Hamiltonians representing respectively the death and reproduction processes of the particles. The operators E^{ab} are defined in (2.21).

A first simple property that can be derived is that the empty lattice is indeed a stationary state of H. This state can be written as a product measure of the form

$$|0\rangle = \bigotimes_{i=1}^{L} \binom{1}{0} \qquad : \text{the empty-lattice state.} \tag{3.10}$$

Note that this vector is properly normalised $\langle s|\, 0\rangle = 1$. To be stationary, $|0\rangle$ has to be a ground state (eigenvalue zero) of H. Using the local description we have, independent of λ,

$$\begin{aligned} h^1 \tbinom{1}{0} &= 0 \\ h^2 \left[\tbinom{1}{0} \otimes \tbinom{1}{0} \right] &= 0 \end{aligned}$$

resulting in $H\,|0\rangle = 0$. This holds for any lattice size and also in the limit $L \to \infty$. Hence, for the contact process this trivial stationary state is always present.

The true challenge is of course the find the second stationary state for the infinite system with large contamination rate. So far this problem has not been solved. However, the existence of a phase transition in the infinite-size limit has been proven [31], [38]: there must be a critical λ_c above which the ground state is twofold degenerate and below which $|0\rangle$ is the only ground state. λ_c can not be calculated exactly, but it is proven that the phase-transition is continuous [39].

Besides these important existence statements, there is a property, known as *self-duality*, that can be derived rigorously for the contact process and that will have a useful consequence. This concept was introduced by probabilists [38] and should not be confused with the duality known from equilibrium statistical mechanics. To avoid this confusion, G. Schütz replaced the term by *enantiodromy* [30]. Since this property is easy to derive in the quantum formalism[40] we will review it here. Two Markov processes, defined by their quantum Hamiltonians H and $\tilde{H}$ are called enantiodromic if an invertible operator B exists for which

$$\tilde{H}^T = BHB^{-1} \tag{3.11}$$

holds. In this context the superscript T means the transposed. For the contact process a B exists for which $\tilde{H} = H$, and therefore it is called self-enantiodromic. Denote the 2×2 matrices

$$b = \begin{pmatrix} 1 & 1 \\ 1 & 0 \end{pmatrix} \qquad b^{-1} = \begin{pmatrix} 0 & 1 \\ 1 & -1 \end{pmatrix}. \tag{3.12}$$

It is easy to check that

$$\begin{aligned} bh^1b^{-1} &= \left(h^1\right)^T \\ (b\otimes b)\, h^2 \left(b^{-1}\otimes b^{-1}\right) &= \left(h^2\right)^T \end{aligned} \tag{3.13}$$

directly implying

$$BHB^{-1} = H^T \tag{3.14}$$

with

$$B = \bigotimes_i b_i \qquad B^{-1} = \bigotimes_i b_i^{-1}. \tag{3.15}$$

The importance of this relation (3.14) lies in the possibility to simplify some expectation values. A particularly useful example is the expression one gets for the particle density at a site i by inserting the identity operator $B^{-1}B$:

$$\begin{aligned} \rho_i(t) &= \langle s|\, E_i^{11} e^{-Ht}\, |P_0\rangle \\ &= \langle s|\, B^{-1}BE_i^{11}B^{-1}Be^{-Ht}B^{-1}B\, |P_0\rangle\,. \end{aligned} \tag{3.16}$$

Operator E_i^{11} transforms to $BE_i^{11}B^{-1} = E_i^{00} - E_i^{01}$. If we denote besides the empty lattice $|0\rangle$, the full lattice as $|L\rangle$ and the transposed of the empty lattice as $\langle 0|$, we get the relations

$$\begin{aligned} \langle s|\, B^{-1} &= \langle 0| \\ B\, |L\rangle &= |0\rangle\,. \end{aligned}$$

Therefore, if we take as initial condition $|P_0\rangle = |L\rangle$ and use the self-enantiodromy, (3.16) becomes

$$\begin{aligned} \rho_i(t)\,\big|_{|P_0\rangle=|L\rangle} &= \langle 0|\left(E_i^{00} - E_i^{01}\right) e^{-H^T t}\, |0\rangle \\ &= \langle 0|\, e^{-Ht}\left(E_i^{00} - E_i^{10}\right)|0\rangle \\ &= \langle 0|\, e^{-Ht}E_i^{00}\, |0\rangle - \langle 0|\, e^{-Ht}E_i^{10}\, |0\rangle \\ &= 1 - \langle 0|\, e^{-Ht}\, |i\rangle \end{aligned} \tag{3.17}$$

with $|i\rangle$ the state with only one particle, at site i. The matrix element $\langle 0|\, e^{-Ht}\, |i\rangle$ gives the probability that starting at $t = 0$ with one particle at site i, no particles are left in the system at time t. If we introduce the *survival probability* $P_i(t)$ as the probability that starting in $|i\rangle$ there are still particles in system, we get

$$\rho_i(t)\,\big|_{|P_0\rangle=|L\rangle} = P_i(t). \tag{3.18}$$

For large times, one expects the particle density to become independent of the initial conditions (provided $\rho(0) > 0$) and one gets

$$\lim_{t\to\infty} \rho_i(t) = \lim_{t\to\infty} P_i(t). \tag{3.19}$$

For simulations this relation is very convenient. One can start with a "seed" of one particle and simulate the time evolution very efficiently since only few particles are in the system. Making several independent runs, one can estimate the survival probability. Equation (3.19) ensures that P_i remains non-zero when the system is in the active phase and goes to zero in the inactive phase. This survival analysis provides a way to determine the critical point λ_c, and as we will show in the next section to find critical exponents.[1]

3.2 Scaling

3.2.1 Critical Exponents

Using the example of the contact process we will now introduce some critical exponents that can be defined around a continuous phase transition out of an absorbing state. Denote the distance away from the critical point as

$$\Delta = \lambda - \lambda_c. \tag{3.20}$$

As an order parameter, we will focus on the particle density. The sites of the lattice are associated with the elements of $\mathbb{Z}$ and since we assume translational invariance, operators will be defined around the origin, indicated with a subindex 0. The stationary particle density, spatial correlation function and time correlation function are defined as

$$\rho^*(\Delta) = \left\langle E_0^{11} \right\rangle^* \tag{3.21}$$

$$C_s(x,\Delta) = \left\langle E_0^{11} E_x^{11} \right\rangle^* - \rho^{*2} \qquad (x \in \mathbb{Z}) \tag{3.22}$$

$$C_t(t,\Delta) = \left\langle E_0^{11} e^{-Ht} E_0^{11} \right\rangle^* - \rho^{*2} \qquad (t \in \mathbb{R}^+) \tag{3.23}$$

where the superscript $*$ in the expectation values indicates that they are to be calculated in the (attractive) stationary state $|P^*\rangle$ for the given value of Δ. In the definition of the exponents we will always assume the system to be infinitely large and the state to be stationary unless stated otherwise. We will be using the symbol $\sim$, to be interpreted in the following two ways. First

$$f(x) \sim x^a \iff \lim_{|x|\to 0} \frac{\ln f(|x|)}{\ln |x|} = a \tag{3.24}$$

[1] In simulations it is nowadays common to study phase transitions out of an absorbing state using this survival analysis. However, it is of importance to remark that this usually implies the assumption $\lim_{t\to\infty} \rho_i(t) \sim \lim_{t\to\infty} P_k(t)$ since the equality as for the contact process cannot be proven in general.

hence the exponent a should by the same for $x \downarrow 0$ and $x \uparrow 0$ unless stated otherwise. Secondly

$$f(x) \sim e^{-ax} \Longleftrightarrow \lim_{x \to +\infty} -\frac{\ln f(x)}{x} = a. \tag{3.25}$$

A first exponent is defined as the power by which the stationary particle density increases as a function of Δ in the active region:

$$\boldsymbol{\beta}: \quad \rho^* \sim \Delta^{\beta} \qquad (\Delta > 0). \tag{3.26}$$

Next, for every value $\Delta \neq 0$ the correlation functions are expected to have an exponential decay for large values of their arguments x and t:

$$C_s(|x|, \Delta) \sim e^{-|x|/\xi(\Delta)} \tag{3.27}$$

$$C_t(t, \Delta) \sim e^{-t/\tau(\Delta)}. \tag{3.28}$$

The *correlation length* ξ and the *relaxation time* τ diverge when the critical point is approached $\Delta \to 0$, resulting in a slower decay. This behaviour is characterised by the two following exponents:

$$\boldsymbol{\nu}_{\perp}: \quad \xi \sim \Delta^{-\nu_{\perp}} \tag{3.29}$$

$$\boldsymbol{\nu}_{\parallel}: \quad \tau \sim \Delta^{-\nu_{\parallel}}. \tag{3.30}$$

The use of $\perp\parallel$ has its origin in directed percolation, where our time-coordinate is a second space-coordinate and the symbols differentiate between the two.

The exponents β, $\nu_{\perp}$ and $\nu_{\parallel}$ are defined in the limit of a stationary and infinitely large system. In practice this is unaccessible, therefore it would be useful to know the behaviour of non-stationary and finite systems. For the latter, one is faced with a technical complication, namely that for a finite system the only stationary state is the absorbing one and no phase transition is present. To get access to the active state, some external intervention is needed. One can use active boundary conditions. Fixing a particle at the boundary of the system destroys the stationarity of the absorbing state and forces the system to be active. Another technique, used in simulations, is to study the *quasistationary* state. One starts of e.g. with a completely filled lattice and makes a lot of independent simulation runs. All these runs will eventually reach the absorbing state, but for every finite time some of them are still surviving. The quasistationary particle density is then defined as the average over the surviving runs. After a transient time, this density will reach a stationary value that can be used to represent the density of the active state [41]. In both of these techniques the calculated particle density will for every Δ converge to the actual stationary value in the limit $L \to \infty$. Later we will

come back to this finite-size/time analysis, but for now we define the exponents for either the finite-size or non-stationary behaviour at the critical point as

$$\boldsymbol{\alpha}_x: \quad \rho^* \sim L^{-\alpha_x} \qquad (L < \infty,\ \Delta = 0) \tag{3.31}$$

$$\boldsymbol{\alpha}_t: \quad \rho \sim t^{-\alpha_t} \qquad (\text{non-stationary},\ \Delta = 0). \tag{3.32}$$

In simulations, the survival analysis, explained in subsection 3.1.2, is an interesting alternative to study critical behaviour. One starts of at $t = 0$ with one particle at the origin of an otherwise empty lattice, denote this state as "00". Making several independent simulation runs, one can approximate $P(t)$: the probability that at time t the system still contains particles. In general one can estimate any expectation value at time t by averaging over all runs (including the non-surviving ones). If we denote this by $\langle \quad \rangle_{t|00}$, we can define the expected total number of particles

$$n(t) = \sum_x \left\langle E_x^{11} \right\rangle_{t|00} . \tag{3.33}$$

An estimate of the spread of the particles is given by the quantity

$$R^2(t) = \frac{1}{n(t)} \sum_x x^2 \left\langle E_x^{11} \right\rangle_{t|00} . \tag{3.34}$$

In the inactive phase $\Delta < 0$, $P(t)$ and $n(t)$ will decay exponentially to zero. In this phase, the spreading of the particles is diffusive (particle create new ones on a neighbouring site and disappear) and one gets $R^2(t) \sim t$. For $\Delta > 0$ however, $P(t)$ will reach a stationary non-zero value, the two boundaries of the occupied region around the origin will on average grow linearly in time, resulting in $n(t) \sim t$ and $R^2(t) \sim t^2$. Exactly at the critical point the survival probability goes to zero, but the average life-time diverges and one gets non-trivial algebraic behaviour, characterised by

$$\boldsymbol{\delta}: \quad P(t) \sim t^{-\delta} \tag{3.35}$$

$$\boldsymbol{\eta}: \quad n(t) \sim t^{\eta} \tag{3.36}$$

$$\tilde{\mathbf{z}}: \quad R^2(t) \sim t^{\tilde{z}}. \tag{3.37}$$

On physical ground one can formulate some bounds for the exponents but exact solutions are not known. They have been studied intensively during the last decades and the accurately known values suggest that not all of them are independent. This existence of scaling relations between critical exponents is known from equilibrium systems where they can be explained by scaling theory. An analogous formalism has been developed for these non-equilibrium phase transitions.

3.2.2 Scaling Theory

The first step towards the modern scaling theory was made by the homogeneity hypothesis of Widom [42] in the context of equilibrium systems. It stated that the free energy of a model does not have to be analytical, but can contain a singular part in the form of a generalised homogeneous function in a set of well chosen parameters that are zero in the critical point. This hypothesis was explained by the renormalisation group (RG), originating from field theory. The idea of rescaling was introduced in statistical mechanics by Kadanoff [43] and the RG was developed by Wilson [44], [45]. Later this was generalised to finite size models by Fisher [46]. This theory is by now well established and used in a wide variety of applications.

In the context of continuous phase transitions out an absorbing state, the generalised homogeneity can be formulated as follows. Suppose the system is close to the critical point: i.e. the contamination rate is close to criticality ($\Delta \approx 0$), the system is large enough ($L \to \infty$) and close to stationarity ($t \to \infty$). $\Delta, \frac{1}{L}$ and $\frac{1}{t}$ form the set of small parameters of the hypothesis and the particle density profile must satisfy

$$\rho(x, \frac{1}{L}, \frac{1}{t}, \Delta) = b^y \rho(\frac{x}{b}, \frac{b}{L}, \frac{b^z}{t}, b^{y_\Delta}\Delta) \qquad (\forall b \in \mathbb{R}). \tag{3.38}$$

This means that when

space	is rescaled with a factor	b
time	is rescaled with a factor	b^z
Δ	is rescaled with a factor	b^{-y_Δ}

(3.39)

the particle density is rescaled with a factor b^{-y}. In principle every macroscopic quantity should scale in this manner with its own y. This puts a big restriction on the form of the function ρ, and can explain why the exponents defined earlier are not independent.

Let us start with the consequences for the correlation length $\xi(\Delta)$ and relaxation time $\tau(\Delta)$. When Δ is rescaled according to (3.39), ξ should be rescaled as a space-coordinate, leading to

$$b\xi(b^{y_\Delta}\Delta) = \xi(\Delta). \tag{3.40}$$

When $b = \Delta^{-\frac{1}{y_\Delta}}$ is chosen, $\xi(b^{y_\Delta}\Delta) = \xi(1)$ becomes a constant and we get

$$\Delta^{-\frac{1}{y_\Delta}} \sim \xi(\Delta),$$

with (3.29) this leads to

$$\frac{1}{y_\Delta} = \nu_\perp. \tag{3.41}$$

For τ we get the relation

$$b^{-z}\frac{1}{\tau(b^{y_\Delta}\Delta)} = \frac{1}{\tau(\Delta)},$$

and

$$z = \frac{\nu_\parallel}{\nu_\perp}. \tag{3.42}$$

Consider next the case of a stationary, translation invariant, infinitely large system. Equation (3.38) becomes

$$\begin{aligned}\rho(\Delta) &= b^y\rho(b^{y_\Delta}\Delta)\\ &= b^y\rho(b^{1/\nu_\perp}\Delta)\end{aligned}$$

and by again choosing $b = \Delta^{-\frac{1}{y_\Delta}}$ one gets $\rho(\Delta) \sim \Delta^{-y\nu_\perp}$. The definition of β (3.26) finally gives

$$y = -\frac{\beta}{\nu_\perp}. \tag{3.43}$$

The generalised homogeneous form of ρ can now be written as

$$\rho(x, \frac{1}{L}, \frac{1}{t}, \Delta) = b^{-\beta/\nu_\perp}\rho(\frac{x}{b}, \frac{b}{L}, \frac{b^{\nu_\parallel/\nu_\perp}}{t}, b^{1/\nu_\perp}\Delta) \qquad (\forall b \in \mathbb{R}). \tag{3.44}$$

and all the critical exponents defined earlier can be expressed in $\beta, \nu_\perp$ and $\nu_\parallel$.

Before doing this, consider first the finite-size/time case. For a translation invariant system with $b = \Delta^{-\nu_\perp}$ one obtains

$$\begin{aligned}\rho(\frac{1}{L}, \frac{1}{t}, \Delta) &= \Delta^\beta f(\frac{\Delta^{-\nu_\perp}}{L}, \frac{\Delta^{-\nu_\parallel}}{t})\\ &= \Delta^\beta f(\frac{\xi}{L}, \frac{\tau}{t}).\end{aligned} \tag{3.45}$$

with f defined as $f(x, y) = \rho(x, y, 1)$. (3.45) is a generally valid form: for a system in the vicinity of the critical point, the correction factor for the thermodynamic-limit scaling (here $\sim \Delta^\beta$), depends on the system size and time only through the ratios $\frac{\xi}{L}$ and $\frac{\tau}{t}$. This gives a criterion to estimate how big your system needs to be and how close stationarity has to be approached to neglect finite-size/time effects. Consider next the exponents α_x and α_t from (3.31) and (3.32). For a homogeneous system in the critical point $\Delta = 0$, the choice $b = L$ and the limit $t \to \infty$ leads to $\rho(\frac{1}{L}) \sim L^{-\beta/\nu_\perp}$and

$$\alpha_x = -\beta/\nu_\perp. \tag{3.46}$$

For $b = t^{\nu_\perp/\nu_\parallel}$ and $L \to \infty$ one gets

$$\alpha_t = -\beta/\nu_\parallel. \tag{3.47}$$

These results are very important to find estimates for the exponents. For example the relation $\rho(\frac{1}{L}) \sim L^{-\beta/\nu_\perp}$ gives a way to find $\beta/\nu_\perp$ of the infinite system by studying the (quasi)stationary particle density of finite systems! This finite-size analysis is an indispensable tool in simulations and numerical techniques.

To find the exponents of the survival analysis, defined in (3.35)-(3.37), the self-enantiodromy property of the contact process is used. Equation (3.19) ensures that for long times, the survival probability is the same as the particle density and should scale in the same way:

$$\delta = -\beta/\nu_\parallel. \tag{3.48}$$

For the determination of η and $\tilde{z}$ a new observable is introduced: $\rho_{00}(x,t) =$ the probability of finding a particle at site x on time t when at time $t = 0$ one particle was present at the origin of an otherwise empty lattice. The scaling hypothesis tells us

$$\rho_{00}(x,t,\Delta) = b^y \rho_{00}(\frac{x}{b}, \frac{b^{\nu_\parallel/\nu_\perp}}{t}, b^{1/\nu_\perp}\Delta). \tag{3.49}$$

The unknown number y can easily be determined. Since for $t \to \infty$, ρ_{00} becomes independent of x and can be written as the product of the survival probability and the stationary particle density one gets

$$\lim_{t\to\infty} \rho_{00}(x,t) = \lim_{t\to\infty} P(t) \cdot \rho(t) = \lim_{t\to\infty} \rho^2(t)$$

and

$$\lim_{t\to\infty} \rho_{00} \sim \Delta^{2\beta} \tag{3.50}$$

leading to $y = -2\beta/\nu_\perp$. In the critical point, (3.49) can now be written as

$$\rho_{00}(x,t) = t^{-2\beta/\nu_\parallel} f(\frac{x}{t^{\nu_\perp/\nu_\parallel}})$$

and the quantities $n(t)$ and $R^2(t)$ can be calculated

$$\begin{aligned} n(t) &= \int_x \rho_{00}(x,t)dx = t^{-2\beta/\nu_\parallel} \int_x f(\frac{x}{t^{\nu_\perp/\nu_\parallel}})dx \\ &\sim t^{-2\beta/\nu_\parallel + \nu_\perp/\nu_\parallel} \\ R^2(t) &= \frac{1}{n(t)} \int_x x^2 \rho_{00}(x,t)dx = \frac{t^{-2\beta/\nu_\parallel}}{n(t)} \int_x x^2 f(\frac{x}{t^{\nu_\perp/\nu_\parallel}})dx \\ &\sim t^{2\nu_\perp/\nu_\parallel} \end{aligned}$$

λ_c	3.29785(2)
β	0.27649(4)
$\nu_\perp$	1.09684(6)
$\nu_\parallel$	1.73383(3)

λ_c from [47], exponents from [48]

Table 3.1: *Critical point and three independent critical exponents of the one-dimensional contact process.*

resulting finally in

$$\eta = -2\beta/\nu_\parallel + \nu_\perp/\nu_\parallel \tag{3.51}$$
$$\tilde{z} = 2\nu_\perp/\nu_\parallel. \tag{3.52}$$

From the eight exponents defined, only three are independent. This can be exploited in approximative techniques. Depending on the specific strengths and weaknesses of a technique some exponents are better accessible then others, but since only three independent ones are needed, one has some freedom of choice.

Some caution is however at place. In equilibrium statistical mechanics this scaling is justified by the renormalisation group theories. In non-equilibrium models no such rigorous evidence is known and the scaling theory has the status of a hypothesis. When studying a model one should in principle always check the assumed relations between the exponents. For the contact process, within numerical precision, no violations are known.

3.2.3 Numerical Values

In subsection 3.1.1 we found using mean-field: $\lambda_c = 1$, and $\rho^* = \frac{\lambda-1}{\lambda}$, $\rho(t) \sim t^{-1}$ leading to $\beta = 1, \nu_\parallel = 1$. To determine the mean-field value of $\nu_\perp$, one needs the generalised form (2.34) to define spatial correlations. A short calculation would result in $\nu_\perp = \frac{1}{2}$. These values are to be compared with those in Table 3.1 which are expected to be correct up to the given precision. As mentioned before, these exponents are not new, and were first found in a model for directed percolation (DP) [20]. The universality class containing all models with this critical behaviour is named after it.

The inaccuracy of mean-field is obvious, and calls for (preferably simple) alternatives. When I started my Ph.D. several approximative techniques existed to find estimates of these exponents: sophisticated simulations, field theoretic renormalisation group techniques, series expansions (obtained from

quantum mechanical perturbation theory in λ or $1/\lambda$), numerical diagonalisations, ... but no real-space renormalisation group (RG) technique existed yet. A simple realisation of such an RG formed the first subject of my research and the result will be elaborated in the next chapter.

Chapter 4

The Standard Real-Space RG

This chapter develops a simple real-space RG to study the stationary critical behaviour of non-equilibrium many particle systems. The RG transformations that are first constructed in a heuristic way, are derived as a first order expansion of the infinite time limit of a more conventional RG. Some general properties of the method are discussed and the chapter concludes with an implementation of the SRG on an exactly solvable model. The contents of this chapter forms the subject of a first publication [49].

4.1 The SRG

The term "renormalisation group" (RG) has its historical origin in particle physics of the 1960s, where its concept was used to study high energy behaviour of renormalised quantum electrodynamics. Since then, the ideas of it have been adapted in several other areas of physics, resulting in a large number of all different realisations of the RG. One of the most prominent properties of the RG is the absence of a general formalism. It is more a set of ideas that has to be implemented each time again, for every new application. The common concept of all these implementations is that the parameters that define the system under investigation, are mapped on new ones, while the physical properties of interest are kept unchanged. In the context of critical phenomena one is interested in the macroscopic, long-distance behaviour of the system and the RG consists of a course-graining of short-distance degrees of freedom.

In a real-space RG for a lattice model one starts by dividing the system into cells. The degrees of freedom in the cells are replaced by new ones, which are smaller in number. Next, new interactions between those degrees of freedom are constructed and the system is mapped on a smaller one: all length scales

are reduced by a factor b. Since this RG is constructed in a way to leave large scale physics invariant, the correlation length ξ, expressed in lattice-size units, is reduced to $\xi' = \xi/b$. This means that under RG-iterations, ξ decreases and hence the system is driven away from a potentially present critical point. However, when the system is exactly at the transition point, ξ is infinite and it is left invariant under the procedure. The study of this *RG flow* around the critical point leads to physical observables behaving in the way predicted by the scaling hypothesis of Widom, in this way justifying it and producing a manner to calculate critical exponents.

We will now introduce such a real-space RG to study the *stationary behaviour* of one-dimensional stochastic lattice models. It is an adaption we made of the standard RG (SRG), also known as the SLAC approach [50], named after the Stanford Linear Accelerator. There it was introduced in the late 1970s and subsequently, during the early 1980s, it was used a lot in the study of ground state properties of quantum spin and fermion chains [51].

4.1.1 Construction of RG flow

We will first introduce the SRG in a manner that might seem somewhat ad hoc, but later we will put it in the broader context of a perturbation theory. Consider a lattice of L sites, for simplicity of notation we will again assume each lattice site to be in one of two possible states, associated with the presence A or absence ϕ of a particle. Next, for the SRG in its simplest form, as we present it here, we can only permit nearest neighbour interactions:

$$H = \sum_{i=1}^{L} h_i \tag{4.1}$$

with h_i a local 2-site operator, acting on site i and $i+1$.

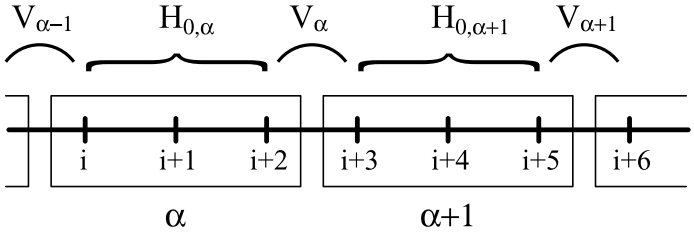

Figure 4.1: *Regrouping of sites and Hamiltonian terms for the case of cell size* $b = 3$.

The first step in the SRG procedure is the division of the lattice into cells,

each containing b sites ($b \geq 2$). The local operators that form the Hamiltonian, are then regrouped into intracell and intercell parts, as visualised in Fig. 4.1. One gets

$$H = \sum_{\alpha}^{L/b} (H_{0,\alpha} + V_\alpha) \tag{4.2}$$

with α the cell index, $H_{0,\alpha}$ the local intracell Hamiltonian containing the terms h_i acting on sites in cell α, and V_α the intercell part containing the interactions between two neighbouring cells.

Next the ground states of $H_{0,\alpha}$ are calculated exactly. It will become clear in a moment that we need them to be doubly degenerated. Assuming this, we denote the two right and left ground states of cell α as

$$\begin{aligned} \left|\psi_{0_1}\right\rangle_\alpha \quad &\text{and} \quad \left|\psi_{0_2}\right\rangle_\alpha \\ {}_\alpha\left\langle\psi_{0_1}\right| \quad &\text{and} \quad {}_\alpha\left\langle\psi_{0_2}\right| \end{aligned} \tag{4.3}$$

after we normalised them:

$$\left\langle\psi_{0_i}\middle|\psi_{0_j}\right\rangle = \delta_{i,j}. \tag{4.4}$$

The idea of the RG is now to map the original lattice on a new one, where each site is represented by one cell. To achieve this, first the 2^b degrees of freedom of each cell are reduced to two, represented by the states (4.3). This means we interpret one of these states as the "cell particle" and the other as the "cell vacancy"[1]:

$$\left|\psi_{0_1}\right\rangle_\alpha \doteq |\phi, 0\rangle_\alpha\,, \qquad \left|\psi_{0_2}\right\rangle_\alpha \doteq |A, 0\rangle_\alpha$$

and the same for the left states. We will use the second parameter in the ket to indicate that we are dealing with eigenstates of the cells, in this case ground states. With these states we construct the configurations of the renormalised lattice

$$|\eta, 0\rangle = \bigotimes_{\alpha=1}^{L/b} |\eta_\alpha, 0\rangle_\alpha \qquad : \eta_\alpha \in \{A, \phi\} \tag{4.5}$$

(and analogous for the left configurations) which span a $2^{L/b}$-dimensional subspace $\mathcal{W}$ of the original configuration space. These configuration (4.5) are in their turn used to construct a projection operator

$$T = \sum_{\eta=1}^{2^{L/b}} |\eta, 0\rangle \langle\eta, 0|\,. \tag{4.6}$$

[1] In general one can use any two independent linear combinations of $\left|\psi_{0_1}\right\rangle_\alpha$ and $\left|\psi_{0_2}\right\rangle_\alpha$ to identify with a particle or a vacancy. In that case redefine them as $\left|\psi_{0_1}\right\rangle_\alpha$ and $\left|\psi_{0_2}\right\rangle_\alpha$.

The actual renormalisation is then performed by projecting any vector $|\psi\rangle$ or $\langle\psi|$, or any operator M of the original system on this subspace $\mathcal{W}$: $|\psi\rangle \to T|\psi\rangle$, $\langle\psi| \to \langle\psi|T$, and $M \to TMT$. To conclude the SRG, a trivial basis transformation is performed: with every configuration $|\eta,0\rangle = \bigotimes_{\alpha}^{L/b} |\eta_\alpha,0\rangle_\alpha \in \mathbb{R}^{2^L}$ of the renormalised lattice we associate the corresponding standard configuration of the smaller lattice $|\eta\rangle = \bigotimes_{i=1}^{L/b} |\eta_i\rangle \in \mathbb{R}^{2^{L/b}}$. This transformation can be implemented by the operators

$$T_1 = \sum_{\eta=1}^{2^{L/b}} |\eta\rangle\langle\eta,0|\,, \qquad T_2 = \sum_{\eta=1}^{2^{L/b}} |\eta,0\rangle\langle\eta|\,. \tag{4.7}$$

Since $T_1T = T_1$ and $TT_2 = T_2$ we finally get the *SRG mapping* $\mathcal{R}$

Lattice of L sites	$\xrightarrow{\mathcal{R}}$	Lattice of L/b sites
$\mathbb{C}^{2^L}$	$\longrightarrow$	$\mathbb{C}^{2^{L/b}}$
$\|\psi\rangle$	$\longmapsto$	$T_1\|\psi\rangle$
$\langle\psi\|$		$\langle\psi\|T_2$
$\mathbb{C}^{2^L} \times \mathbb{C}^{2^L}$	$\longrightarrow$	$\mathbb{C}^{2^{L/b}} \times \mathbb{C}^{2^{L/b}}$
M	$\longmapsto$	T_1MT_2.

(4.8)

The most important renormalisation is that of the Hamiltonian itself, this is now given by

$$\begin{aligned} \mathcal{R}(H) &= T_1HT_2 \\ &= T_1\left(\sum_{\alpha}^{L/b} H_{0,\alpha} + V_\alpha\right)T_2 \\ &= T_1\left(\sum_{\alpha}^{L/b} V_\alpha\right)T_2. \end{aligned} \tag{4.9}$$

Since $|\eta,0\rangle$ are by construction zero-valued eigenstates of $H_{0,\alpha}$ the renormalised Hamiltonian is given by the projection of the intercell Hamiltonian on $\mathcal{W}$.

The SRG mapping (4.8) has two important properties:

1. The SRG conserves probability.

   In the above reasoning we used a two-state lattice: each site could be in one of the two states A or ϕ. We demanded the ground state of the intracell Hamiltonian to be double degenerated because we associated a cell particle and a cell vacancy with these two ground states. Actually this

restriction is nothing but the condition on which the renormalised lattice is again two-stated. The generalisation of this is straightforward. For an n-state lattice to renormalise into another n-state lattice, the ground state of the cells should be n-fold degenerate. This correct degeneracy also has a mathematical implication. In equation (2.50) we proved that the sum over all (normalised) left ground states of a stochastic Hamiltonian is equal to the normalisation vector $\langle s|$. For the ground states $\langle \psi_{0_i \alpha}|$ of the (stochastic) intracell Hamiltonian we have

$$_\alpha \langle s| = \sum_i \left(_\alpha \langle \psi_{0_i}| \right) \tag{4.10}$$

provided the sum runs over *all* the ground states of the cell. If the degeneracy is as described above, this can be applied in the renormalisation of $\langle s|$:

$$\langle s| T = \sum_\eta \langle \eta, 0| = \bigotimes_\alpha \left[\sum_i {}_\alpha \langle \psi_{0_i}| \right]$$

to give

$$\begin{aligned} \sum_\eta \langle \eta, 0| &= \bigotimes_\alpha \left(_\alpha \langle s| \right) \\ &= \langle s| . \end{aligned} \tag{4.11}$$

In words, the normalisation vector $\langle s|$ remains unchanged under the SRG, meaning that there is no loss of probability under renormalisation. As an example take a vector $|\psi\rangle$ of the original system. The normalisation of this vector is not changed by the SRG mapping:

$$\begin{aligned} \langle s\ |\psi\rangle \xrightarrow{\mathcal{R}} \langle s| T_2 T_1\ |\psi\rangle &= \sum_{\eta_1, \eta_2} \langle s\ |\eta_1, 0\rangle \langle \eta_1|\ \eta_2\rangle \langle \eta_2, 0|\ \psi\rangle \\ &= \sum_\eta \langle s\ |\eta, 0\rangle \langle \eta, 0|\ \psi\rangle \\ &= \sum_\eta 1. \langle \eta, 0|\ \psi\rangle \\ &= \langle s\ |\psi\rangle \end{aligned}$$

In the same way one can show that a stochastic matrix remains stochastic.

If the degeneracy of the ground state of the cells is correct, we can conclude that when we start of with a Markov process defined by an Hamiltonian H on an n-state lattice, the renormalised system is again a Markov process on an n-state lattice and with Hamiltonian $T_1 H T_2$.

2. The SRG conserves locality

   In the models we study the only kind of operators we encounter, are local ones. They act like the identity operator on any site except on a few neighbouring ones. We can write a local operator acting non-trivially on k neighbouring sites as

$$M = \left[\bigotimes_{i=1}^{N} \mathbf{1}\right] \bigotimes M_{2^k \times 2^k} \left[\bigotimes_{i=N+k+1}^{L} \mathbf{1}\right].$$

   Let us assume that $k < b$, the cell size of the SRG. Than the operator M acts non-trivially on either one or two neighbouring cells. Consequently the renormalised operator $T_1 M T_2$ acts only non-trivially on respectively one or two neighbouring (renormalised) sites. This is a direct consequence of the tensor construction of $|\eta, 0\rangle$ (4.5) and the fact that the identity operator is invariant under the SRG (4.4). Since the SRG will eventually be performed for large b, any local operator will under SRG be mapped on a one- or two-site operator.

   For a system with a local Hamiltonian this has two important consequences. First, since the SRG mapping can be performed locally, one can renormalise a lattice of infinite length without extra computational effort. This is convenient since we want to study phase transitions, which occur only in the thermodynamical limit. Secondly, any local Hamiltonian will under SRG be mapped on a two-site operator. This can't be correct. The SRG is supposed to map a system on a new one in the same universality class, but one can think of three-site Hamiltonians with (stationary) critical behaviour that cannot be represented by two-site interactions.[2] Hence, at first sight the SRG is only reliable for models with nearest neighbours interactions. However, we will show below how this restriction can be removed, in principle, by putting the SRG in the framework of a perturbation theory.

4.1.2 SRG as a Perturbation Theory

An RG procedure maps a system on a new one by eliminating a fraction of the degrees of freedom, while keeping the physical quantities of interest unaltered. The SRG was introduced above as a ground state RG: expectation values of physical quantities in any ground state of the system should remain invariant.

[2]Example: The BARW model with offspring two, mentioned in the introduction of this thesis, contains three-site interactions on a two-state lattice and belongs to the PC universality class. In this class, no model is known that has only two-site interactions on a two-state lattice.

Let us denote an observable as F and any ground state of the system as $|P^*\rangle$. If the SRG was a perfect ground state RG, it should obey

$$\langle s| F |P^*\rangle = \langle s| T_2 T_1 F T_2 T_1 |P^*\rangle . \tag{4.12}$$

Finding an RG for which this equality holds exactly is seldom possible, but we will now show that the SRG is a first order approximation of a series expansion of the solution of (4.12). This insight came from the discovery of a relation between the SRG and an extension of the more conventional Niemijer-Van Leeuwen real space approach to quantum spin chains [52].

For a one-dimensional *stochastic* system a similar technique can be applied, provided some modifications are made. We will now explain how this works. We start in the same way as the SRG by dividing the system in cells of length b and by regrouping the Hamiltonian terms as in (4.2). But now *all* the 2^b eigenvectors of the intracell Hamiltonian $H_{0,\alpha}$ are calculated exactly and they are split up into two sets according to some criterion (for example a majority rule). One set is associated with an effective "cell particle" and the other with an effective "cell vacancy". Within each set there are 2^{b-1} vectors and these are denoted by $|\eta_\alpha, \tau_\alpha\rangle_\alpha$ with $\eta_\alpha \in \{A, \phi\}$ and $\tau_\alpha \in \{0, 1, ..., 2^{b-1} - 1\}$. Since we assume the ground state of the intracell Hamiltonian to be doubly degenerated, $|\eta_\alpha, 0\rangle_\alpha$ have eigenvalue zero, and the other vectors have an eigenvalue with a strictly positive real part. Tensor products of these states are used to construct 2^L vectors which span the whole configuration space of the original system:

$$|\eta, \tau\rangle = \bigotimes_{\alpha=1}^{L/b} |\eta_\alpha, \tau_\alpha\rangle_\alpha$$

(and the same for the left vectors). In subsection 2.3.2 we saw that eigenstates of a stochastic matrix with a non-zero eigenvalue have a stochastic norm equal to zero. Together with ${}_\alpha\langle s| = {}_\alpha\langle A, 0| + {}_\alpha\langle \phi, 0|$ (2.50) and $\langle s| = \bigotimes_\alpha ({}_\alpha\langle s|)$ this leads to

$$\langle s| = \sum_\eta \langle \eta, 0| \tag{4.13}$$

or

$$\langle s|\, \eta, \tau\rangle = \delta(\tau, 0). \tag{4.14}$$

In this formula $\tau = 0$ means $\tau_\alpha = 0 \quad \forall \alpha$. Next denote

$$H_0 = \sum_{\alpha=1}^{L/b} H_{0,\alpha} \qquad \text{and } V = \sum_{\alpha=1}^{L/b} V_\alpha \tag{4.15}$$

respectively the intra- and intercell Hamiltonian. The vectors $|\eta, \tau\rangle$ are eigenvectors of H_0. When we write the corresponding eigenvalue as $E(\eta, \tau)$ we

have

$$\begin{aligned} &H_0 \left|\eta,\tau\right\rangle = E(\eta,\tau)\left|\eta,\tau\right\rangle \\ &E(\eta,\tau=0)=0 \\ &\mathrm{Re}\left[E(\eta,\tau\neq 0)\right]>0. \end{aligned} \tag{4.16}$$

The $2^{L/b}$ states $|\eta,0\rangle$ have eigenvalue zero, while the rest of the vectors has an eigenvalue with a strictly positive real part.

We are now ready to construct the RG. We start by rewriting the expectation value for an observable F as

$$\begin{aligned} \left\langle s\right| F\left|P(t)\right\rangle &= \left\langle s\right| Fe^{-Ht}\left|P_0\right\rangle \\ &= \sum_{\eta'}\left\langle \eta',0\right| Fe^{-Ht}\left|P_0\right\rangle \end{aligned}$$

where $|P_0\rangle$ is the initial state at $t=0$ and we used formula (4.13). Next we insert the identity operator $\sum_{\eta,\tau}|\eta,\tau\rangle\langle\eta,\tau|$ in this expression to get

$$\left\langle s\right| Fe^{-Ht}\left|P_0\right\rangle = \sum_{\eta'}\sum_{\eta,\tau}\left\langle \eta',0\right| Fe^{-Ht}\left|\eta,\tau\right\rangle\left\langle \eta,\tau\right.\left|P_0\right\rangle .$$

If we can construct an RG for which the long time limit of this expectation value remains unaltered under its mapping, this would be a correct ground state RG. For the renormalised system, the expectation value is

$$\left\langle s\right|\mathcal{R}(F)e^{-\mathcal{R}(H)t'}\left|\mathcal{R}(P_0)\right\rangle = \sum_{\eta'}\sum_{\eta}\left\langle \eta'\right|\mathcal{R}(F)e^{-\mathcal{R}(H)t'}\left|\eta\right\rangle\left\langle \eta\right.\left|\mathcal{R}(P_0)\right\rangle$$

and hence the RG transformation $\mathcal{R}$ should be defined through the trace over τ in the relation[3]

$$Tr_\tau\left\langle \eta',0\right| Fe^{-Ht}\left|\eta,\tau\right\rangle\left\langle \eta,\tau\right.\left|P_0\right\rangle = \left\langle \eta'\right|\mathcal{R}(F)e^{-\mathcal{R}(H)t'}\left|\eta\right\rangle\left\langle \eta\right.\left|\mathcal{R}(P_0)\right\rangle . \tag{4.17}$$

In general it is however not possible to work out this equation exactly and one needs to turn to approximative solutions. One of the options is to make a series expansion. In the original Hamiltonian we consider the intercell Hamiltonian V as a perturbation and the renormalised Hamiltonian will be expanded into a sum of operators of successive order:

$$H = H_0 + V \tag{4.18}$$

$$\mathcal{R}(H) = H_0' + H_1' + H_2' + \ldots \tag{4.19}$$

[3]We allow a rescaling of time $\mathcal{R}(t)=t'$. It doesn't change the critical behaviour and it gives us the possibility to divide the renormalised Hamiltonian by a factor, which can be incorporated in t'. In the examples it will be clarified that this can be used to find a renormalised Hamiltonian of the same form as the original.

Next the expansion in the evolution operators of (4.17) is performed by the Schwinger-Dyson relation. Up to second order this is given by

$$\begin{aligned} e^{-(H_0+V)t} &= e^{-H_0 t} - \textstyle\int_0^1 e^{-H_0 t\lambda}\,(Vt)\,e^{-H_0 t(1-\lambda)}d\lambda \\ &\quad + \textstyle\int_0^1\int_{\lambda_1}^1 e^{-H_0 t\lambda_1}\,(Vt)\,e^{-H_0 t(\lambda_2-\lambda_1)}\,(Vt)\,e^{-H_0 t(1-\lambda_2)}d\lambda_1 d\lambda_2 \\ &\quad + \dots \end{aligned}$$

$$\begin{aligned} &e^{-(H_0'+H_1'+H_2')t'} \\ &\quad = e^{-H_0' t'} - \textstyle\int_0^1 e^{-H_0' t'\lambda}\,(H_1' t')\,e^{-H_0' t'(1-\lambda)}d\lambda \\ &\quad + \textstyle\int_0^1\int_{\lambda_1}^1 e^{-H_0' t'\lambda_1}\,(H_1' t')\,e^{-H_0' t'(\lambda_2-\lambda_1)}\,(H_1' t')\,e^{-H_0' t'(1-\lambda_2)}d\lambda_1 d\lambda_2 \\ &\quad - \textstyle\int_0^1 e^{-H_0' t'\lambda}\,(H_2' t')\,e^{-H_0' t'(1-\lambda)}d\lambda + \dots \end{aligned}$$

We plug these expansions in (4.17) and solve the equation order by order in the $t \to \infty$ limit.

- Order zero

  Collecting the terms of zeroth order gives

  $$\begin{aligned} \langle\eta'|\,\mathcal{R}\,(F)\,e^{-H_0' t'}\,|\eta\rangle\,\langle\eta\,|\mathcal{R}(P_0)\rangle &= Tr_\tau\,\langle\eta',0|\,F e^{-H_0 t}\,|\eta,\tau\rangle\,\langle\eta,\tau\,|P_0\rangle \\ &= Tr_\tau e^{-E(\eta,\tau)t}\,\langle\eta',0|\,F\,|\eta,\tau\rangle\,\langle\eta,\tau\,|P_0\rangle\,. \end{aligned}$$

  Since we are interested in the long time limit, (4.16) implies that in the trace only the term $\tau = 0$ is relevant, and we obtain

  $$\langle\eta'|\,\mathcal{R}\,(F)\,e^{-H_0' t'}\,|\eta\rangle\,\langle\eta\,|\mathcal{R}(P_0)\rangle = \langle\eta',0|\,F\,|\eta,0\rangle\,\langle\eta,0\,|P_0\rangle\,.$$

  To zeroth order the solution is

  $$H_0' = 0 \tag{4.20}$$

  $$\langle\eta\,|\mathcal{R}(P_0)\rangle = \langle\eta,0\,|P_0\rangle \tag{4.21}$$

  $$\langle\eta'|\,\mathcal{R}\,(F)\,|\eta\rangle = \langle\eta',0|\,F\,|\eta,0\rangle\,. \tag{4.22}$$

- First order

  Using $H_0' = 0$ and inserting the identity operator $\sum_{\eta''}|\eta''\rangle\langle\eta''|$ in the renormalised system and $\sum_{\eta'',\tau''}|\eta'',\tau''\rangle\langle\eta'',\tau''|$ in the original system, the first order terms give

  $$\begin{aligned} &\textstyle\sum_{\eta''}\langle\eta'|\,\mathcal{R}\,(F)\,|\eta''\rangle\,\langle\eta''|\,H_1' t'\,|\eta\rangle\,\langle\eta\,|\mathcal{R}\,(P_0)\rangle \\ &\quad = Tr_\tau \textstyle\sum_{\eta'',\tau''}\Big\{\langle\eta',0|\,F\,|\eta'',\tau''\rangle \\ &\qquad \Big[\textstyle\int_0^1 e^{-E(\eta'',\tau'')t\lambda}\,\langle\eta'',\tau''|\,Vt\,|\eta,\tau\rangle\,e^{-E(\eta,\tau)t(1-\lambda)}d\lambda\Big]\;\langle\eta,\tau\,|P_0\rangle\Big\}. \end{aligned}$$

In the limit $t \to \infty$, (4.16) implies that the integral is only non-zero for $\tau = \tau'' = 0$. Hence we obtain

$$\sum_{\eta''} \langle \eta' | \mathcal{R}(F) | \eta'' \rangle \langle \eta'' | H_1' t' | \eta \rangle \langle \eta | \mathcal{R}(P_0) \rangle$$
$$= \sum_{\eta''} \langle \eta', 0 | F | \eta'', 0 \rangle \langle \eta'', 0 | Vt | \eta, 0 \rangle \langle \eta, 0 | P_0 \rangle .$$

and

$$\langle \eta'' | H_1' t' | \eta \rangle = \langle \eta'', 0 | Vt | \eta, 0 \rangle \tag{4.23}$$

Up to first order in the long time limit, the initial state $|P_0\rangle$, an observable F and the Hamiltonian H transform according to:

$$\langle \eta | \mathcal{R}(P_0) \rangle = \langle \eta, 0 | P_0 \rangle$$
$$\langle \eta' | \mathcal{R}(F) | \eta \rangle = \langle \eta', 0 | F | \eta, 0 \rangle$$
$$\langle \eta' | \mathcal{R}(H) t' | \eta \rangle = \langle \eta', 0 | Vt | \eta, 0 \rangle .$$

These three relations are exactly the same as those defined by the SRG in (4.8) and (4.9), proving the statement that the SRG is a first order expansion of a more general ground state RG theory.

- Second order

  An analogous calculation can be made for the second order terms, leading to

  $$\langle \eta' | H_2' t' | \eta \rangle = \sum_{\eta'', \tau'' \neq 0} \frac{\langle \eta', 0 | Vt | \eta'', \tau'' \rangle \langle \eta'', \tau'' | Vt | \eta, 0 \rangle}{-tE(\eta'', \tau'')}.$$

  When a local operator is renormalised, the first order contribution is always a two-site operator, and as we can see now, the second order correction can contain three-site interactions.

To conclude this subsection we can state that we have constructed the SRG as a renormalisation group that keeps expectation values in the ground state approximatively invariant. A stochastic Hamiltonian with two-site interactions on a two-state lattice of length L is mapped on a new system with a lattice of length L/b that is again two-stated and with again a stochastic two-site Hamiltonian. A generalisation to an n-state lattice is trivial, as long as the number of ground states in a cell is equal to n. More involved is a possible generalisation to Hamiltonians with n-site interactions. If n is bigger than 2, higher orders need to be calculated in the expansion explained above, but this exceeds the framework of the simple SRG.

Remark 4 When applying the SRG one always has some freedom of choice in the regrouping of the Hamiltonian into the intracell $H_{0,\alpha}$ and the intercell part V_α. And also after the calculation of the ground states $\left|\psi_{0_1}\right\rangle_\alpha$ and $\left|\psi_{0_2}\right\rangle_\alpha$ of $H_{0,\alpha}$ the matter of which linear combination to associate with the cell particle $|A,0\rangle_\alpha$ and which with the cell vacancy $|\phi,0\rangle_\alpha$ is not uniquely defined. In these decisions symmetry arguments can sometimes be helpful, but it remains a question that has to be sorted out for each model again. Finally it is clear from the perturbation formulation that in general the SRG will not produce exact results, but since the intercell Hamiltonian can be seen as a perturbation term, one expects the procedure to become more accurate for increasing b.

4.1.3 SRG and Critical Behaviour

We introduced the SRG for the study of stationary critical behaviour of stochastic systems. To see how an RG procedure can describe critical phenomena, we start by collecting the rates of the model in a vector $\vec{K} = (K_1, \ldots, K_k)$, which represents uniquely our model. As an example one could think of the contact process in which case this vector would be just a number, the contamination rate. Next, all interactions that can be created by RG mappings are also included in $\vec{K}$. In other words, we take the dimension of the vector space big enough to ensure that under repeated application of the RG, the system can still be represented by a vector $\vec{K}$ in our space. If some of these interactions are not present in the original model, the corresponding components of $\vec{K}$ are just set to zero. We can now write the SRG mapping in the k-dimensional parameter space:

$$\vec{K} \to \mathcal{R}\left(\vec{K}\right).$$

Each vector $\vec{K}$ is a model that by RG is mapped on another one. When this transformation is iterated, the successive vectors form a flow, as e.g. the one sketched in Fig. 4.2. In principle this flow can contain cycles, but in practice on usually finds trajectories becoming attracted to fixed points. The analysis start be finding these fixed points of the RG flow. Depending one the correlation length of the corresponding system, one distinguishes two kinds of fixed points. Since the correlation length ξ of a system is invariant under SRG (in lattice units this means $\xi \to \xi/b$), we obtain that ξ must be either zero or infinite. In the former case the corresponding fixed point $\vec{K}_t$ is called trivial, while in the latter case we have a critical fixed point $\vec{K}_c$. Since the RG flow is assumed to be analytical, all systems that flow to the same fixed point have the same macroscopic properties: they belong to the same phase. This has two important consequences. First, the subspace that flows into a critical point

(critical surface), serves as a separatrix that divides the parameter space into phases with the same macroscopic physics (cf Fig. 4.2). Secondly, all vectors (read all systems) that are attracted to the same critical point by the RG flow, have the same critical behaviour. This latter point, is the explanation for the existence of universality classes. To determine the critical exponents of a class, we have to study the RG flow around the corresponding critical fixed point

$$\mathcal{R}\left(\vec{K}_c\right) = \vec{K}_c. \tag{4.24}$$

The analysis starts by the linearisation of $\mathcal{R}\left(\vec{K}\right)$ in $\vec{K}_c$. We assume the RG flow to be differentiable in the fixed point and write

$$\mathcal{R}\left(\vec{K}_c + \delta\vec{K}\right) = \vec{K}_c + A\delta\vec{K}$$

with $\delta\vec{K}$ a small deviation and A a linear operator: the first derivative of $\mathcal{R}$. Next we diagonalise A, and denote the eigenvectors as $\vec{v}_i$ and the corresponding eigenvalues, which are in practice always real, as λ_i. It is convenient to write $\lambda_i = b^{y_i}$ with b the rescaling factor (cell size of the SRG). y_i is (for an exact RG) independent of b, while λ_i is not. Next, these eigenvectors are used as a basis in which we expand the deviation vector $\delta\vec{K}$

$$\delta\vec{K} = \sum_{i=1}^{k} \Delta_i \vec{v}_i.$$

And we can finally write the RG flow in the form we need:

$$\mathcal{R}\left(\Delta_1, \Delta_2, \ldots, \Delta_k\right) = \left(b^{y_1}\Delta_1, b^{y_2}\Delta_2, \ldots, b^{y_k}\Delta_k\right). \tag{4.25}$$

The quantities Δ_i which transform in this linear way are called *the scaling variables* and the corresponding y_i the *RG eigenvalues*. According to the value of y_i one differentiates three groups of scaling variables:

- $\underline{y_i < 0}$

  When the system is close to the critical point, this scaling variable Δ_i decreases to zero under the RG flow. Δ_i is in this respect not a measure for the distance away from the critical point, and the critical behaviour is not influenced by the values of negative y_i. These Δ_i are called *irrelevant scaling variables.*

- $\underline{y_i > 0}$

  The RG flow drives these variables away from the critical point, the corresponding y_i determine the critical exponents and the Δ_i are called the *relevant scaling variables.*

- $y_i = 0$
  A scaling variable with zero RG eigenvalue is called *marginal*. In the linear approximation it is not clear whether Δ_i will increase or decrease under RG transformations.

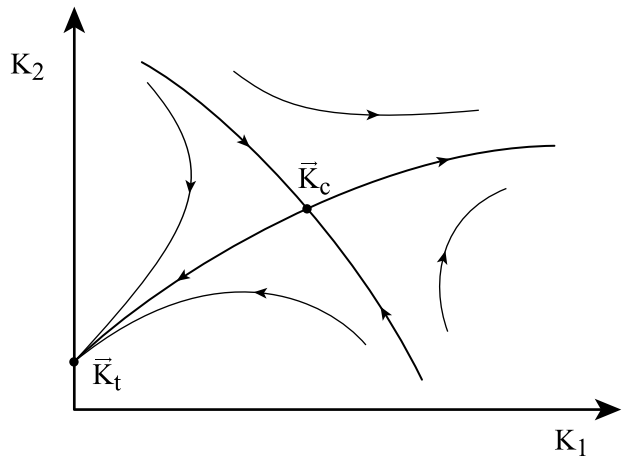

Figure 4.2: *Typical RG flow in a two dimensional parameter space. The critical point has one relevant and one irrelevant scaling variable.*

Let us consider the case of a critical point with one relevant scaling variable, cf Fig. 4.2, to explain how the SRG provides us a way the calculate critical parameters of a system. Since the SRG is a ground state RG, we will only talk about stationary behaviour and we will assume the system to be infinitely large. Under these conditions the phase diagram and the position of the critical point can directly be derived from the SRG flow. Denote the relevant scaling variable by Δ and the corresponding RG eigenvalue as y. In subsection 3.2.2 we saw that the rescaling of the parameter Δ, measuring the distance away from the critical point, determines the exponent $\nu_\perp$, which describes the divergence of the correlation length. This provides us the first critical exponent, which can be calculated by taking the derivative of the SRG flow in the critical point. Close to the critical point we have

$$\begin{aligned} \mathcal{R}(\Delta) &= \frac{\partial \mathcal{R}}{\partial \Delta}|_{\Delta=0}\, \Delta \\ &= b^y \Delta \end{aligned}$$

and

$$\nu_\perp = \frac{1}{y} = \frac{\ln b}{\ln\left(\frac{\partial \mathcal{R}}{\partial \Delta}|_{\Delta=0}\right)} \tag{4.26}$$

To get access to the exponent β, we study the stationary particle density. Denote a stationary state of the system as $\left|P^*(\vec{K})\right\rangle$. The particle density in the stationary state of a translational invariant system can be written as

$$\rho^*(\vec{K}) = \langle s| E_i^{11} \left|P^*(\vec{K})\right\rangle .$$

The SRG gives us $\langle s| E_i^{11} \left|P^*(\vec{K})\right\rangle = \langle s| T_2 T_1 E_i^{11} T_2 T_1 \left|P^*(\vec{K})\right\rangle$. We assume that the renormalisation of E_i^{11} is proportional to E^{11}, i.e. $T_1 E_i^{11} T_2 = a(\vec{K}) E_\alpha^{11}$. We then obtain[4]

$$\rho^*(\vec{K}) = a(\vec{K}) \rho^*(\mathcal{R}(\vec{K})). \tag{4.27}$$

The relation (4.27) can be iterated along the SRG flow, and hence the particle density can be obtained as an infinite product if one knows the density at the (trivial) fixed point $\vec{K}_t$ that attracts $\vec{K}$,

$$\rho^*\left(\vec{K}\right) = \left[\prod_{k=0}^{\infty} a\left(\mathcal{R}^k\left(\vec{K}\right)\right)\right] \rho^*\left(\vec{K}_t\right) \tag{4.28}$$

In principle other expectation values can be calculated in a similar way. Since we now know how ρ^* behaves we can determine the exponent β by looking at the particle density in the neighbourhood of the critical point. For the critical behaviour the distance away from $\vec{K}_c$ is measured by the relevant scaling variable Δ and we can write near the critical point $\vec{K}_c$

$$\rho^*(\Delta) = a\left(\vec{K}_c\right) \rho^*(b^{1/\nu_\perp}\Delta). \tag{4.29}$$

This is exactly the generalised homogeneous function postulated by Widom (3.44) and we obtain finally

$$a\left(\vec{K}_c\right) = b^{-\beta/\nu_\perp} \tag{4.30}$$

or

$$\frac{\beta}{\nu_\perp} = -\frac{\ln\left(a\left(\vec{K}_c\right)\right)}{\ln b}. \tag{4.31}$$

This exponent $\beta/\nu_\perp$ can be related to the fractal dimension of the occupied sites in the stationary state of the critical system. If a d-dimensional space

[4] To be precise, we should mention that the value of $a(\vec{K})$ can depend on i by the position of i in the cell of the SRG. A more correct way of renormalising ρ^* in a translational invariant system and with cell size b is then given by $\rho^*(\vec{K}) = \lim_{L\to\infty} \frac{1}{L}\sum_{i=1}^{L} \langle s| E_i^{11} |P^*\rangle = \lim_{L\to\infty} \frac{\sum_{i=1}^{L} a_i}{L} \rho^*(\mathcal{R}(\vec{K})) = \frac{\sum_{i=1}^{b} a_i}{b} \rho^*(\mathcal{R}(\vec{K}))$.

that contains a fractal structure is uniformly rescaled by a factor b, the volume of the space is rescaled with a factor b^d and that of the fractal with b^D. D is the dimension of the fractal, and its density rescales consequently as b^D/b^d. For the particle density in stationary state of the critical system we obtain

$$\frac{\rho^*}{\mathcal{R}(\rho^*)} = b^{D-d} = b^{-\beta/\nu_\perp}$$

and the fractal dimension of the occupied sites is

$$D = d - \frac{\beta}{\nu_\perp}. \tag{4.32}$$

4.2 An Exactly Solvable Example

4.2.1 Diffusion, Coagulation, Decoagulation

To test the concepts of the SRG, we first use it to study a model that can be solved exactly. Consider the following reaction-diffusion system.

$$\begin{array}{lcll} \phi A & \longleftrightarrow & A\phi & \text{with rate } 1 \quad : \text{Diffusion} \\ AA & \longrightarrow & \begin{array}{l}\phi A \\ A\phi\end{array} & \text{with rate } c \quad : \text{Coagulation} \\ \begin{array}{l}\phi A \\ A\phi\end{array} & \longrightarrow & AA & \text{with rate } d \quad : \text{Decoagulation} \end{array} \tag{4.33}$$

The evolution operator of a stochastic system can be written as e^{-Ht}, and one notices that a multiplication of the Hamiltonian H by a constant is merely a rescaling of time. Such a rescaling does not affect the true physics of a system. Moreover, for the stationary behaviour it does not matter at all. It is therefore always possible to take one reaction rate equal to one by multiplying H with the inverse of that rate. We took the diffusion rate equal to one, hereby reducing the dimension of the parameter space to two.

It is immediately clear that this system has an absorbing state given by the empty lattice. Since competition is present between a particle creation and destruction process, one has the possibility of an active stationary state for which the particle density is non-zero. Unlike for the contact process, this active state can be calculated exactly. Denote the Hamiltonian as $H = \sum_i h_i$ with the local Hamiltonian given by

$$\begin{aligned} h_i \;=\; & -\left(E_i^{01}E_{i+1}^{10} + E_i^{10}E_{i+1}^{01}\right) + \left(E_i^{11}E_{i+1}^{00} + E_i^{00}E_{i+1}^{11}\right) \\ & -c\left(E_i^{01}E_{i+1}^{11} + E_i^{11}E_{i+1}^{01}\right) + 2c\left(E_i^{11}E_{i+1}^{11}\right) \\ & -d\left(E_i^{10}E_{i+1}^{11} + E_i^{10}E_{i+1}^{11}\right) + d\left(E_i^{00}E_{i+1}^{11} + E_i^{11}E_{i+1}^{00}\right). \end{aligned} \tag{4.34}$$

When the coagulation rate c equals one, this operator can be mapped on that of a free fermion system by using a well chosen basis transformation [53]. In this case one can solve the time evolution of any observable. However, since we are only interested in the stationary states, a simpler approach will suffice. In subsection 2.2.3 we introduced the product measure (2.25). We will use that now as an ansatz to find the ground states. It is convenient to first write the local Hamiltonian in an explicit matrix form. If we number the configurations of a 2-site system as

$$|1\rangle = |\phi\phi\rangle\,, \quad |2\rangle = |\phi A\rangle\,, \quad |3\rangle = |A\phi\rangle\,, \quad |4\rangle = |AA\rangle \tag{4.35}$$

we can write

$$h_i = \begin{pmatrix} 0 & 0 & 0 & 0 \\ 0 & 1+d & -1 & -c \\ 0 & -1 & 1+d & -c \\ 0 & -d & -d & 2c \end{pmatrix} \text{ and } \tbinom{1-\rho}{\rho} \bigotimes \tbinom{1-\rho}{\rho} = \begin{pmatrix} (1-\rho)^2 \\ \rho\,(1-\rho) \\ \rho\,(1-\rho) \\ \rho^2 \end{pmatrix}. \tag{4.36}$$

The vector $\bigotimes_i \binom{1-\rho}{\rho}$ is a ground state of H if

$$\begin{gathered} h_i \tbinom{1-\rho}{\rho} \bigotimes \tbinom{1-\rho}{\rho} = 0 \\ \Updownarrow \\ d(1-\rho)\rho = c\rho^2 \end{gathered}$$

and we obtain two solutions for the stationary particle density

$$\rho^* = 0 \text{ and } \quad \rho^* = \frac{d/c}{1+d/c}. \tag{4.37}$$

The second one is plotted in Fig. 4.3. The active solution is valid for any value of the rates and is different from the absorbing state except when the decoagulation rate is zero. In other words, the system is always active, and we do not have a real phase transition. The point $d = 0$, which could be named a transition point is not critical: the state is a product measure and has consequently zero correlation length. We can however associate an exponent β (3.26) with the density profile. From equation (4.37) we obtain $\beta = 1$.

The reason why we take this system as a first test-case for the SRG is two-fold. First it has a phase transition (although trivial) that can be calculated exactly. Secondly, the ground states are product measures and we can expect the SRG to reproduce the exact solution since any ground state of the system of length $2L$ can be expressed exactly in the ground states of the system of length L.

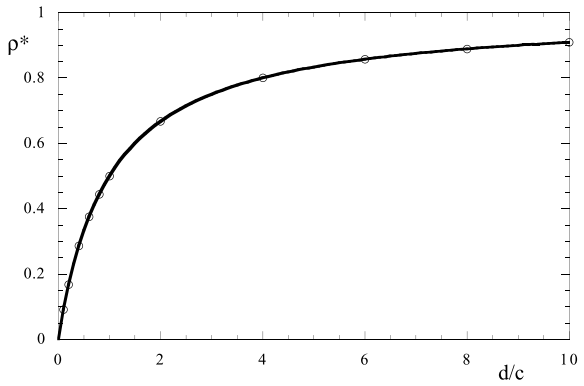

Figure 4.3: *The active stationary particle density as a function of the ratio of the decoagulation over the coagulation rate. The full curve represents the exact result, the circles are numerically evaluated points of the SRG.*

4.2.2 Application of SRG

We will perform the SRG with a cell size $b = 2$ and we group the lattice in a way that site i and $i+1$ are in cell α. Next we define the intracell Hamiltonian as $H_{0,\alpha} = h_i$ and the intercell as $V_\alpha = h_{i+1}$. In this case $H_{0,\alpha}$ has a doubly degenerated ground state, as it should be, and we choose the cell states as

$$\begin{aligned} |\phi,0\rangle_\alpha &= |\phi\phi\rangle \\ |A,0\rangle_\alpha &= \tfrac{1}{2+d/c}\left[|\phi A\rangle + |A\phi\rangle + \tfrac{d}{c}\,|AA\rangle\right] \\ {}_\alpha\langle\phi,0| &= {}_\alpha\langle\phi\phi| \\ {}_\alpha\langle A,0| &= {}_\alpha\langle\phi A| + {}_\alpha\langle A\phi| + {}_\alpha\langle AA| \end{aligned} \tag{4.38}$$

It is easy to check that they are indeed right and left ground states of H_i (4.36). We are now ready to perform the SRG projection (4.9) of the Hamiltonian, for which it suffices to project $V_\alpha = h_{i+1}$ on the space spanned by the four vectors $|\eta,0\rangle_\alpha \bigotimes |\eta,0\rangle_{\alpha+1}$. This can on its turn be reduced to the projection of the operators E^{ab}_{i+1} and E^{ab}_{i+2} on respectively the vectors $|\eta,0\rangle_\alpha$ and $|\eta,0\rangle_{\alpha+1}$. Since the $|\eta,0\rangle_\alpha$ have left right symmetry the following relations are all we

need to perform the SRG

$$T_1 E^{11}_{i+1} T_2 = \left(\frac{1+d/c}{2+d/c}\right) E^{11}_\alpha \tag{4.39}$$

$$T_1 E^{00}_{i+1} T_2 = E^{00}_\alpha + \left(\frac{1}{2+d/c}\right) E^{11}_\alpha \tag{4.40}$$

$$T_1 E^{01}_{i+1} T_2 = \left(\frac{1}{2+d/c}\right) E^{01}_\alpha + \left(\frac{d/c}{2+d/c}\right) E^{11}_\alpha \tag{4.41}$$

$$T_1 E^{10}_{i+1} T_2 = E^{10}_\alpha + \left(\frac{1}{2+d/c}\right) E^{11}_\alpha \tag{4.42}$$

If we use these renormalised operators to construct $\mathcal{R}(H)$ we find that there is no proliferation of interactions, the system contains again the reactions (4.33) and no other. The renormalised diffusion rate is however given by $\frac{1}{2+d/c}$. We therefore divide the renormalised Hamiltonian by this factor (merely a rescaling of time) and can then synthesise the SRG by the resulting transformations

$$\mathcal{R}(d) = d\frac{1+c+d}{c} \tag{4.43}$$

$$\mathcal{R}(c) = c\frac{1+c+d}{2c+d}. \tag{4.44}$$

The flow generated by these equations is shown in Fig. 4.4. There is a trivial

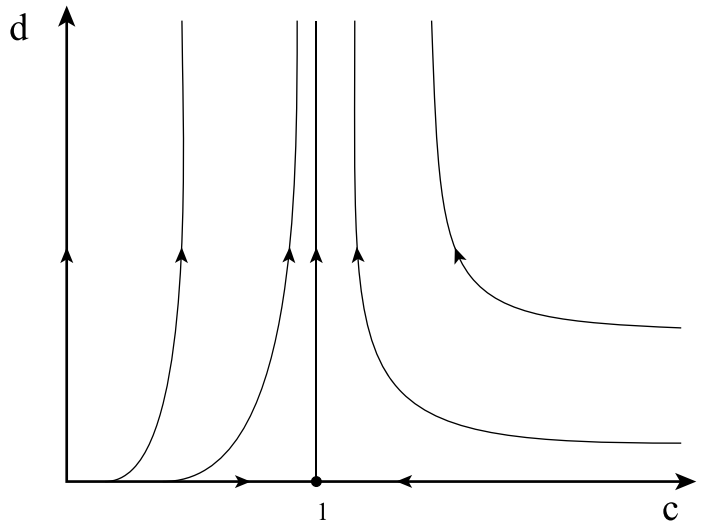

Figure 4.4: *Schematic RG flow in the* (c, d)*-plane.*

fixed point in $(c, d) = (1, 0)$ and the line $c = 1$ is an invariant line. The line $d = 0$ is attracted by the fixed point an would in the case of a real phase transition separate the parameter space into two phases. In this case however, the whole space $d > 0$ is attracted to the region of infinite decoagulation rate, indicating that the system is always active. The RG equations, linearised at the fixed point, have d as the relevant scaling variable with RG eigenvalue $y = 1$, while $(c-1)$ is irrelevant. Since the system is not critical, the interpretation of y as one over the exponent defining the divergence of the correlation length (3.41) is not meaningful. In the derivation of this divergence we used $\xi(\Delta) = b\xi(b^{y_\Delta}\Delta)$ (3.40) to arrive at $\xi(\Delta) = \Delta^{-1/y_\Delta}\xi(1)$ (where Δ is the relevant scaling variable). This indeed implies a divergence, except of course when $\xi(1) = 0$. In this model any ground state is a product measure, and we find $\xi(1) = 0$: no divergence.

Next we turn to the calculation of the particle density as described by (5.19). The renormalisation prefactor of E^{11}, calculated in (4.39), only depends on d and c through the ratio d/c. Since (4.43) and (4.44) imply that also the rescaling of d/c depends only on d/c itself:

$$\mathcal{R}\left(\frac{d}{c}\right) = \frac{d}{c}(2 + \frac{d}{c}), \tag{4.45}$$

we obtain

$$\rho^*\left(\frac{d}{c}\right) = \frac{1 + \frac{d}{c}}{2 + \frac{d}{c}}\rho^*\left(\mathcal{R}\left(\frac{d}{c}\right)\right). \tag{4.46}$$

ρ^* is thus a function of d/c, which is consistent with the exact solution. The precise value of ρ^* can now be calculated by iterating this relation along the RG flow. In Fig. 4.4 we see that for every $d > 0$ the flow ends up in $d/c = \infty$. In that limit $\rho^* = 1$, hence formula (4.46) becomes finally

$$\rho^*\left(\frac{d}{c}\right) = \lim_{n\to\infty}\left[\prod_{k=0}^{n} a\left(\mathcal{R}^k\left(\vec{K}\right)\right)\right]. \tag{4.47}$$

One can show analytically [49] that (4.47) converges to the exact result (4.37) as we expected for a system with product measures as ground states. When performing this calculation numerically, one finds the product converging very quickly to the limiting value. In Fig. 4.3 the circles are the densities calculated with 5 iteration steps. Further we use the SRG to calculate the exponent β characterising the particle-density profile near $d = 0$. From (4.46) we obtain that the prefactor of the density in the fixed point is $1/2$, which should be equal to $b^{-\beta\cdot y}$. Since $b = 2$ and $y = 1$ we recover the exact result $\beta = 1$.

Finally we mention a remarkable observation. In the RG flow of Fig. 4.4 we find an invariant line $c = 1$. This coincides exactly with the subspace

where the systems dynamics can be solved by a mapping on free fermions [53]. We observed the same when we renormalised the diffusion annihilation model. The SRG flow had a invariant point for *annihilation rate/diffusion rate* equal to two. Again the system can only be solved completely in this point of the parameter space. We have at the moment no explanation for this phenomenon.

In conclusion we can say that the concept of the SRG works well for this problem with trivial ground states. It indeed nicely maps a stochastic system on a new one, producing an analytical RG flow. The flow gives a correct phase diagram and the linearisation of it in the fixed point produces the correct exponent. The main question is now of course whether the SRG can do the same approximatively for non-trivial models. In the next chapter we will show that for the contact process, it certainly can.

Chapter 5

SRG and Contact Process

In the first section of this chapter the SRG is applied to the contact process. First the absence of proliferation of interactions is proven and a general form for the RG flow is derived. Next the results of explicit calculations for different cell sizes b are presented and the critical parameters are approximated by an extrapolation $b \to \infty$. The outcome of these calculations can be found in reference [54]. In the second section the SRG is applied to a generalised version of the contact process, which has two equivalent absorbing states. This model was introduced in 1997 [55] and belongs to a different universality class. The chapter concludes with a short evaluation of the SRG method.

5.1 Contact Process

5.1.1 Regrouping of Local Hamiltonians

The one-dimensional contact process with contamination rate λ was defined in Chapter 3, the dynamics are given by the reactions

$$\begin{array}{lcll} \phi A \\ A\phi & \to & AA & \text{decoagulation with rate } \frac{\lambda}{2} \\ A & \to & \phi & \text{death with rate 1.} \end{array} \tag{5.1}$$

The Hamiltonian of this process can be written as

$$H = \sum_i h_i^1 + h_i^2 \tag{5.2}$$

with

$$h_i^1 = -E_i^{01} + E_i^{11} \tag{5.3}$$

$$h_i^2 = -\frac{\lambda}{2}E_i^{11}E_{i+1}^{10} + \frac{\lambda}{2}E_i^{11}E_{i+1}^{00} - \frac{\lambda}{2}E_i^{10}E_{i+1}^{11} + \frac{\lambda}{2}E_i^{00}E_{i+1}^{11}, \tag{5.4}$$

which are respectively the Hamiltonians for the death process on site i and decoagulation on sites $i, i+1$.

We start the SRG by dividing the lattice in cells of length b, labelled by α. Next we have to decide how to group the local operators of H in the

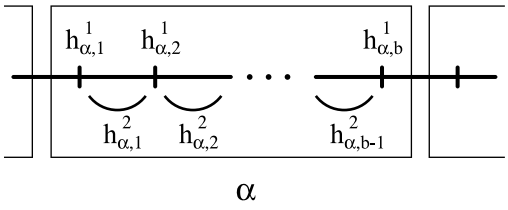

Figure 5.1: *Cell and site numbering of the SRG.*

intra- and intercell Hamiltonian $H_{0,\alpha}$ and V_α. A natural attempt is to take into $H_{0,\alpha}$ all the terms that act only on sites inside cell α, hence $H_{0,\alpha} = \sum_{i=1}^{b} h_{\alpha,i}^1 + \sum_{i=1}^{b-1} h_{\alpha,i}^2$ (here the first subindex labels the cell, while the second indicates the site in the cell, see Fig. 5.1). This choice is however not suitable for the application of the SRG. Defined in this way, $H_{0,\alpha}$ is the Hamiltonian of the contact process on a (finite) lattice of b sites with open boundary conditions and it only has the empty lattice as a ground state. In subsection 4.1.1 we showed that for conservation of probability the intracell Hamiltonian needs two ground states, one representing the effective cell vacancy and the other the effective cell particle. It is the second one that is missing. To solve this problem we force $H_{0,\alpha}$ to have an active state by removing $h_{\alpha,i}^1$ on the central site of the cell.

From now on we choose the cell size b odd, $b = 2n-1$, and take

$$H_{0,\alpha} = \sum_{i=1}^{n-1} h_{\alpha,i}^1 + \sum_{i=n+1}^{b} h_{\alpha,i}^1 + \sum_{i=1}^{b-1} h_{\alpha,i}^2 \tag{5.5}$$

$$V_\alpha = h_{\alpha,n}^1 + h_{\alpha,b}^2 \tag{5.6}$$

as visualised in Fig. 5.2.

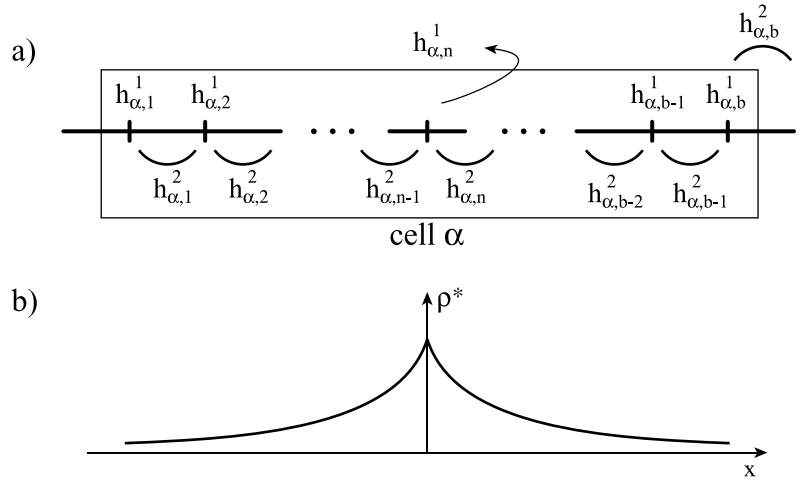

Figure 5.2: *a) gives the regrouping of the Hamiltonian into an intracell part (terms inside the rectangle), and an intercell part (terms outside the rectangle). The removal of $h^1_{\alpha,n}$ forces the intracell Hamiltonian to have an active ground state with a particle-density profile sketched in b).*

The next step is to calculate the two right and left ground states of $H_{0,\alpha}$. Since the SRG for the contact process will be an approximation, it has to be performed for cell sizes b as large as possible. The determination of these ground states will become the most time consuming part of the procedure. Analytically this calculation is limited to cell sizes of just a few sites. To make a reliable extrapolation $b \to \infty$ possible, we need a good numerical algorithm to get to larger b. We will return to this issue later. If these ground states are available, we can calculate the renormalised Hamiltonian $\mathcal{R}(H)$. For small cell sizes, this can be done by hand and one can show that $\mathcal{R}(H)$ contains the same reactions as H, there is no proliferation of interactions. This is certainly not trivial and it would be interesting if this "conservation of form" could be derived rigorously for any cell size b. In the next section we make some analytical considerations that will lead to this result and that will also simplify the numerical calculations.

5.1.2 Conservation of Form

In the ground state calculation of $H_{0,\alpha}$ some simplifications can be carried through. Let us start with the right ground states. The first one is trivial $|\phi,0\rangle_\alpha = \bigotimes_{i=1}^b \binom{1}{0} = \bigotimes_{i=1}^b |\phi\rangle_{\alpha,i}$: the empty lattice. The get some insight in

the active ground state $|A,0\rangle_\alpha$, we rewrite (5.5). The absence of $h^1_{\alpha,n}$ makes it possible to split $H_{0,\alpha}$ into two parts which can be mapped on each other by left-right reflection:

$$H_{0,\alpha} = H^l_\alpha + H^r_\alpha, \tag{5.7}$$

where

$$H^r_\alpha = \sum_{i=1}^{n-1} h^1_{\alpha,i} + \sum_{i=1}^{n-1} h^2_{\alpha,i}, \tag{5.8}$$

$$H^l_\alpha = \sum_{i=n+1}^{b} h^1_{\alpha,i} + \sum_{i=n}^{b-1} h^2_{\alpha,i}. \tag{5.9}$$

Physically H^r_α (H^l_α) is the Hamiltonian of the contact process on a lattice of n sites without the death process $A \to \phi$ on the right (left) site. Besides the empty lattice as the trivial right ground state, these operators have a non-trivial, *active* right ground state. To get a better grasp on the latter one, we first notice that H^r_α has no reaction that destroys a possibly present particle A at site (α, n), i.e. there are no transitions possible from configurations with a particle at site (α, n) to configurations without a particle on that site. Denote the subspace spanned by the former configurations by $\mathcal{V}$. Then, H^r_α defines a stochastic process on $\mathcal{V}$, implying that H^r_α must have a ground state in this subspace. This state clearly cannot be the empty lattice since this is not an element of $\mathcal{V}$. We therefore conclude that this state is the active ground state of H^r_α and that it has with probability one a particle on site (α, n). The same reasoning can be made for H^l_α and the active ground state can be written as

$$\begin{aligned} &|\psi\rangle^r_\alpha \otimes |A\rangle_{\alpha,n} && \text{for } H^r_\alpha \\ &|A\rangle_{\alpha,n} \otimes |\psi\rangle^l_\alpha && \text{for } H^l_\alpha. \end{aligned}$$

$|\psi\rangle^r_\alpha$ and $|\psi\rangle^l_\alpha$ are states on a lattice of $n-1$ sites and can be mapped on each other by reflection. Using equation (5.7) we immediately obtain that $|\psi\rangle^r_\alpha \otimes |A\rangle_{\alpha,n} \otimes |\psi\rangle^l_\alpha$ is the active ground state of $H_{0,\alpha}$. This is the state drawn in Fig. 5.2 b). In conclusion we now have

$$|\phi,0\rangle_\alpha = \bigotimes_{i=1}^{b} |\phi\rangle_{\alpha,i} \tag{5.10}$$

$$|A,0\rangle_\alpha = |\psi\rangle^r_\alpha \otimes |A\rangle_{\alpha,n} \otimes |\psi\rangle^l_\alpha . \tag{5.11}$$

To determine the active ground state of the "contact process" defined by $H_{0,\alpha}$ on a lattice of $2n-1$ sites, we only need to find the active ground state of the process defined by H^r_α on a lattice of n sites.

The left ground states of $H_{0,\alpha}$ are found by use of the self-enantiodromy. In (3.13) we showed that the local operators h^1 and h^2 are self-enantiodromic, implying that $BH_{0,\alpha}B^{-1} = (H_{0,\alpha})^T$ with B an invertible operator defined in (3.15). Consequently, $(B\,|\phi,0\rangle_\alpha)^T$ and $(B\,|A,0\rangle_\alpha)^T$ are left ground states of the intracell Hamiltonian. They can be written as

$$\begin{aligned}(B\,|\phi,0\rangle_\alpha)^T &= {}_\alpha\langle s| \\ (B\,|A,0\rangle_\alpha)^T &= {}^r_\alpha\langle\zeta| \otimes {}_{\alpha,n}\langle\phi| \otimes {}^l_\alpha\langle\zeta|\,.\end{aligned}$$

The former one is nothing but the trivial left ground state ${}_\alpha\langle s|$ (the normalisation vector), in the latter one we wrote ${}^{r,l}_\alpha\langle\zeta| = \left(B\,|\psi\rangle^{r,l}_\alpha\right)^T$. Since state $|A,0\rangle_\alpha$ is orthogonal on $(B\,|A,0\rangle_\alpha)^T$, the orthonormality relations $\langle\eta,0\,|\eta',0\rangle = \delta_{\eta,\eta'}$ are satisfied by choosing

$$\begin{aligned}{}_\alpha\langle\phi,0| &= {}^r_\alpha\langle\zeta| \otimes {}_{\alpha,n}\langle\phi| \otimes {}^l_\alpha\langle\zeta| &(5.12)\\ {}_\alpha\langle A,0| &= {}_\alpha\langle s| - {}_\alpha\langle\phi,0| &(5.13)\end{aligned}$$

for the left ground states of $H_{0,\alpha}$.

To conclude the analytical aspect of the RG we have to perform the projection of the intercell Hamiltonian (5.6) as defined in (4.9). (5.3) and (5.4) imply that the only projections needed are given in (5.14). Using no more than the structure of the states (5.10)-(5.13) we can say that these transformations are independent of α and are of the form:

$$\begin{aligned}E^{11}_{\alpha,b}, E^{11}_{\alpha,1} &\overset{T^1\ldots T^2}{\longrightarrow} vE^{11}_\alpha \\ E^{00}_{\alpha,b}, E^{00}_{\alpha,1} &\overset{T^1\ldots T^2}{\longrightarrow} E^{00}_\alpha + (1-v)\,E^{11}_\alpha \\ E^{10}_{\alpha,b}, E^{10}_{\alpha,1} &\overset{T^1\ldots T^2}{\longrightarrow} vE^{10}_\alpha + (1-v)\,E^{11}_\alpha + (1-v)\,E^{00}_\alpha \\ E^{01}_{\alpha,n} &\overset{T^1\ldots T^2}{\longrightarrow} w^2E^{01}_\alpha + \left(1-w^2\right)E^{11}_\alpha \\ E^{11}_{\alpha,n} &\overset{T^1\ldots T^2}{\longrightarrow} E^{11}_{\alpha,n}\end{aligned} \qquad (5.14)$$

with

$$\begin{aligned}v &= \langle s|\,E^{11}_{\alpha,1}\,|\psi\rangle^r_\alpha &(5.15)\\ w &= {}^r_\alpha\langle\zeta|\,\psi\rangle^r_\alpha = {}^r_\alpha\langle\psi|\,B^T\big|\,\psi\rangle^r_\alpha &(5.16)\end{aligned}$$

The renormalised Hamiltonian $\mathcal{R}(H)$, following from (5.14) contains the same reactions as H. Hence we find no proliferation of interactions for any cell size

b. After dividing the $\mathcal{R}(H)$ by its death rate (again merely a rescaling of time) the renormalisation flow is given by

$$\mathcal{R}(\lambda) = \lambda \frac{v^2}{w^2}. \tag{5.17}$$

We can now generate the RG map of the contact process with cell length $b = 2n-1$ by calculating two matrix elements in the active right ground state of the contact process H^r_α on a lattice of only n sites. In this way, it is possible to perform the RG for rather large cell sizes. Moreover, for each cell size, the needed calculations are limited.

To conclude we consider the exponent β. Here some more information is needed. We have to determine the renormalisation of the particle density or the operators $E^{11}_{\alpha,i}$. In the case of the contact process this depends on the site $i = 1, \ldots, b$. Using (5.10)-(5.13) one can see that

$$\mathcal{R}\left(E^{11}_{\alpha,i}\right) = a_i E^{11}_\alpha \begin{cases} a_i = \langle s| E^{11}_{\alpha,i} |\psi\rangle^r_\alpha & \text{for } i = 1, \ldots, n-1 \\ a_i = 1 & \text{for } i = n \\ a_i = a_{2n-i} & \text{for } i = n+1, \ldots b. \end{cases} \tag{5.18}$$

Clearly these transformed operators are not all equal. Consequently, the renormalisation of ρ^* can be performed in several ways. We choose to average over all, leading to

$$\begin{aligned} \rho^*(\lambda) &= \sum_{i=1}^{b} \frac{1}{b} \langle s| E^{11}_{\alpha,i} |P^*\rangle \\ &= \frac{\sum_{i=1}^{b} a_i(\lambda)}{b} \rho^*\left(\mathcal{R}(\lambda)\right). \end{aligned}$$

The fact that for $i = n$ we find $a_i = 1$ is an artifact of the Hamiltonian grouping introduced to force an active ground state in the intracell Hamiltonian. We therefore leave it out of the summation. Finally, since $a_i = a_{2n-i}$ for $i > n$ we arrive at

$$\rho^*(\lambda) = \frac{\sum_{i=1}^{n-1} a_i(\lambda)}{n-1} \rho^*\left(\mathcal{R}(\lambda)\right). \tag{5.19}$$

Notice that again only the active right ground state of H^r_α is needed to perform the calculation.

5.1.3 Results

We applied the RG to the contact process for cell sizes $b = 2n-1 = 3, 5, \ldots 37$. For each cell size we had to calculate the non-trivial ground state of the non-symmetrical $2^n \times 2^n$ matrix H^r_α. Analytically, this was possible for $b = 3, 5, 7, 9$.

For larger cells we worked numerically and noticed that from $b \geq 5$ the critical parameters approached their limit in a monotonic way. Before we go into this let us consider the case $b = 5$ explicitly.

Using software that can perform symbolical calculations, it is fairly easy to construct the RG flow for a cell size $b = 5$. The result is given by

$$\mathcal{R}(\lambda) = \lambda \frac{\lambda^4 (2+\lambda)^2 \left(8 + 10\lambda + 4\lambda^2 + \lambda^3\right)^2}{16 \left(16 + 40\lambda + 37\lambda^2 + 18\lambda^3 + 4\lambda^4\right)^2}. \tag{5.20}$$

The function $\mathcal{R}(\lambda) - \lambda$ is plotted in Fig. 5.3. The RG equation (5.20) has

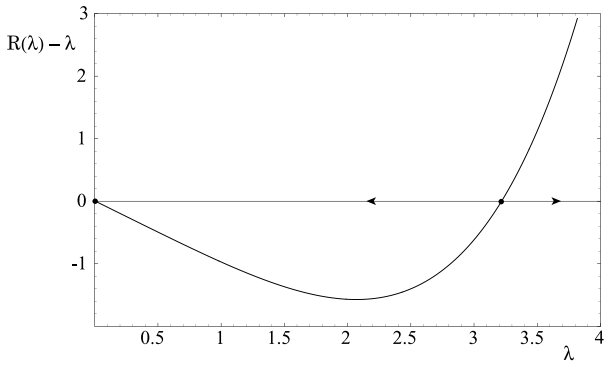

Figure 5.3: *Plot of the function $\mathcal{R}(\lambda) - \lambda$ and the resulting SRG flow for cell size $b = 5$.*

a non-trivial repulsive fixed point at $\lambda_c = 3.2231....$ Considering the very small cell size $b = 5$ this value is surprisingly close to the best known value $\lambda_c = 3.2979....$ From a linearisation of the flow around the fixed point, we get for the relevant scaling variable $(\lambda - \lambda_c)$ the RG eigenvalue $y = 0.9075...$, from which we obtain $\nu_\perp = 1.1018....$ This is a very good estimate, to be compared with $1.0972....$ Less precise is the value of $\beta/\nu_\perp$. It is known to be $\beta/\nu_\perp = 0.2521...$ while we find $\beta/\nu_\perp = 0.3473...$ after the calculation of the extra matrix elements for (5.19). Finally the particle density can be approximated by iterating (5.19). Since the fixed point $\lambda_c = 3.2231...$ is repulsive, we get for $\lambda < \lambda_c$ that $\lim_{k\to\infty} \rho^* \left(\mathcal{R}^k(\lambda)\right) = \rho^*(0) = 0$ and hence $\rho^*(\lambda) = 0$. For $\lambda > \lambda_c$ we obtain $\lim_{k\to\infty} \rho^* \left(\mathcal{R}^k(\lambda)\right) = 1$ and $\rho^*(\lambda)$ can be written as an infinite product with a non-zero limit. This leads to the density profile given in Fig. 5.4.

For larger cell sizes we performed the ground state calculations of the intracell Hamiltonian numerically. We used the Arnoldi Algorithm [56], which is designed to calculate the eigenvectors with lowest or highest eigenvalue of

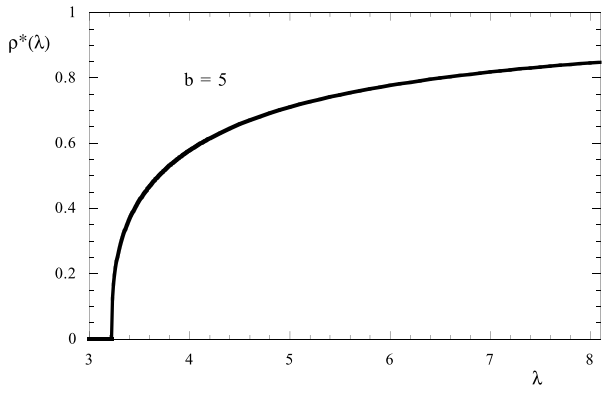

Figure 5.4: *The stationary particle density of the contact process, as obtained from the SRG with cell size* $b = 5$.

large (non-symmetrical) matrices. When the algorithm converges, it produces very precise estimates. Since for stochastic systems we know the eigenvalue of the ground state exactly, we have a reliable criterion to decided on convergence and hence a very powerful diagonalisation tool. Using this method we were able to perform the RG calculations up to $b = 37$. The results are presented in Table 5.1. The extrapolations $b \to \infty$ of the RG results are made using the BST algorithm [61], which is known to be a good tool to extrapolate finite lattice data [62]. The error bars given on our results are those of the extrapolation and not those of the approximations made in SRG procedure. The latter ones cannot be estimated and are simply assumed to go to zero for $b \to \infty$. Our results are also compared with those that can be found in literature and are based on a variety of other techniques. The results in the second row of Table 5.1 were obtained from a numerical diagonalisation of the Hamiltonian for the contact process on a finite lattice. In that case the exponent β was not calculated, but we used a scaling relation to obtain this exponent from estimates of $\nu_\perp$ and the exponent δ. The estimates in the three last rows are not for the contact process itself, but for other models in the same universality class.

As can be seen, the results of our SRG technique compare very well with those of the other techniques, especially for the location of the critical point and the correlation length exponent. The value of $\beta/\nu_\perp$ is somewhat less precise. However, in comparison with the standard of real space renormalisation calculations, the current results must be considered as extremely accurate.

Considering the success of the SRG to determine the stationary behaviour of the contact process, it is tempting to apply it to models for which it is

b	λ_c	$\nu_\perp$	$\beta/\nu_\perp$
9	3.228740192229	1.100222670443	0.300770659640
11	3.232841532095	1.099704726572	0.291239313449
13	3.236622341324	1.099306840428	0.284829626291
15	3.240001893307	1.098993499409	0.280220582724
17	3.243002363779	1.098741258486	0.276745857289
19	3.245669884031	1.098534370274	0.274032449042
21	3.248051604747	1.098361971472	0.271855062319
23	3.250189366461	1.098216363626	0.270069478446
25	3.252118590397	1.098091954504	0.268579043181
27	3.253868772889	1.097984591005	0.267316523888
29	3.255464377754	1.097891127814	0.266233690895
31	3.256925727824	1.097809141091	0.265295037853
33	3.258269778268	1.097736734033	0.264473840447
35	3.259510752614	1.097672401665	0.263749596182
37	3.260660654464	1.097614935125	0.263106311367
$b \to \infty$	3.2982(2)	1.09682(2)	0.2534(4)
series expansion [47][57]	3.29785(2)	1.0969(1)	0.2520(1)
diagonalisation [58]	3.29792(2)	1.09681(1)	0.256(1)
simulations [59]		1.09684(1)	0.25208(1)
series expansions [60]		1.096854(4)	0.252072(11)
DMRG [15]		1.08(2)	0.249(3)

Table 5.1: *Critical parameters as calculated by the SRG method for a cell size of b sites, together with the results coming from other approaches. The number between brackets is the uncertainty on the last digit.*

known or suspected that they belong to a different universality class. In the next section we discuss these possibilities.

5.2 Generalised Contact Process

5.2.1 Introduction

It is in general believed that all absorbing-state phase transition can be classified in a finite number of universality classes. But it has not been cleared out sufficiently which properties are decisive for the type of critical behaviour a model exhibits. In the introduction of my thesis I mentioned the conjecture of directed percolation (DP), giving the sufficient (but not needed) conditions for a transition to belong to the DP universality class. Since this hypothesis

has up to now not been contradicted, it forms a good starting point:

DP Conjecture: *In the absence of any special conservation laws and quenched disorder, continuous phase transitions between an active and a single absorbing state of many particle systems with local interactions and a scalar order parameter are of the directed percolation (DP) type.*

One of the puzzles of this research area is that it seems to be very hard to find physical realisations of DP transitions [63], although the conjecture states the robustness of the class. The understanding of the universality classification for absorbing-state transitions is clearly incomplete and could use further research. In order to gain insight it is always important to find simple models that exhibit the wanted behaviour. One can think of several ways to violate the conditions of the DP conjecture in attempting to find simple realisations of non-DP behaviour. In my research I looked at two possibilities: the introduction of quenched disorder or extra symmetry. The former case is still the subject of my current research and will be the last topic of this thesis. First I will consider the latter possibility, which is represented by the existence of the parity-conserving (PC) universality class. A first realisation of this class was found by Grassberger *et al.* [64] in 1984. However, the dynamical rules of that model were very complicated and at that time it was unclear what caused the non-DP exponents. By now it has been recognised that two different symmetries can lead to the PC behaviour.

First there is the conservation of the number of particles modulo two: parity conservation. This symmetry gave the name to the universality class and is most prominently represented by the *Branching and Annihilating Random Walks* (BARW) [65]. These models, which I also mentioned in the introduction of my thesis, have (one type of hard core) particles making random walks and upon meeting they can annihilate $AA \to \phi\phi$. Competing with this annihilation the model has a branching process with a fixed number of offsprings: if a particle A has m empty neighbouring sites, it can produce an offspring of m particles on these sites:

$$A \to (m+1)A.$$

When the branching rate is bigger than a critical value, the model has besides the absorbing state a stationary state with a non-zero particle density. With this density as the order parameter, the BARW models have a continuous phase transition out of the absorbing state. When m is odd, the transition belongs to the DP universality class. When m is even, parity conservation is present and the critical behaviour turns out to be characterised by a different set of exponents: they belong to the PC class[1]. The fact that the slightest

[1]Note that the introduction of higher symmetries (e.g. conservation of particles modulo

violation of the conservation law (in the form of a very small rate for a death process $A \to \phi$) throws the system back into the DP class proves that it plays a crucial role [66]. Since these models contain $(m+1)$-site interactions, they are difficult to study using real-space renormalisation techniques. As mentioned before, the first order approximation of our SRG technique can only handle nearest neighbour interactions, consequently the case $m > 1$ is out of the scope of it. However, it is interesting to mention that when we apply our SRG to the BARW with $m = 1$, after one RG step the system is transformed into the contact process, which is consistent with the fact that it belongs to the DP class.

A second option to access the non-DP class is the introduction of more absorbing states. But just this violation of the DP conjecture does not automatically imply non-DP behaviour. As an example consider the pair contact process, defined by

$$\begin{array}{rcl} AA & \to & AAA \\ AA & \to & \phi\phi. \end{array} \tag{5.21}$$

This model has infinitely many absorbing states, given by all configurations without neighbouring particles. The model has a continuous phase transition out of the absorbing states, but it does belong to the DP class [67]. Non-DP behaviour only occurs when there is *symmetry* among these states. It turns out that when a model has two equivalent absorbing states, the competition between them results in a critical behaviour described by the PC exponents. This symmetry is denoted as Z_2 and has been found in various models like some cellular automata [64], non-equilibrium Ising models [68] or Z_2 generalisations of DP models [55]. The model in the last reference was introduced by Hinrichsen in 1997. It gives a clear realisation of this Z_2 symmetry and can be seen as a *generalised contact process*. In this system each lattice site can be occupied by, at most, one particle (called active) or can be in any of n inactive states ϕ_k, $k \in \{1, \ldots, n\}$. The dynamical rules are described by

1. Spreading of activity : particles can create extra particles at neighbouring inactive sites.

2. Spontaneous decay : particles can turn spontaneously into an inactive state of a random type k

3. At the boundary between two inactive sites of a different type, a particle can be created.

three) does not automatically imply new critical behaviour, it can even lead to a transition that can be described by mean-field exponents.

Rule 3 implies that the system has only n absorbing states, being the configurations with all sites in the *same* inactive state. Rule 1 and 2 are similar to the dynamics of the contact process. In the absence of rule 3 these dynamics are not different from a system with only one inactive state $n = 1$ and consequently produce DP behaviour. Rule 3 distinguishes different types of inactive sites but treats them equivalently. To understand its effect we consider the case of $n = 2$. Assume that the system is in its critical point. Eventually all particles will disappear and the system will get stuck in one of the two absorbing states. But before such a state is reached, a typical configuration in the long-time limit looks like an alternation of inactive domains of type 1 and type 2. Between these domains particles will be present as a consequence of rule 3. The effect of the two other rules on these particles makes that such a domain "interface" is a fluctuating entity. Some of the domains will grow at the cost of other domains, which will disappear, until finally one is occupying the complete lattice. This domain competition can be described by constructing effective dynamics for the domain *interfaces*. Later we will come back to this point, but it is not difficult to see that for $n = 2$ domain boundaries can only be created or destroyed in pairs, cf Fig. 5.5. Hence, the coarsegrained

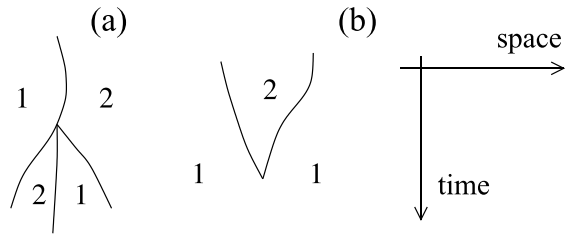

Figure 5.5: *Possible creation a) and destruction b) of domain interfaces for the generalised contact process with two absorbing states. The numbers indicate the domains of inactive sites of type* 1 *and* 2.

critical dynamics of the generalised contact process with two absorbing states can be described by domain interfaces performing a branching and annihilating random walk with offspring 2. This relation with the BARW model with parity conservation suggests that the model belongs to the same PC universality class. Another important difference between $n = 1$ and $n = 2$ that can be understood by this picture, is the dynamical behaviour in the inactive phase. For the case $n = 1$ the decay of the particle density is dominated by the reaction $A \to \phi$ and is consequently exponentially fast. For $n = 2$ this temporal evolution is governed by diffusion and annihilation of (active) domain interfaces. In a

one-dimensional system this results in an algebraic decay of $\rho(t) \sim t^{-1/2}$ (cf introduction of this thesis).

When Hinrichsen introduced the generalised contact process he used simulation techniques to determine the critical behaviour. For $n = 1$ he found a phase transition in the DP class and for $n = 2$ the critical exponents were consistent with PC, as suggested. The data he found for $n \geq 3$ were inconclusive.

Note that the PC behaviour of the $n = 2$ case is however not trivial. The given picture of the domain interfaces only holds globally while on a microscopic scale it is not well-defined. And there are models known with global but not local parity conservation, belonging to the DP class [69]. Recently the study of the pair contact process (5.21) with diffusion raised a lot of questions in this respect. This model does not have parity conservation even on a microscopic scale, but some authors found that some exponents belong to the PC class [70], while others think the system is in a new universality class [71].

Most of the results mentioned above come from simulations or numerical diagonalisation techniques (DMRG). When studying universality, a renormalisation group approach is always very useful. It would therefore be interesting if we could apply our SRG to a model in the PC class. The generalised contact process with $n = 2$ absorbing states is an obvious candidate, which we will discuss next.

5.2.2 Results

The dynamics of the generalised contact process as introduced in [55] are defined in (6.1)-(6.4). For the present purpose we introduce a variant with a closer connection to the original contact process[2]. Denote a particle by A and the possible inactive states of each site as ϕ_k $k \in \{1, \ldots, n\}$. The following dynamical rules define the model:

$$\text{Rule 1}: \quad \begin{matrix} A\phi_k \\ \phi_k A \end{matrix} \quad \rightarrow \quad AA \qquad \text{with rate } 1 \tag{5.22}$$

$$\text{Rule 2}: \quad A \quad \rightarrow \quad \phi_k \qquad \text{with rate } \mu \tag{5.23}$$

$$\text{Rule 3}: \quad \phi_k\phi_l \quad \rightarrow \quad \begin{matrix} \phi_k A \\ A\phi_l \end{matrix} \quad (k \neq l) \quad \text{with rate } \kappa \tag{5.24}$$

In order to find PC behaviour we consider the case of two inactive states $n = 2$, which need to be equivalent. Hence all rates are taken independent of k.

[2] One could also implement the SRG on the model given by (6.1)-(6.4). One RG step would map it on the model we introduce here as our starting point.

We denote the local two-site Hamiltonian defined by the reactions (5.22) and (5.24) on site i and $i+1$ by h_i^2 and the Hamiltonian of (5.23) on site i by h_i^1. We divide the lattice in cells of length b and use the numbering with the index α as given in Fig. 5.1. Just as for the contact process, the regrouping into the intra- and intercell Hamiltonian is again performed as indicated in Fig. 5.2. Now the intracell Hamiltonian has two absorbing ground states and one (forced) active ground state: the degeneracy of the ground state equals three as it should for a three-state lattice. The absorbing states are equivalent, which is needed since we want to preserve this symmetry under the SRG procedure.

Analogous to (5.7)-(5.9) we can rewrite the intracell Hamiltonian as a sum of two operators working on the left and right half of the cell:

$$H_{0,\alpha} = H_\alpha^r + H_\alpha^l.$$

Since this model does not have the property of self-enantiodromy we have to calculate both left and right ground states of these operators. Apart from this technical problem we can proceed in the same way as for the original contact process. It is again possible to proof that there is no proliferation of interactions and the SRG flow is given by

$$\mathcal{R}(\mu) = \mu \frac{v^2}{[1+w_1(\kappa-2)](1-w_2)} \tag{5.25}$$

$$\mathcal{R}(\kappa) = \kappa \frac{1}{[1+w_1(\kappa-2)]} \tag{5.26}$$

with[3]

$$\begin{aligned} w_1 &= \langle s| E_{\alpha,1}^{00} |A,0\rangle_\alpha^r \\ w_2 &= {}_\alpha^r\langle \phi_1,0| E_{\alpha,1}^{20} |\phi_1,0\rangle_\alpha^r \\ v &= {}_\alpha^r\langle \phi_1,0| E_{\alpha,\frac{b+1}{2}}^{02} |A,0\rangle_\alpha^r \end{aligned}$$

and $|\eta,0\rangle_\alpha^r$ (${}_\alpha^r\langle\eta,0|$) are the right (left) ground states of H_α^r. From (5.25) and (5.26) we can deduce that the lines $\kappa=2$ and $\kappa=0$ are invariant under the RG flow, independent of the cell size b.

[3]Since the lattice is now three-stated we have to make a convention regarding the representation of the states. As an extension of (2.17) we define the single-site states by:

$$|\phi_1\rangle = \begin{pmatrix} 1 \\ 0 \\ 0 \end{pmatrix}, |\phi_2\rangle = \begin{pmatrix} 0 \\ 1 \\ 0 \end{pmatrix}, |A\rangle = \begin{pmatrix} 0 \\ 0 \\ 1 \end{pmatrix}$$

For the case of the small cell size $b = 3$ the complete RG flow can easily be calculated analytically. This results in

$$\begin{aligned} \mathcal{R}(\mu) &= \mu \frac{16\mu^2(1+\mu)^2}{(2+\mu)(1+\kappa\mu)(2+7\mu+6\mu^2)} \\ \mathcal{R}(\kappa) &= \kappa \frac{1+2\mu}{1+\kappa\mu}. \end{aligned}$$

A sketch of the RG flow can be found in Fig. 5.6. Let us first analyse this flow

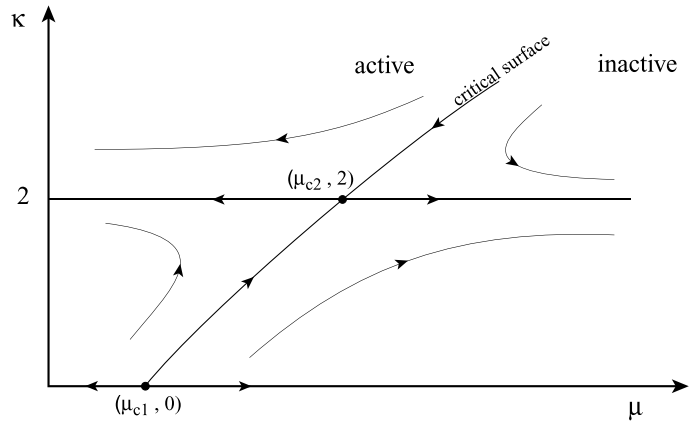

Figure 5.6: *Schematic parameter flow of the generalised contact process with two absorbing states, as produced by the SRG.*

qualitatively. One clearly recognises a critical surface acting as a separatrix. The parameter space to the left of this curve is attracted to $\mu = 0$, representing the active phase, while the other half is attracted to $\mu = \infty$ and forms the inactive region. On this critical surface two fixed points are present. One is repulsive and located at $(\mu_{c1}, \kappa = 0)$. The line $\kappa = 0$ is invariant under RG transformations and represents the models without Rule 3 (5.24). Hence this first fixed point must be the critical point of the DP phase transition. The rest of the critical surface with $\kappa > 0$ is attracted to a second fixed point at $(\mu_{c1}, 2)$, indicating that the presence of rule 3 changes the critical behaviour. This point is expected to represent the PC universality class. Considering the slope of the critical surface, one finds the active region of the PC models to be larger than that of the DP type. Finally the line $\kappa = 2$ is invariant and we can immediately see that $(\mu - \mu_{c2})$ is the relevant scaling variable at the PC fixed point. Since we proofed that this line is invariant under SRG transformations for *every* cell size b, we can restrict ourselves to this subspace when evaluating the critical behaviour of the PC point.

So far everything looks very promising and consistent with the knowledge about the model. However, when we evaluated the quantitative aspect of the RG in the PC fixed point, it didn't turn out as expected. The results of this calculation are presented in Table 5.2. If we compare these sequences

b	μ_{c2}	$\nu_\perp$	$\beta/\nu_\perp$
5	3.59073840237405	3.84957107827342	0.77606122804702
7	3.17405007983074	3.55241121447515	0.74430908143347
9	2.95801300580053	3.40871145273645	0.72572996656579
11	2.81969425036648	3.32221357209652	0.71322533401272
13	2.72094710034720	3.26369199161513	0.70409359105930
15	2.64562474086776	3.22112387966619	0.69705935726526
17	2.58555702819569	3.18859584859303	0.69143275221699
19	2.53609988871684	3.16283594505297	0.68680400916693
21	2.49438790888701	3.14187578139579	0.68291252317888
23	2.45854189627294	3.12445470449951	0.67958367219083
$b \to \infty$	1.5(1)	2.95(5)	0.62(1)
PC [72]		1.83(3)	0.50(2)

Table 5.2: *Critical parameters as calculated by the SRG method for a cell size of b sites. The extrapolated values are compared with the PC values.*

with those for the contact process we find that the estimated values for finite b are much further away from their limiting value. And since we are now dealing with a three-stated lattice, the maximum cell size manageable was $b = 23$. This makes an extrapolation less accurate. The error bars are 100 to a 1000 times larger then those of the contact process, but nevertheless they are still acceptable. When we now compare these extrapolated values for $\nu_\perp$ and $\beta/\nu_\perp$ with the corresponding PC exponents (cf Table 5.2) we find them to be incompatible!

This discrepancy could be related to several causes. The most likely option is that the SRG is not powerful enough and produced inaccurate numerical results. One of the main drawbacks of a real-space RG approach, is that is difficult to estimate the effect of the introduced approximations. Consequently, it is very hard to check this option without further information. A second possibility is that the values that we found are correct and that the system simply does not belong to the PC universality class. Since we used a variant of the generalised contact process that has not been studied by other means, this option can at the moment not be excluded. A third interpretation is that the SRG does reproduce the PC exponents, but that larger cell lengths are needed to reach the true behaviour. It would be interesting to perform some

simulations to decide between these three options, but at the moment this has not been done.

5.3 Conclusions

Concluding the topic of the SRG we can say that we successfully adapted the method from quantum spin chains to stochastic multi particle systems on a one-dimensional lattice. We were able to construct the method as a first order expansion of an exact RG procedure in a late-time limit and we showed how conservation of probability can be assured.

When we applied the method to the exactly solvable system with coagulation, decoagulation and diffusion, the correct stationary behaviour was recovered: the produced RG flow gave an exact image of the phase diagram and the stationary particle density could be derived.

For the contact process, which contains a non-trivial critical point, rather accurate estimates for the location of the critical point, the values of the critical exponents and the profile of the stationary particle density were obtained from a calculation on a system of no more than three sites. We proved that no proliferation of interactions occurs for any cell size and using some analytical properties such as the duality of the process, we were able to extend the computations up to cell sizes of 37 sites. A suitable extrapolation yielded estimates for the critical properties that are of very high accuracy.

When we used the method to the generalised contact process with two absorbing states, the resulting RG flow produced a qualitatively correct phase diagram. The resulting estimates for the critical parameters are however expected to be incorrect.

Considering the simplicity of the method, I think it is fair to conclude that the SRG can be a handy tool to study the stationary and critical behaviour for this kind of systems. In Chapter 7 yet another application of the SRG will confirm this statement. It has of course to be admitted that real-space RG methods in general involve some ill understood approximations. Furthermore, it is not possible to predict for which systems an approach such as the one we presented can be successful. For each model one has to investigate independently how to perform the RG, taking into account all known symmetries, dualities and so on.

Chapter 6

DMRG and Generalised Contact Process

In this chapter a non-hermitian density-matrix renormalisation group (DMRG) is used to investigate the critical properties of the generalised contact process with n (permutation symmetric) absorbing states. After the introduction of the model the principles of the DMRG method are explained. Next an analysis of the cases $n \leq 4$ is presented. For $n = 1$ and $n = 2$ respectively the DP and PC universality classes are recovered, consistent with previous studies. For $n = 3$ and $n = 4$, the model is active in the whole parameter space and the critical point is shifted to the limit of one infinite reaction rate. A proof is given that in this limit the dynamics can be mapped onto that of a zero temperature n-state Potts model. For $n = 3$ the effect of breaking the permutation symmetry between the inactive states is studied.

This research was published in reference [73].

6.1 Introduction of the Model

The generalised contact process was introduced by Hinrichsen [55] to gain insight in the classification of universality classes for absorbing state phase transitions. In the previous chapter the general concept was already explained, but we didn't give the original setup yet. The model consists of a one-dimensional lattice where each site can be occupied by, at most, one particle A, or can be in any of n inactive states $\phi_1, \phi_2, \ldots \phi_n$. The reactions are:

$$AA \rightarrow \begin{matrix} A\phi_k \\ \phi_k A \end{matrix} \quad \text{with rate } \tfrac{\lambda}{n} \tag{6.1}$$

$$\begin{matrix} \phi_k A \\ A\phi_k \end{matrix} \rightarrow \phi_k\phi_k \quad \text{with rate } \mu_k \tag{6.2}$$

$$\begin{matrix} \phi_k A \\ A\phi_k \end{matrix} \rightarrow AA \quad \text{with rate 1} \tag{6.3}$$

$$\phi_k\phi_l \rightarrow \begin{matrix} A\phi_l \\ \phi_k A \end{matrix} \quad (k \neq l) \quad \text{with rate 1.} \tag{6.4}$$

Let us summarise the results found by Hinrichsen in [55]. The essential difference with the original contact process is reaction (6.4). For $n = 1$ this reaction can not take place and the model has a phase transition in the directed percolation (DP) class. For $n = 2$ the system has two absorbing states represented by the configurations with all sites in the same inactive state ϕ_i. When μ_1 is taken equal to μ_2 these states are treated equivalently and the system has absorbing states that have a permutation symmetry group Z_2. In this case the dynamics of the system is governed by a competition between the two absorbing states and the critical behaviour belongs to the parity conserving (PC) universality class. The particle-density decay in the inactive phase is algebraic $\rho \sim t^{-1/2}$ while for $n = 1$ this is exponential. On a coarsegrained level the dynamics can be described by domain interfaces performing branching and annihilating random walks with conservation of parity. This links the Z_2 symmetry with parity conservation. When the symmetry is broken by taking $\mu_1 \neq \mu_2$, the system falls back into the DP class. One of the two absorbing states becomes dominant and the system behaves as if only one absorbing state was present. To come to these results Hinrichsen made use computer simulations and for the case $n \geq 3$ the data he found were inconclusive.

There are several reasons why we investigated this particular model. First, the model incorporates the two well understood universality classes of absorbing-state phase transitions (DP and PC), and is consequently an ideal study object. Secondly, it is interesting to see the effect of breaking the permutation symmetry, especially for $n \geq 3$ when there are different ways in breaking it. Finally, since the simulation techniques were not able to provide insight into the cases with $n \geq 3$, it is useful to see whether this can be reached with a different technique. In the previous chapter (cf subsection 5.2.2) I showed that the SRG method is probably not capable of tackling the problem. A more powerful (but purely numerical) technique, which was having its first successful

applications to stochastic systems at that time [14][15], is the density-matrix renormalisation group (DMRG). This is the method we used.

Besides the physics of the model, it was interesting to investigate the performance of the DMRG. The generalised contact process contains for $n > 1$ several absorbing configurations and several states per site, a situation that was definitely more complicated than what was considered before.

6.2 The DMRG

The density-matrix renormalisation group (DMRG) was introduced in the early 90's [12][13] as a numerical technique to determine a particular part of the spectrum of Hamiltonians of one-dimensional quantum spin chains of finite length. The method is able to approximate eigenvalues and eigenvectors of very large systems with an amazing accuracy and caused a revolution in this field of research. Most interesting for us, one could even reach system sizes big enough to study phase transitions and critical phenomena if the technique is combined with finite-size scaling. More recently, the technique has been adapted to the study of low-lying spectra of generators of Markov processes [14],[15], giving yet another example of a quantum mechanical tool used in a stochastic context.

The DMRG is a very powerful algorithm but its application to stochastic processes is still recent and it is not yet widely spread. Therefore it will, to some extend, be described in this section and the application to the generalised contact process is postponed to the next section. For simplicity, we will explain the technique first in the context of a quantum chain.

6.2.1 Diagonalisation

The name DMRG is a bit misleading since it does not concern a renormalisation in the strict sense. No renormalisation flow is constructed and the typical techniques of renormalisation to study critical properties are not used. The DMRG is actually an approximative extension of diagonalisation techniques, inspired by renormalisation. Let us first take a look at exact diagonalisation of Hamiltonians of quantum chains with short range interaction. If we have a lattice of L sites with two states per site, we have $n = 2^L$ degrees of freedom. In general a representation of the Hamiltonian will be a $n \times n$ matrix, but when the operator is local, this matrix will be extremely sparse. If one wants to diagonalise it for a large lattice size L, one should take advantage of this sparseness. For this purpose very good techniques exist, like the Lanczos method or the Arnoldi method [56]. These algorithms do not need the matrix representation itself, but only the effect of the operator on a vector. Since a

large amount of the matrix elements is zero, this makes a big difference. Using the sparseness, a multiplication of the matrix with a vector can be made very efficient, resulting in a computational effort $\sim n$ rather than $\sim n^2$. These algorithms can produce eigenvectors and eigenvalues of the low or high lying part of the spectrum with very high accuracy. We will refer to them as 'exact diagonalisation'.

Nevertheless, this exact diagonalisation is still very limited with respect to the lattice size L since the dimension n of the vector space grows exponentially in L. To reach larger systems, one needs a way to limit the degrees of freedom without destroying the quantities of interest. This idea could be implemented as follows. Suppose that one wants to find the ground state of a system and the

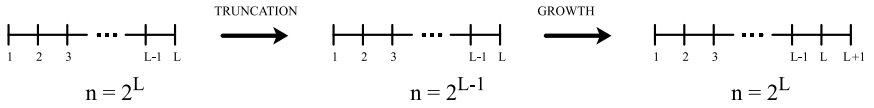

Figure 6.1: *General idea how to keep the number of degrees of freedom n fixed*

exact diagonalisation technique can manage the problem for an Hamiltonian H_L on a lattice of L sites. Before going on to a lattice of $L+1$ sites, one first performs a truncation: $\frac{n}{2}$ carefully chosen vectors are used to represent the n-dimensional vector space. Then H_{L+1} is constructed and the vectors are used to perform a projection of H_{L+1}, a $2n \times 2n$ matrix, onto $\tilde{H}_{L+1}$, an $n \times n$ matrix. $\tilde{H}_{L+1}$ can now be handled using exact diagonalisation and its ground state will serve as an approximation of the ground state of H_{L+1}. This whole procedure, represented in the diagram of Fig. 6.1, can now be iterated to handle systems of increasing size. The crucial step in this reasoning is of course the choice of the vectors used to truncate the vector space. Here we arrive at the problem of the procedure. This choice should be based on the minimisation of the difference between the ground state of H_{L+1} and $\tilde{H}_{L+1}$, but the former one is not known!

The DMRG method contains a clever trick to solve this problem. One usually defines two different DMRG algorithms: the *infinite size algorithm*, which is the procedure to approximate eigenstates of increasing system sizes, and the *finite size algorithm*, which consists of an iterative way to improve the approximation of an eigenstate of a system with a fixed length.

6.2.2 Infinite System Algorithm

Assume one wants to know a particular eigenstate of the Hamiltonian, often the ground state. This state of interest will be called the *target state*. Con-

sider a system of size L, for which the target state can be found using exact diagonalisation. (One usually takes open boundary conditions, for which the DMRG works best.) To perform the truncation of the vector space, a different setup is used than the simple one presented in Fig. 6.1. The system is divided into two parts. One will be called the system block, the other the environment. The whole system is called the superblock. Both parts are taken of equal size and the number of degrees of freedom for each is $n = 2^{L/2}$. The orthonormal basis vectors representing the configuration space will be denoted respectively by $|i\rangle$ and $|j\rangle$, cf Fig. 6.2. Denote the target state of the superblock as $|\psi\rangle$.

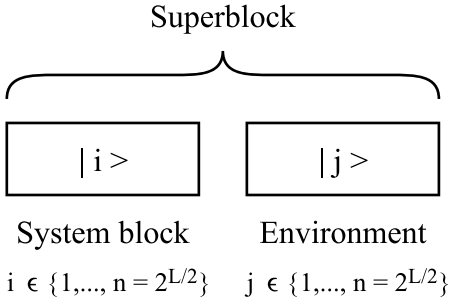

Figure 6.2: *A system block together with its environment form the superblock.*

The aim is to reduce the number of states n used to describe the system block, without destroying the target state $|\psi\rangle$ of the superblock. We will make this statement more precise. Assume one wants to reduce n to $m < n$: the n vectors $|i\rangle$ are to be replaced by m vectors $|u^\alpha\rangle, \alpha = 1, \ldots, m$. In combination with the environment states $|j\rangle$, these vectors should be able to make an accurate representation $\left|\tilde{\psi}\right\rangle$ of the target state $|\psi\rangle$:

$$|\psi\rangle \approx \left|\tilde{\psi}\right\rangle = \sum_{\alpha=1}^{m}\sum_{j=1}^{n} a_{\alpha,j}\,|u^\alpha\rangle\,|j\rangle \tag{6.5}$$

where $|u^\alpha\rangle\,|j\rangle$ is shorthand for $|u^\alpha\rangle \otimes |j\rangle$. This means one needs to minimise

$$S = \left||\psi\rangle - \left|\tilde{\psi}\right\rangle\right|^2 \tag{6.6}$$

with respect to all $a_{\alpha,j}$ and $|u^\alpha\rangle$. Since not the $|u^\alpha\rangle$ themselves, but only the space spanned by them is relevant, one can without loss of generality, demand these vectors to form an orthonormal set

$$\left\langle u^\beta \,|u^\alpha\right\rangle = \delta_{\beta,\alpha}. \tag{6.7}$$

The solution of this minimisation problem is the heart of the DMRG, and is given in a more general form in the following theorem

Theorem 5 *The Density Matrix*

Let the dimension of the configuration space of the system block and the environment respectively be given by n_1 and n_2. Furthermore, denote the two sets of orthonormal basis vectors of the system block and the environment respectively as $|i\rangle, i = 1, \ldots, n_1$ and $|j\rangle, j = 1, \ldots, n_2$, and the target state of the superblock as $|\psi\rangle$. Take $m \in \mathbb{N}$ with $m < n_1$ and denote any vector of the system block as $|u\rangle$.

If one wants to minimise

$$S = \left| |\psi\rangle - \sum_{\alpha=1}^{m} \sum_{j=1}^{n_2} a_{\alpha,j} |u^\alpha\rangle |j\rangle \right|^2 \tag{6.8}$$

by varying over all $a_{\alpha,j}$ and $|u^\alpha\rangle$ subject to $\langle u^\beta | u^\alpha\rangle = \delta_{\beta,\alpha}$, the solution for the vectors $|u^\alpha\rangle$ is given by the following procedure.

Take $|\psi\rangle\langle\psi|$ the density matrix of the target state on the superblock and construct the reduced density matrix on the system block

$$\rho_{ii'} = \sum_{j=1}^{n_2} \langle i| \langle j| \quad |\psi\rangle\langle\psi| \quad |i'\rangle |j\rangle . \tag{6.9}$$

ρ is an hermitian operator with n_1 real eigenvalues. The m eigenvectors of ρ with largest eigenvalue are the vectors $|u^\alpha\rangle$ in the solution of the minimisation problem.

A proof is given in Appendix B. For a quantum spin chain it is possible to get some insight in the theorem by physical arguments. Let A be an operator restricted to the system block. From quantum mechanics it is known that the reduced density matrix ρ contains all information needed to calculate the expectation value of A in the target state. This can be written as

$$\langle A\rangle = \text{Tr } \rho A. \tag{6.10}$$

Eigenvalues w_α of the density matrix ρ have the properties: $w_\alpha \geq 0$ and $\sum_{\alpha=1}^{n_1} w_\alpha = 1$. Each w_α gives the probability to find the system block in eigenstate $|u^\alpha\rangle$ of ρ when the superblock is in the state $|\psi\rangle$. One can now rewrite

$$\langle A\rangle = \sum_{\alpha=1}^{n_1} w_\alpha \langle u^\alpha| A |u^\alpha\rangle \tag{6.11}$$

If one was to choose m of these vectors $|u^\alpha\rangle$ to approximate any $\langle A\rangle$, one should keep the vectors with a big eigenvalue w_α and to neglect those with a small eigenvalue. This is exactly what the theorem states. Moreover, ordering the eigenvalues of ρ $w_1 \geq w_2 \geq \ldots$ the value

$$\varepsilon = 1 - \sum_{\alpha=1}^{m} w_\alpha = \sum_{\alpha=m+1}^{n_1} w_\alpha \tag{6.12}$$

is the discarded weight and gives an estimate for the error made in the truncation. It is clear that the spectrum of ρ is very important: the faster w_α decreases for increasing α, the more accurate the approximation is.

Let us now return to the situation of Fig. 6.2. For a given target state of the superblock, we obtain in this way an optimal strategy to truncate the configuration space of the system block. The vectors $|u^\alpha\rangle, \alpha = 1, \ldots, m$ form the best set of m vectors to approximate the target state when the system block has an environment of $L/2$ sites. The algorithm is now as follows. We start with a system of L sites and $n \cdot n = 2^L$ degrees of freedom. Using the truncation strategy on both left and right part of the superblock, we reduce number of degrees of freedom to $m \cdot m$. Next the Hamiltonian is projected on these reduced vector space. Now we increase the system size by putting two new sites in the centre of the superblock. The Hamiltonian of this system is now an operator on a vector space of dimension $m \cdot 2 \cdot 2 \cdot m = 4m^2$. If m is chosen small enough (but large enough for a good approximation) this reduced Hamiltonian can be handled with exact diagonalisation. In this way we find an approximation of the target state of a system of $L + 2$ sites. The procedure can be iterated to study increasing system sizes, cf Fig. 6.3, and is given in the following algorithm.

Algorithm 6 *Infinite System Algorithm*
Outline is given in Fig. 6.3

1. *Construct the Hamiltonian H_L on a superblock of L sites, which can be handled using exact diagonalisation.*

2. *Using exact diagonalisation, determine the target state $|\psi\rangle$ and its eigenvalue of the Hamiltonian H_L on the superblock.*

3. *Construct the reduced density matrix ρ on the left half of the system. Diagonalise ρ using an algorithm for dense matrices (e.g. the standard technique of Householder transformation + diagonalisation of tridiagonal matrix). Find the orthonormal set of m eigenvectors $|u^\alpha\rangle$ with largest eigenvalues.*

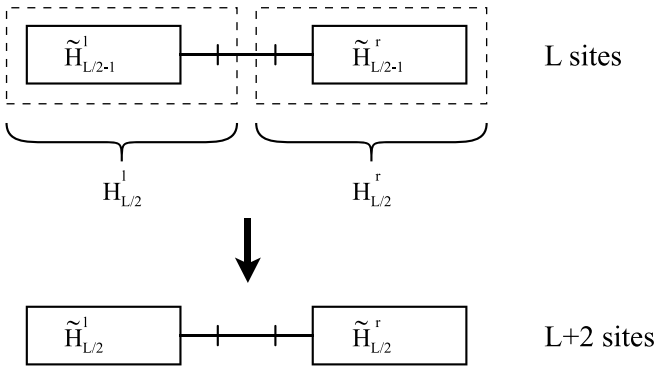

Figure 6.3: *Outline of the infinite system algorithm. The dashed lines indicate the system block and the environment. Operators without a tilde are before truncation of configuration space, with a tilde, after truncation.*

4. *Construct $H^l_{L/2}$, the Hamiltonian on the left half of the system. Project this $H^l_{L/2}$ on the truncated basis $|u^\alpha\rangle$, resulting in an $m \times m$ matrix*

$$\left(\tilde{H}^l_{L/2}\right)_{\alpha\beta} = \langle u^\alpha | \, H^l_{L/2} \, \left| u^\beta \right\rangle \tag{6.13}$$

5. *Repeat step 3 and 4 for the right half of the system. If the system has left-right symmetry this can be done without further calculation.*

6. *Construct a superblock of $L+2$ sites, using the effective Hamiltonians $\tilde{H}^l_{L/2}$ and $\tilde{H}^r_{L/2}$, and two single sites.*

7. *Go to step 2, substituting $L+2$ for L.*

This is the way the DMRG controls the number of degrees of freedom. Every time the algorithm gets to point 2, it finds an Hamiltonian matrix of the same size (determined by m), for which the target state can be found using exact diagonalisation. Iterating the algorithm one finds approximations for the target state and its eigenvalue for increasing system sizes. These sizes would not be accessible by 'direct' exact diagonalisation.

Note that the crucial step is where the vectors $|u^\alpha\rangle$, optimised in a superblock of L sites for an environment of $L/2$ sites, are used in a system where they have an environment of $2 + L/2$. This is how the DMRG avoids the problem mentioned at the end of the previous subsection. Even though this approximation seems crude, it often gives good results. However, it can be made much more accurate if it is combined with the finite size DMRG

algorithm. Before we turn to this point in the next subsection, we first say a few words about observables.

When iterating the DMRG algorithm, one is permanently making truncations of the vector space. This can be seen as a change of coordinates where the original basis is replaced by a truncated new one. Suppose that at a certain moment in the procedure one wants to calculate the expectation value of an observable A in the approximated target state. This can only be performed if A is written in the same basis as the state. Consequently, one has to keep track of all basis transformations one performs. Every time a truncation is made of a configuration space the operator A is active on, A should be projected on the truncated basis too. In practice, one decides, before the algorithm is started, which observables A are of interest, and the transformations of A are performed while iterating the algorithm. An exception are those operators that are only active on the two central sites of the superblock. These sites are always explicitly present, and no transformation is needed.

6.2.3 Finite System Algorithm

The weak spot of the infinite system algorithm is step 6. The effective Hamiltonians $\tilde{H}^l_{L/2}$ and $\tilde{H}^r_{L/2}$ are optimised for an environment of $L/2$ sites, the algorithm uses them however in a superblock where they have an environment of $2 + L/2$ sites. It is not a priori clear how precise this is. For an homogeneous system this might be acceptable, but a system with quenched disorder for example, can not be approached in this manner. More generally, in the absence of translational invariance, one is faced with a problem. At this point the finite system algorithm comes into play. It is applied after the insertion of two new sites, and before the next application of the infinite system algorithm. By "probing" the environment iteratively the finite system algorithm improves the truncated basis $|u^\alpha\rangle$ and hence the effective operators $\tilde{H}^l_{L/2}$ and $\tilde{H}^r_{L/2}$. The heart of the method is the same as for the infinite system algorithm, but instead of increasing both left and right system blocks at each step, it increases one and decreases the other, keeping the system length L fixed. The first iteration step of the algorithm is outlined in Fig. 6.4.

Algorithm 7 *Finite System Algorithm*

1. *Iterate the infinite system algorithm (alternated with this finite system algorithm) to reach in step 6 of the infinite system algorithm a superblock of L sites. While performing the iterations, store all the effective Hamiltonians* $\tilde{H}^{r,l}_{L/2-1}, \tilde{H}^{r,l}_{L/2-2}, \tilde{H}^{r,l}_{L/2-3}, \ldots$ *used to reach this point.*
   Denote $s^l = s^r = L/2-1$ *the size of respectively the left and right system block. (cf Fig. 6.4)*

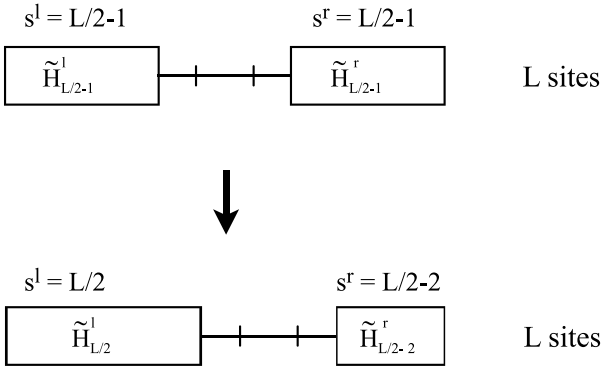

Figure 6.4: *First iteration step of the finite size algorithm. The total number of sites is fixed at L.*

2. *Determine the target state of the superblock. To increase the left system block construct and diagonalise the reduced density matrix ρ on the left $s^l + 1$ sites. Construct $\tilde{H}^l_{s^l+1}$ using the m eigenvectors of ρ with largest eigenvalue. Store $\tilde{H}^l_{s^l+1}$.*

3. *Form a superblock of size L using $\tilde{H}^l_{s^l+1}$, $\tilde{H}^r_{s^r-1}$ and two single sites.*

4. *Replace s^l by $s^l + 1$ and s^r by $s^r - 1$ and repeat step 2, 3 until $s^r = 1$. This is the left to right part of the algorithm.*

5. *Repeat step 2, 3, 4 reversing the role of left and right: build up the right system block starting at $s^r = 1$ and ending at $s^l = 1$.*

6. *Again apply the left to right procedure until one reaches the starting point $s^l = s^r = L/2 - 1$.*

The method can be seen as a zipper running trough the superblock from one side to the other. Hamiltonians for increasing system blocks are updated, while for decreasing system blocks the old Hamiltonians are used. Note that for the calculation of expectation values, also permanent updating of the operators of the observables is needed, just as in the infinite system algorithm. While zipping, the effective Hamiltonians and operators get better adapted to their environment, making up for the error caused by the infinite system method. The procedure above describes one complete zipping movement, ending with the zipper halted in the central position. This whole procedure can be repeated until convergence is reached (the operators stay invariant under

the transformations), and next another step of the infinite system algorithm can be applied. It is the combination of these two algorithms that produces high precision results for big systems.

Until now, we assumed that we were interested in only one particular state $|\psi\rangle$ (e.g. the ground state) of the Hamiltonian. This restriction can be removed. One can show that the same DMRG procedure can be used to approximate two (or in principle more) target states $|\psi_1\rangle$ and $|\psi_2\rangle$ simultaneously. One only needs to replace the density matrix $|\psi\rangle\langle\psi|$ by $\frac{1}{2}[|\psi_1\rangle\langle\psi_1| + |\psi_2\rangle\langle\psi_2|]$. (Here we used the same weight for both states, but this can be chosen differently.) It is however clear that the efficiency of the truncation strategy will be reduced when targeting two states. In general the number of vectors m kept in the truncation, should be increased to reach the same accuracy when approximating two target states simultaneously.

This concludes the main idea of the DMRG. There is lot more to say about it. I did not cover issues like how to choose m, the number of states kept in the truncation step, how to decide on convergence of the finite system method, how to minimise computer memory and computation time, ... Answers to these questions and much more can be found in [74].

6.2.4 The DMRG for Markov Processes

Since the formalism of a Markov process for an interacting particle system on a one-dimensional lattice is very similar to that of a one-dimensional quantum spin chain, the possibility of an application of the DMRG to it is an interesting question. For a Markov process, the Hamiltonian H (generator) is non-hermitian. The heart of the DMRG, the density-matrix theorem 5 depends however only on an eigenvector of H and not on H itself. Although the theorem was inspired by the density matrix from quantum mechanics, it is just an algebraic technique, and it should work for any form of H [14], [15]. But to apply the full DMRG algorithm, two adaptations are necessary. The first one is straightforward: one needs an exact diagonalisation tool capable of handling non-hermitian matrices to perform step 2 in the DMRG algorithms. These tools exist (e.g. the Arnoldi algorithm [56]) but are much more time consuming than their hermitian counterparts. The second problem concerns the fact that left and right eigenvectors are not related by transposition. Suppose one wants to approximate the ground state. If the effective Hamiltonian is to reproduce this extreme part of the spectrum accurately, both left and right eigenvectors should be targeted. When choosing the truncated basis of the system block, this should now be optimised to approximate *two* vectors simultaneously. To target several states at the same time, one needs another density matrix on the superblock. Let us consider the case

of a non-degenerated ground state. Denote the right ground state as $|\psi_0\rangle$, the left is the normalisation vector $\langle s|$. For the hermitian case $|\psi_0\rangle\langle\psi_0|$ was used to minimise the distance of the trial ground state $\left|\tilde{\psi}_0\right\rangle$ to $|\psi_0\rangle$. For the non-hermitian case several options are open [14],[15], but the one used in this thesis is

$$\rho = \frac{1}{2}\left[|\psi_0\rangle\langle\psi_0| + |s\rangle\langle s|\right]. \tag{6.14}$$

Combining the two with equal weight minimises simultaneously the distance of $\langle\tilde{s}|$ and $\left|\tilde{\psi}_0\right\rangle$ to respectively $\langle s|$ and $|\psi_0\rangle$. (Note that targeting $\langle s|$ is always needed when calculating expectation values (2.11).) This choice also has the advantage of keeping the density matrix symmetric, avoiding further problems like complex eigenvalues. Nevertheless, since now two states need to be approximated, the number of states m kept in the truncated basis needs to be higher to get the same accuracy.

The DMRG has by now been tested for Markov processes and was found to work. Although its performance is in general less good than for the hermitian case, it remains an excellent tool to study the low lying spectrum of the generators.

6.3 Results

In this section we describe how we used the DMRG to study the critical behaviour of the generalised contact process with n absorbing states (6.1)-(6.4). Since it was the first time that the DMRG was applied to a stochastic model of this complexity, we started with the cases $n = 1, 2$, where our results could be compared with those of ref. [55]. As long as not stated otherwise, we take the rates independent of the type of inactive state, i.e. $\mu_1 = \mu_2 = \ldots = \mu_n \doteq \mu$.

6.3.1 The Cases $n = 1$ and $n = 2$

A first quantity that can be studied using the DMRG is the gap Γ between (the real part of) the eigenvalue of the first excited state and the ground state of the model. Γ is the inverse of the relaxation time and enables us to determine the phase diagram and the critical exponent $z = \frac{\nu_\parallel}{\nu_\perp}$ of the model. A direct implementation of the DMRG is however very unpractical since for $n > 1$ we have a degenerate ground state, and the DMRG is known to work best for gapped systems. We alleviate this problem by adding at the two boundary sites the following reactions

$$\phi_k \to \phi_1 \qquad (k \neq 1) \text{ with rate } p \tag{6.15}$$

(Recall that it is customary to use open boundary conditions in DMRG [74]). If we denote the n absorbing states as $\left|\psi_k^0\right\rangle$ $k = 1, \ldots n$, we find that with the presence of (6.15) only state the $\left|\psi_1^0\right\rangle$ remains absorbing. The bulk critical behaviour is however expected to be unchanged. Denote the Hamiltonian of the generalised contact process plus the reaction (6.15) at the boundary sites as H. Next, we perform the transformation[1]

$$H' = H + \Delta \left|\psi_1^0\right\rangle \langle s| \,, \tag{6.16}$$

with $\Delta > 0$. H' is no longer a stochastic Hamiltonian, the zero eigenstate is shifted to Δ, but the rest of the spectrum is equal to that of H. The calculation of the gap Γ of the original Hamiltonian, with an n-fold degenerate ground state, is hereby reduced to the calculation of the lowest eigenvalue of H' (obviously provided Δ is bigger than the gap of H). Using this strategy we apply the DMRG to find the gap Γ as a function of the rates and the system size.

Before we turn to the analysis of the data it is instructive to take a look at the phase diagram in Fig. 6.5. Depending on the rates μ and λ the (infinite)

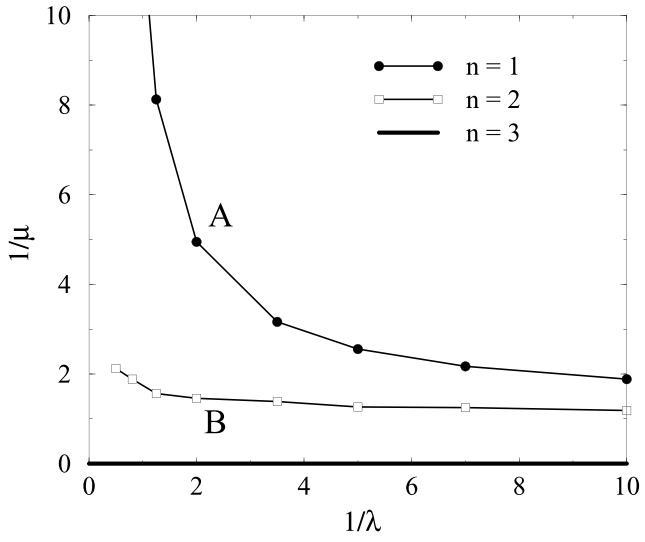

Figure 6.5: *Phase diagram of the generalised contact process with n absorbing states for* $\mu_1 = \mu_2 = ... = \mu_n \doteq \mu$, *as obtained by the DMRG. The region above the curves is the active phase, while the region below is inactive.*

[1] This transformation was also performed in [70].

	Inactive	**Critical line**	**Active**
$n = 1$	$\Gamma \sim \Gamma_0 > 0$	$\Gamma \sim L^{-z}$	$\Gamma \sim e^{-aL}$
$n = 2$	$\Gamma \sim L^{-2}$	$\Gamma \sim L^{-z}$	$\Gamma \sim e^{-aL}$

Table 6.1: *The behaviour of the gap as a function of the system size L in the different regions of the phase diagram.*

system is in the active or the inactive phase. Below the curve the system is inactive, the ground state is n-fold degenerate and the only stationary states are the absorbing ones. In the region above the curve the system has an attractive stationary state with a non-zero particle density, hence the ground state is $(n+1)$-fold degenerate. Along the curve the system is critical. We find (see below) that the critical exponents are the same all along this critical line, and are those of DP for $n = 1$ and PC for $n = 2$. We note that the active region increases from $n = 1$ to $n = 2$. The location of the critical lines agrees well with the Monte Carlo simulations by Hinrichsen [55].

We will now present how we arrived at these phase diagrams. For each value of (λ, μ) we can, in the way explained above, calculate the gap Γ_L of the Hamiltonian on a system of L sites. As a function of L this gap behaves differently in the three regions of the phase diagram. Exactly at the boundary of the two phases, the system is critical and from finite size scaling we obtain $\Gamma_L \sim L^{-z}$ with $z = \frac{\nu_\parallel}{\nu_\perp}$. In the inactive phase we have to differentiate between $n = 1$ and $n = 2$. For $n = 1$ we know that the decay in time towards stationarity is exponentially fast, also for the infinite system. Since the gap Γ_L is the inverse of the relaxation time this must remain finite: $\lim_{L\to\infty} \Gamma_L = \Gamma_0 > 0$. For $n = 2$ the scenario is different. Since in the inactive phase the dynamics are governed by diffusing and annihilating domain interfaces, the decay in time is known to be algebraic with power 1/2: the system is critical in the whole inactive phase. Finite size scaling implies here $\Gamma_L \sim L^{-2}$. Finally, in the active phase the (infinite) system has an extra degeneracy. The first excited state has become a ground state with a non-zero particle density. Consequently, in the active region we expect the gap to decay exponentially in L. The behaviour of Γ is summarised in Table 6.1.

Let us now focus on the case $n = 2$. In the three regions of the phase diagram, the gap goes to zero for increasing system sizes. To differentiate between the three regimes, the gap Γ_L can best be monitored by plotting the discrete logarithmic derivative of it:

$$Y_L = \frac{\ln\left(\Gamma_{L+1}/\Gamma_{L-1}\right)}{\ln\left[(L+1)\,/\,(L-1)\right]} \approx \frac{\partial \ln \Gamma}{\partial(\ln L)}. \tag{6.17}$$

In the active phase the exponential decay of the gap implies $Y_L \sim -aL$, while

in the inactive phase we obtain $Y_L \sim -2$. Exactly on the critical line we expect $Y_L \sim -z$, with z the dynamical exponent of the PC universality class.

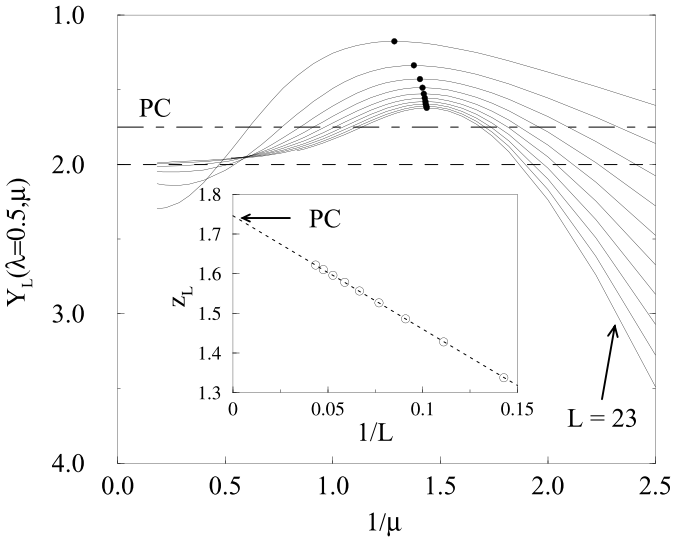

Figure 6.6: *Plot of Y_L for $n = 2$ as a function of μ and for $\lambda = 0.5$. The system sizes are $L = 5, 7, \ldots 23$. Inset: plot of the effective exponent z_L as a function of the inverse system length. The horizontal lines indicate the values 2 and 1.74. The latter one is the exponent z for the PC universality class.*

Fig. 6.6 shows Y_L as a function of μ for $\lambda = 0.5$. For this calculation the DMRG algorithm was iterated up to $L = 24$. One can clearly distinguish the three different scaling regimes. In the right part of the plot, the system is active and Y_L tends to $-\infty$ when L increases. In the left part the curves flatten out and approach the value -2 of the inactive phase. In between we marked the maxima of Y_L with a dot. The horizontal values of these maxima give successive estimates for the position of the critical point, while the vertical values are estimates for the critical exponent z. From an $L \to \infty$ extrapolation we find $\mu_c = 0.69(1)$ for our choice of $\lambda = 0.5$, which determines the point B of the critical line in Fig. 6.5. The inset in Fig. 6.6 gives the effective exponents z_L as a function of the inverse system size. An extrapolation of this curve yields the result $z = 1.747$, which is in accurate agreement with the corresponding value known for the PC class $z = 1.750(5)$ [72].

In this way the DMRG enables us to determine the phase diagram and the exponent z. As we will show in the following subsection, using different boundary conditions we can also find values for $\beta/\nu_\perp$. In Table 6.2, we show

	our result $\mathbf{n=1}$	**DP [41]**	our result $\mathbf{n=2}$	**PC [72]**
μ_c	0.20(1)		0.69(1)	
$z = \frac{\nu_\parallel}{\nu_\perp}$	1.575(5)	1.58074(4)	1.747(5)	1.750(5)
$\frac{\beta}{\nu_\perp}$	0.255(5)	0.25208(5)	0.49(1)	0.50(5)

Table 6.2: *Estimates for some critical parameters calculated by the DMRG with* $\lambda = 0.5$. *The exponents are compared with those from the DP and PC class.*

the estimates of the critical parameters we find for $n = 1$ and $n = 2$ when we fix the rate $\lambda = 0.5$ (point A and B in Fig. 6.5). When we repeated the calculations for different values of λ, we found the same exponents. We recover the exponents of DP and PC as expected, indicating that the DMRG is performing well.

6.3.2 The Case $n = 3$

Since the results of the DMRG are consistent with the Monte Carlo results for $n = 1$ and $n = 2$, we can confidently use it to study also the case $n = 3$. We proceed in the same way by calculating the gap. In Fig. 6.7 we plot the

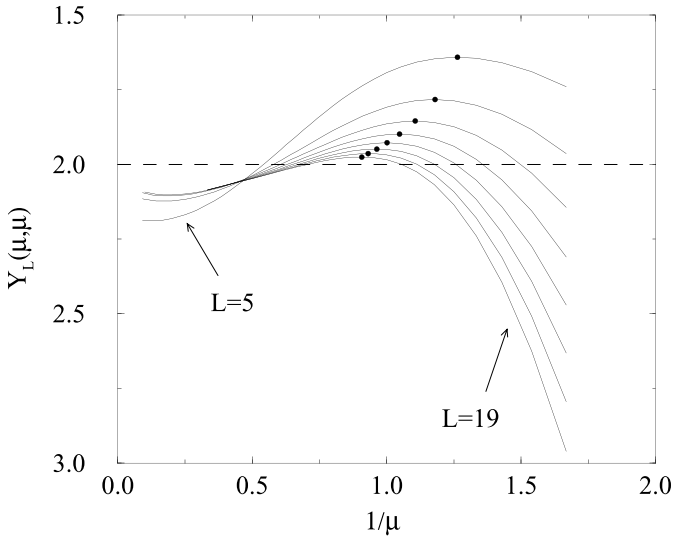

Figure 6.7: *Plot of* Y_L *for the model with* $n = 3$ *absorbing states along the line* $\lambda = \mu$.

quantity Y_L along the line $\lambda = \mu$. For this system with four states per site we calculated the gap with the DMRG for system sizes up to $L = 20$. In the right part of the plot we again clearly find the evidence of an active state $Y_L \sim -aL$. But the difference with the case $n = 2$ is that the maxima of the curves seem to shift towards $(Y_L = -2, 1/\mu = 0)$ for increasing system sizes. In other words, in the limit $L \to \infty$ the system is always active and the critical point is located at $1/\mu = 0$. This numerical evidence together with an analytical argument, which we will present later, leads us to expect that the model is critical only if $1/\mu = 0$, as indicated in the phase diagram in Fig. 6.5. When we extrapolate the estimates for the exponent, we find $z = 2.00(3)$.

To get access to more critical exponents we impose different boundary conditions. We replace (6.15) with

$$\phi_k \to A \qquad \text{with rate } p' \qquad \forall k. \tag{6.18}$$

For finite system lengths, these conditions destroy the stationarity of the absorbing states and the system has only one ground state, which has a non-zero particle density. Again we start with an analysis of the gap Γ'_L to the first excited state of the Hamiltonian.[2] At the critical point, the behaviour is as before $\Gamma'_L \sim L^{-z}$. However, in the active phase the gap is no longer asymptotically degenerate, as with the previous boundary conditions. The active state is stationary for every system length and the gap to the first excited state remains non-zero: for every lattice length L, the system decays exponentially in time towards the active state: $\lim_{L\to\infty} \Gamma'_L = \Gamma'_0 > 0$. The advantage is that we can use the gap itself to discriminate between the active and the critical phase, we do not need the logarithmic derivative.

Fig. 6.8 shows a plot of the gap Γ'_L along the line $\lambda = \mu$. For every non-zero value of μ an extrapolation of the gap for $L \to \infty$ yield a non-zero limit, i.e. we find the system to be active throughout the whole parameter space, consistent with the previous analysis.

These data also give the possibility to estimate the correlation length exponent along the time direction: $\nu_{||}$. Finite size scaling around the critical point $1/\mu = 0$ gives us the following scaling relation:

$$\Gamma'_L(\lambda = \mu) = \mu^{-\nu_{||}} f\left(\mu L^{-z/\nu_{||}}\right) \tag{6.19}$$

For μ fixed and $L \to \infty$, Γ'_L remains finite, so the scaling function should behave like $\lim_{x\to 0^+} f(x) = f_0$. As a consequence in the thermodynamic limit

[2] The ground state of this Hamiltonian is not trivial. Consequently it cannot be shifted out as in (6.16) and a calculation of the gap demands an explicit determination of the eigenvalue of the first excited state. In the DMRG we have to target the two lowest eigenvectors of the Hamiltonian simultaneously.

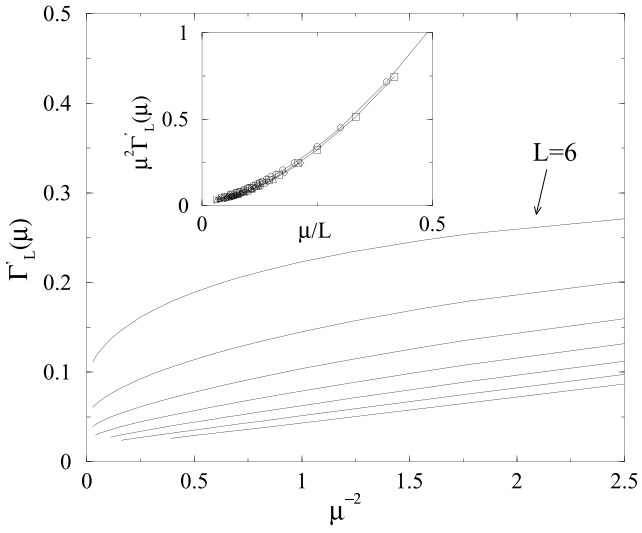

Figure 6.8: *Plot of the gap* Γ'_L*, for the model with* $n = 3$ *absorbing states along the line* $\lambda = \mu$ *and for system lengths* $L = 6, 8 \ldots, 18$*. Inset: scaling collapse of* $\mu^{\nu_{||}}\Gamma'_L(\mu)$ *as a function of* $\mu L^{-1/\nu_\perp}$ *with* $\nu_{||} = 2$ *and* $\nu_\perp = 1$ *for system lengths* $L = 10, 12, \ldots, 18$*.*

$L \to \infty$ the gap should vanish at the critical point as $\Gamma'_L \sim \mu^{-\nu_{||}}$. The linear behaviour of the gap for large L in Fig. 6.8, when plotted as a function of μ^{-2}, already indicates that $\nu_{||} = 2$ and this results is also consistent with the scaling collapse reported in the inset, where we took $\nu_{||} = 2$ and $z = 2$.

Finally, using the same boundary conditions we can calculate the expectation value of the particle density in the ground state. For finite systems this is non-zero, and we calculated this density, which we denote as ρ_L, at a central site of the lattice. When the system is on the critical line, the density should decay with L as $\rho_L \sim L^{-\beta/\nu_\perp}$. This is the technique we used to determine $\beta/\nu_\perp$ for $n = 1$ and $n = 2$ in the previous subsection. However, for $n = 3$ the critical line is at $\mu = \infty$ and can't be reached numerically. Hence we are forced to analyse ρ_L as a function of μ and L (we again use $\lambda = \mu$). For large L and large μ the particle density is expected to behave as $\rho_L \sim \mu^{-\beta}$. Therefore we define the effective exponent β as

$$\beta_{\text{eff}}(\mu, L) = -\frac{\partial \ln \rho_L(\lambda = \mu)}{\partial (\ln \mu)}, \tag{6.20}$$

which in the limit $L \to \infty$ and $\mu \to \infty$ converges to β.

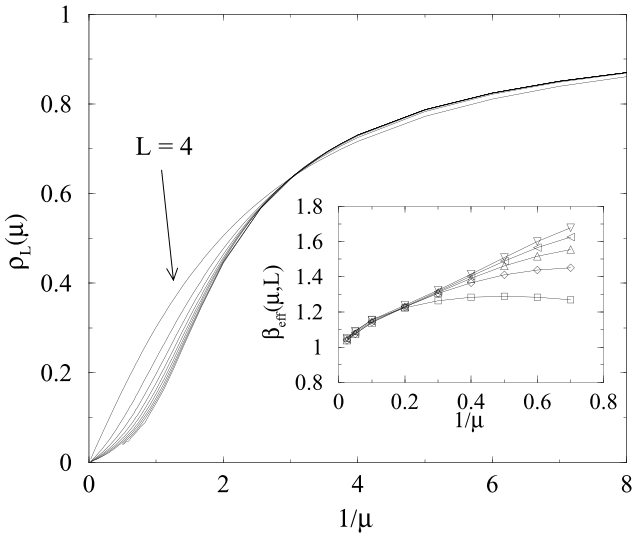

Figure 6.9: *Plot of the stationary particle density ρ_L at the centre of the system for the model with $n = 3$ absorbing states, along the line $\lambda = \mu$. The system sizes are $L = 4, 6 \ldots, 24$. For large μ the calculations were limited to $L = 14$. Inset: plot of the effective exponent β as a function of $1/\mu$ for system sizes $L = 6$ (lower curve) up to $L = 14$ (upper curve).*

In Fig. 6.9 we find that the $L \to \infty$ limit of the particle density (calculated along the line $\lambda = \mu$) only vanishes for $\mu \to \infty$, again indicating that the system is always active. The inset shows a plot of β_{eff} as a function of $1/\mu$ for various systems lengths. The extrapolated values for $L = 12$ and $L = 14$ is $\beta = 1.00(1)$.

In summary, we found that for $n = 3$, the system is always active, except for $1/\mu = 0$ where it is critical and we have exponents consistent with $z = 2$, $\nu_{||} = 2$, $\beta = 1$.

6.3.3 The Case $n = 4$

To conclude our numerical calculations for the case of permutation symmetric ground states, we studied the system with four inactive states per site. Here, we restricted ourselves to a calculation of the particle density ρ_L with boundary conditions (6.18). Our results are shown in Fig. 6.10.

From these data we find, as was the case for $n = 3$, that the system is active for any finite value of μ, and that the critical exponent $\beta = 0.98(4)$.

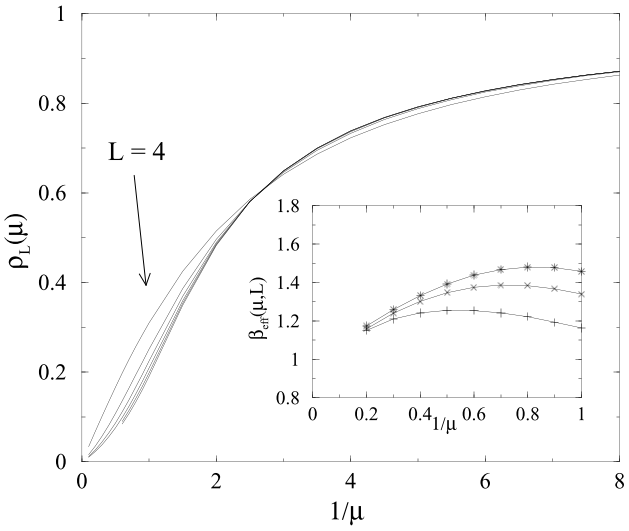

Figure 6.10: *Plot of the stationary particle density ρ_L at the centre of the system for the model with $n = 4$ absorbing states, along the line $\lambda = \mu$. The system sizes are $L = 4, 6 \ldots, 14$. For large μ the calculations were limited to $L = 10$. Inset: plot of the effective exponent β as a function of $1/\mu$ for system sizes $L = 6$ (lower curve) up to $L = 10$ (upper curve).*

6.3.4 Fast Rate Expansion for μ or $\lambda \to \infty$

In subsection 5.2.1 we mentioned an intuitive coarse-grained picture for the dynamics in the inactive phase of the $n = 2$ model. For long times, the dynamics were governed by interfaces between inactive domains, which performed annihilating random walks. On this basis the particle density was predicted to decay as $\rho \sim t^{-1/2}$. In the limit for the rate $\mu \to \infty$ this picture can be made mathematically exact.

For this purpose we apply the infinite-rate expansion, elaborated in subsection 2.3.4. There it was shown that when a certain reaction rate becomes infinite, the time evolution can be described by effective dynamics on a subspace of the original configuration space. These dynamics are constructed by projecting the original Hamiltonian on the subspace spanned by the groundstates of that one infinitely fast reaction process. In our model we first consider the case where the reaction rate for

$$\begin{matrix} \phi_k A \\ A\phi_k \end{matrix} \quad \to \quad \phi_k \phi_k \qquad \text{with rate } \mu_k$$

becomes infinite: $\mu \to \infty$. The ground states of this process are given by all configurations without particles[3]. Denote the subspace spanned by them as $\mathcal{W}$. In practice, the projection of the original Hamiltonian on $\mathcal{W}$ is performed by perturbing a state of $\mathcal{W}$ by one reaction of the model and projecting this again on $\mathcal{W}$. As a possible effective reaction consider :

$$\ldots\phi_k\phi_k\phi_k\phi_l\phi_l\ldots \overset{\text{perturbation (6.4)}}{\to} \ldots\phi_k\phi_k A\phi_l\phi_l\ldots \overset{\text{projection}}{\to} \ldots\phi_k\phi_k\phi_l\phi_l\phi_l\ldots$$

For a complete derivation we refer to our article [73]. The resulting effective dynamics in the limit $\mu \to \infty$ are determined by the processes

$$\phi_k\phi_l\phi_k \quad \to \quad \phi_k\phi_k\phi_k \quad \text{rate } 2 \tag{6.21}$$

$$\phi_k\phi_l\phi_l \quad \longleftrightarrow \quad \phi_k\phi_k\phi_l \quad \text{rate } 1/2 \tag{6.22}$$

$$\begin{array}{lcll} \phi_k\phi_l\phi_m & \to & \phi_k\phi_k\phi_m & \text{rate } 1 \\ & \to & \phi_k\phi_m\phi_m & \text{rate } 1. \end{array} \tag{6.23}$$

Note that this same result holds in the limit $\mu = \lambda \to \infty$, which was the case we investigated numerically.

Let us first review the case $n = 2$. When only two inactive states are present, reaction (6.23) is not possible and we indeed get diffusion and annihilation of domain walls and we recover the exponent $z = 2$. For a more general result, it is interesting to interpret the n inactive states as the possible spin values of an n-Potts model. In this language, the processes (6.21)-(6.23) obey the following rule: the central spin assumes the value of one of its neighbour spins with equal probability. The dynamics of our model in the limit $\mu \to \infty$ are therefore consistent with the requirements of detailed balance for an n-state Potts model at zero temperature. It is generally expected that if such dynamics include a domain wall diffusion, the system is critical with a dynamical exponent $z = 2$ [75], independent of n. In fact, the exponent $z = 2$ can be derived exactly when the rate of process (6.21) equals one and that of (6.23) equals 1/2 [76].

In conclusion we find that for $n \geq 3$ the system is critical when $\mu \to \infty$ and the dynamical exponent is $z = 2$. This value is in agreement with the numerical results of the previous subsections. Moreover, we numerically found that for $n = 3$ and $n = 4$ also the exponent β was the same. These facts together lead us to the conjecture that for all $n \geq 3$, the phase diagram is identical and the critical exponents are given by $\beta = 1, z = 2$ and $\nu_{||} = 2$.

[3] Also the configuration with all sites occupied by a particle is a ground state. However, this state can't survive any perturbation, and it is consequently irrelevant for the fast rate expansion.

It is also possible to draw some conclusions from an analogous expansion for $\lambda \to \infty$

$$AA \quad \to \quad \begin{matrix} A\phi_k \\ \phi_k A \end{matrix} \qquad \text{with rate } \tfrac{\lambda}{n}.$$

For this process the ground states are all configurations without neighbouring particle pairs and the effective dynamics can be constructed on the subspace spanned by these states. Each particle in this system separates two domains of inactive sites. Therefore, particles can be labelled by two indices. We denote A_{ij} a particle with an inactive site ϕ_i to its left and ϕ_j to its right. In the limit $\lambda \to \infty$ it is instructive to look at the dynamics of these particles. For the case $n = 1$ only one type of particle is present and when the effective dynamics are constructed [73] we find diffusion, $AA \to A$ and $A \to \phi$. The presence of the latter reaction ensures that the particle density decays exponentially in time. Consequently, for $n = 1$ in the limit $\lambda \to \infty$ the system is non-critical and inactive, independently of μ. This is in agreement with our numerical results: see phase diagram in Fig. 6.5.

For $n > 1$ the situation is less clear. Now the effective dynamics contain both processes that destroy and create particles. It is therefore in principle possible to have both an active and an inactive phase, depending on the value of μ. At this moment, we can draw no firm conclusions for the form of the phase diagram when $\lambda \to \infty$. On the basis of our numerical work and on the basis of our results for $\mu \to \infty$, we believe that the model is probably always active along that line when $n > 2$.

6.3.5 Relation with Branching and Annihilating Random Walks

In this subsection we do not take μ or λ infinite, but we still want to describe the dynamics on the level of domain boundaries. It is analogous to the reasoning Hinrichsen made in his paper [55] to relate the $n = 2$ case to the BARW with offspring two. This argument works as follows: indicating with X_{ij} the domain wall between two configurations ϕ_i and ϕ_j he considered an effective dynamics for the variables X_{ij}. As seen in the previous section such representation of the original model becomes exact either in the limit $\lambda \to \infty$ and then X_{ij} coincides with the particle A_{ij}, or in the limit $\mu \to \infty$ where X_{ij} coincides with the bond variable $\phi_i\phi_j$. For finite values of these rates one can still apply this reasoning at a coarse-grained level. In this case X_{ij} is not a sharp domain wall, but an object with a fluctuating thickness. Hinrichsen argued that in this coarse-grained representation the most likely reactions for $n = 2$ are:

$$X_{ij} \overset{(a)}{\to} X_{ij}X_{ji}X_{ij} \qquad X_{ij}X_{ji} \overset{(b)}{\to} \phi, \tag{6.24}$$

(For $n = 2$ one has obviously $i = 1, j = 2$ or vice versa). These reactions

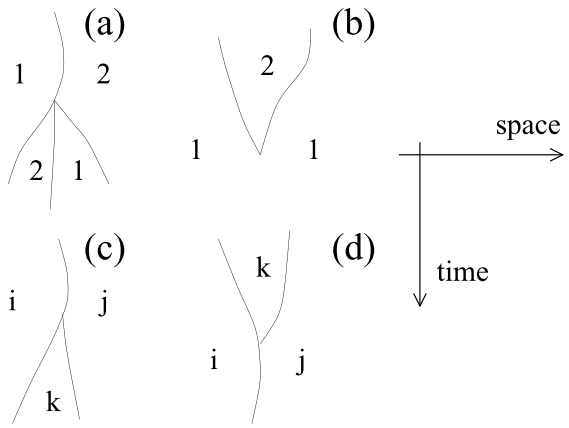

Figure 6.11: *Possible reactions in the coarse-grained representation of the generalised contact process for $n = 2$ (a)-(b) and $n \geq 3$ (a)-(d).*

are sketched in Fig. 6.11(a) and (b). They coincide with those of the BARW model with offspring two, suggesting that the universality class is PC.

We can extend these arguments to the case $n > 2$, where there is still the possibility of having reactions of type (a) and (b), but also reactions involving three different domains ($i \neq j$, $i \neq k$ and $j \neq k$).:

$$X_{ij} \stackrel{(c)}{\rightarrow} X_{ik}X_{kj} \qquad X_{ik}X_{kj} \stackrel{(d)}{\rightarrow} X_{ij} \tag{6.25}$$

When $n > 2$ there are actually $n(n-1)/2$ domain walls, and the model described by reactions (6.24) and (6.25) is now a BARW with more than one type of particles. To our knowledge this type of model has not been studied yet, but we expect it to be in the same universality class as the GCP with $n > 2$, i.e. always in an active state except when the rates for the processes (a) and (c) are zero, and with exponents $z = 2$, $\beta = 1$ and $\nu_{||} = 2$.

However, there is a BARW with more than one type of particles that has attracted some attention recently. The model was introduced by Cardy and Täuber [18] [19], who considered a system with N different particles A^α, where $\alpha = 1, 2, N$ which diffuse and undergo the reactions:

$$2A^\alpha \rightarrow 0 \qquad \text{with rate } 1 \tag{6.26}$$

$$A^\alpha \rightarrow A^\alpha A^\alpha A^\alpha \qquad \text{with rate } \sigma \tag{6.27}$$

$$A^\alpha \rightarrow A^\alpha A^\beta A^\beta \qquad (\alpha \neq \beta), \text{ with rate } \sigma'/(N-1). \tag{6.28}$$

These authors used a renormalisation approach based on a field theoretic description for stochastic processes. This method, which is bosonic of nature, yielded the same exponents we determined for the generalised contact process with $n \geq 3$ [19]. Notice that the coarse-grained representation of the GCP as defined by the reactions in Fig. 6.11 and the model defined by the reactions (6.26)-(6.28) do not actually coincide. While there is an obvious correspondence between (6.26), (6.27) with (b), (a) of Fig. 6.11, the reaction (6.28) does not have any obvious counterpart. It is not a priori clear therefore that the two models are in the same universality class. The coincidence of the critical exponents therefore suggests that one could replace (6.28) with other reactions, as for instance $A^\alpha \to A^\gamma A^\delta$, without changing the universality class. To our knowledge, BARW models with this kind of reactions have not been studied yet. They form an interesting subject for further investigation.

The model of Cardy and Täuber has raised some interest recently since it has been found that "fermionic" and "bosonic" versions of the model are in different universality classes [77]. In the fermionic version only one particle per lattice site is allowed, which implies that particles of different species block each other, whereas in the bosonic variant more particles can be on the same site and no blocking effects are present. In the fermionic version of the model it makes for instance a difference whether the two offsprings produced by the reaction (6.28) are placed to the same side or at opposite sides of the parent particle [77], [78]. If, for instance, they are placed at opposite sides the offsprings cannot annihilate through the reaction (6.26) because of the presence of the parent particle that blocks them. In the bosonic model the two offspring can instead always recombine.

It is important to stress here that in the multispecies BARW model we constructed [(6.24)-(6.25)] from a coarse-grained representation of the GCP there are no blocking effects. By the very construction of the model, two domain walls approaching each other can always annihilate. Therefore even if the model is clearly of fermionic nature its universality class, as found numerically, is that of the bosonic multispecies BARW.

6.3.6 The Effect of Breaking the Symmetry

As a final point we consider the effect of breaking the permutation symmetry of the inactive states of the model. For $n = 2$, Hinrichsen [55] explicitly broke the Z_2 symmetry by choosing $\mu_1 \neq \mu_2$ in the reaction (6.2). As a result he found the system to switch from PC to DP behaviour, which was understood as PC being related to the presence of an exact Z_2 symmetry.

For $n = 3$, we now perform a similar symmetry-breaking by considering the following two cases: (a) $\mu_1/2 = \mu_2 = \mu_3$ and (b) $2\mu_1 = \mu_2 = \mu_3$. In both

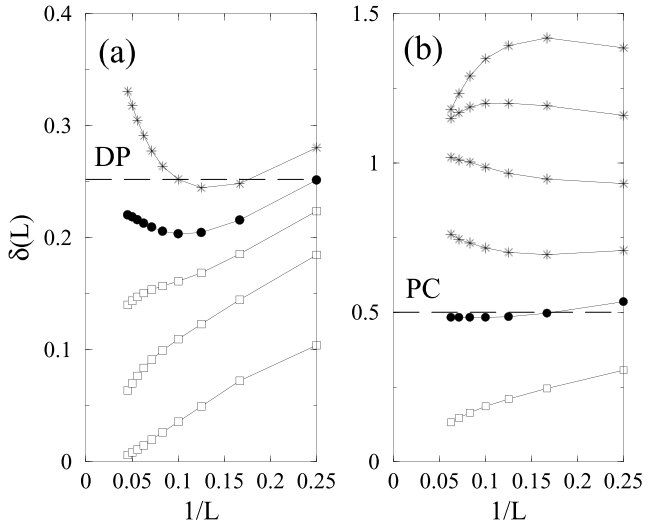

Figure 6.12: *Plot of δ for the generalised contact process with $n = 3$ for $\lambda = 0.5$, $p' = 1.5$ and (a) $\mu_1/2 = \mu_2 = \mu_3$, (b) $2\mu_1 = \mu_2 = \mu_3$. Symbols refer to curves calculated in the inactive phase (stars), at the critical point (filled circles) and in the active phase (empty squares). At criticality $\delta(L)$ converges towards the values of $\beta/\nu_\perp$ expected for DP (a) and PC (b), and indicated by horizontal dashed lines in the figure. Notice the two distinct behaviours of δ in the inactive phase.*

cases the system has a Z_2 symmetry due to the equivalence of the states ϕ_2 and ϕ_3. The difference is that starting from a random configuration in the second case the system is more likely to reach the absorbing states $(\phi_2, \phi_2, \phi_2, \ldots)$ and $(\phi_3, \phi_3, \phi_3, \ldots)$ compared with $(\phi_1, \phi_1, \phi_1, \ldots)$, while in the first case the reverse is true. We calculated the particle density $\rho_L(\lambda, \mu_1, \mu_2, \mu_3)$ as before, using the boundary-term (6.18). Depending on the phase in which the model is, the density will behave as $\rho_L = \rho_0 + Ce^{-aL}$ (in the active region), $\rho_L \sim L^{-\beta/\nu_\perp}$ (at criticality), or $\rho_L \sim e^{-aL}$ (in the inactive phase). If we define

$$\delta(L) = -\frac{\ln\left[\rho_{L+1}/\rho_{L-1}\right]}{\ln\left[(L+1)/(L-1)\right]}, \tag{6.29}$$

we expect $\lim_{L\to\infty} \delta(L)$ to be zero in the active phase, to be $\beta/\nu_\perp$ at critical points, and $+\infty$ in the inactive phase.

In Fig. 6.12 we plotted $\delta(L)$ as a function of $1/L$ for cases (a) and (b) with the choice $\lambda = 0.5$ and injection rate $p' = 1.5$. In both cases for small

μ one finds the typical scaling behaviour of the active phase with $\delta(L) \to 0$ just as for the case $\mu_1 = \mu_2 = \mu_3$. For large μ_k however the situation differs from the symmetric model. For (a), we find $\delta(L) \to +\infty$ for large μ, i.e. one has a standard inactive phase with a particle density exponentially small in L. In case (b), $\delta(L)$ becomes equal to 1, implying that the inactive phase is itself critical with $\beta/\nu_\perp = 1$. In between the active and the inactive phase we have a critical point where $\delta(L)$ is going to a distinct finite value. The critical point estimates of $\delta(L)$ are marked by filled circles in Fig. 6.12. For case (a) the critical point is at $\mu_1 \approx 0.64$, while for (b) it is at $\mu_1 \approx 0.42$. The value of $\beta/\nu_\perp$ agrees with that of DP and PC respectively, as can be seen in Fig. 6.12 where the critical values of these universality classes are indicated with a dashed line.

This indicates that on breaking the symmetry of the inactive states the remaining symmetry of the *dominant* rates μ_i determines the critical behaviour. In case (b) $\mu_1 < \mu_2 = \mu_3$ the dominant rates still have a Z_2 symmetry leading to the PC universality class, while in case (a) $\mu_1 > \mu_2 = \mu_3$, DP critical behaviour is recovered.

6.4 Conclusions

We studied a generalised contact process first introduced by Hinrichsen, mainly by applying the DMRG. With this technique we verified that for $n = 2$, the critical line of the model is in the PC universality class, consistent with earlier results coming from simulations.

A first set of new results was obtained for the case $n = 3$, for which we found that the model is always active, except when $\mu \to \infty$, which corresponds to the critical line of the model. From our numerical work we determined the critical exponents to be equal to $z = 2, \nu_{||} = 2$ and $\beta = 1$. Using well established scaling laws (cf section 3.2), other exponents can be determined from these three. For $n = 4$, we found evidence that the phase diagram is the same, and that the critical exponent β also equals 1. Secondly, using a fast rate expansion that becomes exact for $\mu \to \infty$, we were able to argue that in that limit $z = 2$ for $n \geq 2$. It can be hoped that by examining the model for μ^{-1} small using perturbation techniques, it may be possible to determine also the exponents β and $\nu_{||}$ exactly. On the basis of these numerical and exact results we conjectured that the universality class of the model is the same for all $n \geq 3$.

The exponent values that we found for $n \geq 3$ coincide with those of the BARW model with more than one type of particles introduced by Cardy and Täuber [18], [19]. We were able to give an heuristic argument that explains

why the two models could be in the same universality class. It is interesting to remark that despite many attempts the number of universality classes found for phase transitions out of an adsorbing phase, remains very limited. It could have been hoped *a priori* that for the generalised GCP studied here, new universality classes could appear for $n > 2$. In a sense our results show that this is true, but only in the least exciting way possible: the universality class does not depend on n, and moreover the exponents take on rather trivial values. One could hope that by lowering the permutation symmetry of the absorbing states to a cyclic Z_n-symmetry, other universality classes could appear for $n \geq 4$. This could be done, e.g. by having the rates of the process (6.4) depend on $|k-l| \bmod(n)$. But since this would only make a difference for $n \geq 4$, it will probably be difficult to investigate such a model with the numerical techniques currently available.

We also verified that if one breaks the permutation symmetry of the model with $n = 3$, one recovers a DP or PC universality, suggesting that it is the symmetry of the largest rates that determines the universality class.

Finally, we remark that the consistency of the DMRG results with those coming from simulation for $n = 2$, or with the exactly determined value of z for $n \geq 3$, shows convincingly that the DMRG can be trusted as a powerful method in the study of (criticality in) non equilibrium systems.

Chapter 7

Contact Process with Quenched Disorder

This chapter investigates the critical properties of the contact process with quenched random rates. In the limit of very small disorder the SRG is applied to argue that disorder is relevant. Using this SRG a numerical and analytical calculation show that the Harris criterion can be applied in this non-equilibrium context. For strong disorder the SRG procedure is reformulated in the spirit of a SDRG like that of Ma, Dasgupta and Hu [79], [80]. The resulting RG flow can be handled analytically and has an attractive fixed point at infinite disorder which represents a new universality class of absorbing state phase transitions. The critical exponents can be proven to be those of the RTIM model [81], [82] and are expected to be exact. Finally a DMRG calculation numerically recovered the strong disorder exponents and was used to probe the intermediate disorder regime.

The results of this project can be found in [83].

7.1 Introduction

In subsection 5.2.1 I spoke about possibilities to find absorbing state phase transitions with critical behaviour *not* belonging to the class of directed percolation. Besides the previously discussed option of extra symmetries, there is that of disorder. We will in this chapter discuss the contact process with *quenched disorder*. Disordered, because the reaction rates can change from site to site and quenched because the rates do not change in time. We will mainly consider the case where the rates are independently and identically distributed stochastic variables.

Very little is known yet about non-equilibrium phase transitions in disor-

dered systems. Earlier work on the contact process and directed percolation with quenched disorder focused mainly on dynamical properties. As an example it was predicted rigorously, that there exists a phase in which, starting from one seed particle, the average number of particles grows in time in a sublinear way [84]. Remember that for the homogeneous process this quantity decays exponentially to zero in the inactive phase, while it grows linear in time in the active phase. This intermediate phase with sublinear behaviour was confirmed in numerical studies [85], [86], [87] and the corresponding exponents were found to be non-universal but depending on the probability distribution the rates were drawn from. A scaling theory has been established [87], relating various dynamical exponents. Other authors argued on the basis of numerical work that the model's dynamics has features of slow, glassy behaviour [88]. The phase where these phenomena are occurring has some parallels with the Griffiths phase, known from disordered *equilibrium* systems [1].

In our research, we mainly considered the stationary behaviour of the model. Given the slow relaxation properties, this late-time regime cannot easily be studied with simulations. We used real-space renormalisation and DMRG techniques, which suffer less from this slow dynamics. In the strong disorder limit, we found a new universality class of absorbing state phase transitions. The critical properties can be determined exactly and are related to those of the random transverse field Ising model (RTIM). Since quenched disorder in this latter model and in equilibrium models in general is better understood we give a short introduction to it.

7.2 Quenched Disorder in Quantum Systems

The (one-dimensional) RTIM model is a quantum spin chain in thermal equilibrium. Its Hamiltonian is defined by

$$H = -\sum_i J_i \sigma_i^z \sigma_{i+1}^z - \sum_i h_i \sigma_i^x. \tag{7.1}$$

The operators σ are Pauli matrices and J_i, h_i are positive constants. h_i is a transverse field along the X-axis and J_i is a ferromagnetic coupling constant. Consider first the homogeneous (TIM) model $h_i = h, J_i = J$. In this model, the possible order created by the alignment of spins due to the coupling constant J is opposed by both temperature effects and the presence of the transverse field h. When the temperature is strictly positive, the quantum effects are however irrelevant and the system is essentially a one-dimensional classical system which is always in the disordered phase [89]. The interesting behaviour is located at zero temperature where h/J becomes a relevant parameter. When h/J is small enough a macroscopic magnetisation is present

$\langle \sigma^z \rangle = m \neq 0$, whereas for large h/J the system is in the disordered phase with $m = 0$. In between is a critical point where a continuous "quantum" phase transition occurs [89]. Around this critical point the traditional scaling theory is valid. However, when the TIM contains disorder (J_i and h_i are quenched random variables), the physics of this phase transition changes radically.

Consider all J_i and h_i to be drawn independently from respectively the probability distribution $P(J_i)$ and $\Pi(h_i)$. The order parameter is then defined as $m = [\langle \sigma^z \rangle]_{\text{av}}$: the expectation value of the magnetisation, averaged over the disorder ($[\quad]_{\text{av}}$). Next, one can define $\Delta = [\ln (h_i/J_i)]_{\text{av}}$ as the control parameter. When Δ is small the system is in the ordered phase with a non-zero magnetisation m and if Δ is increased beyond a critical value Δ_c the system has again a continuous quantum phase transition from an ordered to a disordered phase. But this is as far as the equivalence with the homogeneous model goes.

First, it was known for a long time that around the quantum critical point of the RTIM there exists a whole phase where the free energy of the system is non-analytical. This region of the phase diagram is called the Griffiths phase [90], [91]. For example, in the disordered part of this phase the susceptibility is infinite. The magnetisation is zero but extremely sensitive to the application of an external field along the Z-axis. The physical reason for this singular behaviour is the existence of "rare events". When averaging over the probability distributions P and Π, for strongly disordered systems one encounters sometimes very large regions of strongly coupled spins. These realisations are very rare, but their contribution to the susceptibility is also very large since these regions are extremely sensitive to an external field. It is true for several other observables that in the Griffiths phase of the RTIM the presence of rare but large ordered regions controls the expectation values. This phenomenon implies that the system is not self-averaging: taking one realisation of an infinitely large system, does not produce the same result as averaging over all realisations.

More recently, D.S. Fisher used a *strong disorder renormalisation group* (SDRG) approach, originally introduced by Ma, Dasgupta and Hu [79], [80], to explain a lot of the properties of the RTIM model [81], [82]. This renormalisation exploits the dominance of the rare events by concentrating the RG on them. The resulting RG flow for P and Π can be determined analytically and is expected to be exact in the limit of infinite disorder. It turns out that the RG has an attractive fixed point for this limit. Hence, the critical exponents in this infinite randomness fixed point (IRFP) are expected to give a correct description of the late-time behaviour for strongly disordered systems. Moreover, for this RTIM model, Fisher found that the *whole* parameter space

is attracted to the IRFP [81], [82]. This means that even for systems with a minimal disorder the critical behaviour is described by the IRFP. Let us summarise some of the critical features.

Denote $\delta = (\Delta - \Delta_c)$ the distance away from the critical point. First, one can calculate the spatial correlation function $C(x,\delta) = \left[\left\langle \sigma_i^z \sigma_{i+x}^z \right\rangle\right]_{\text{av}}$. This behaves in the familiar way: it decays exponentially in $|x|$ and the corresponding correlation length diverges as $\xi \sim \delta^{-\nu_\perp}$ with

$$\nu_\perp = 2. \tag{7.2}$$

It is interesting to mention that in this case one can show the effect of the rare events very nicely. When averaging over the random realisations to calculate $\left[\left\langle \sigma_i^z \sigma_{i+x}^z \right\rangle\right]_{\text{av}}$, one will almost every time find a very small number for $\left\langle \sigma_i^z \sigma_{i+x}^z \right\rangle$. However, every now and than one encounters a rare realisation for which $\left\langle \sigma_i^z \sigma_{i+x}^z \right\rangle$ is of order unity. To eliminate the contribution of these rare events, one could define a correlation function as

$$C_{\text{typ}}(x,\delta) = \exp\left[\ \left[\ln \left\langle \sigma_i^z \sigma_{i+x}^z \right\rangle\right]_{\text{av}}\ \right].$$

This is called the *typical* correlation function since it characterises the behaviour of the most likely realisations. If the system was self-averaging, the behaviour of $\left\langle \sigma_i^z \sigma_{i+x}^z \right\rangle$ would in the limit $x \to \infty$ not depend on the specific realisation of the quenched randomness and C_{typ} would be equal to C. However, the correlation length associated with C_{typ}, called the *typical* correlation length, diverges as $\xi_{\text{typ}} \sim \delta^{-1}$ and we find

$$(\nu_\perp)_{\text{typ}} = 1. \tag{7.3}$$

This deviation from the exponent $\nu_\perp$ is a sign of the domination of the rare events.

Next the dynamical exponent $z = \frac{\nu_\parallel}{\nu_\perp}$ can be determined. In traditional scaling z can be defined as the exponent relating the spatial correlation length with the relaxation time $\tau \sim \xi^z$. In the disordered quantum chains one can calculate the average (time and space) correlation functions and the corresponding τ and ξ turn out to be related by $\tau \sim e^{a\sqrt{\xi}}$with $a > 0$ a constant, or

$$\ln \tau \sim \sqrt{\xi} \tag{7.4}$$

This implies

$$z = \infty \quad \text{and} \quad \nu_\parallel = \infty. \tag{7.5}$$

Finally we consider the magnetisation exponent in the ordered phase $\delta \leq 0$. One distinguishes the surface magnetisation m_s at a boundary site of a semi-infinite system and the bulk magnetisation m_b in an infinite system. In a

numerical study of systems with finite length L, they can be determined by fixing a spin on site 1 and calculating the expectation value of the magnetisation on site $L/2$ (m_b) and site L (m_s). In the limit $L \to \infty$ one gets[1]

$$\begin{array}{ll} m_b \sim \delta^{\beta_b} & \text{with } \beta_b = 2 - \frac{1+\sqrt{5}}{2} = 0.381966... \\ m_s \sim \delta^{\beta_s} & \text{with } \beta_s = 1 \end{array} \tag{7.6}$$

The SDRG has been applied to several random quantum chains (Ising, Potts, clock, Ashkin-Teller model, etc.) leading to presumably exact results, both at the quantum critical point and in the Grifiths phase [93], [94]. In these models it was sometimes observed that a minimum disorder is needed before the critical behaviour is described by the IRFP. In these cases the basin of attraction of the IRFP in the RG flow is limited. Recently, it was found that in such a situation there may appear an intermediate disorder regime with continuously varying critical exponents [95].

In the subsequent sections, we will study the critical behaviour of the quenched random contact process and find results very similar to those of the random quantum chains.

7.3 Small Disorder

Let us start by defining the model. The two possible reactions of the contact process are now site-dependent and defined as

$$\begin{array}{lcll} \phi_i A_{i+1} \\ A_i \phi_{i+1} & \to & A_i A_{i+1} & \text{with rate } \frac{\lambda_i}{2} \\ A_i & \to & \phi_i & \text{with rate } \mu_i. \end{array} \tag{7.7}$$

The rates λ_i and μ_i are independently distributed according to the probability distributions

$$\lambda \sim P(\lambda) \tag{7.8}$$

$$\mu \sim \Pi(\mu). \tag{7.9}$$

Analogous to the RTIM we will be using the logarithm of these rates, which we define as

$$\begin{array}{lcl} \Lambda_i & = & \ln \lambda_i \\ M_i & = & \ln \mu_i. \end{array} \tag{7.10}$$

[1] The exponent β_s was known before the introduction of the SDRG [92].

Finally we introduce two control parameters

$$A = \left[\ln \frac{\lambda_i}{\mu_i}\right]_{\text{av}} = [\Lambda_i]_{\text{av}} - [M_i]_{\text{av}} \tag{7.11}$$

$$R = var\left(\ln \frac{\lambda_i}{\mu_i}\right) = var\left(\Lambda_i\right) + var\left(M_i\right), \tag{7.12}$$

where we used the independence of λ_i and μ_i, and the average and variance are with respect to the distributions (7.8)(7.9). Since λ_i/μ_i can be seen as the local activity (with respect to the creation of particles) the control parameter A is a measure for the "Activity" and R for the "Randomness" of the model.

We explained in Chapter 5, that the standard renormalisation can be used to accurately determine the critical behaviour of the homogeneous contact process. We therefore expect the procedure to work as well for the quenched random contact process when the disorder R is small.

7.3.1 The SRG

In the previous applications of the SRG to non-trivial absorbing state phase transitions, we forced the intracell Hamiltonian to have an active state by removing on the *central* site the reactions that destroy particles (cf Fig. 5.2). In the current situation is will turn out to be more useful if we perform the grouping of the operators in a different way. Denote h_i^1 the one-site Hamiltonian representing the reaction $A \to \phi$ on site i with rate μ_i, and h_i^2 the two-site Hamiltonian for the reaction $A\phi, \phi A \to AA$ on site $i, i+1$ with rate $\lambda_i/2$. Using the same α-index notation for the cell as in Chapter 5, we regroup the Hamiltonian terms as given in Fig. 7.1. The intercell Hamiltonian between cell

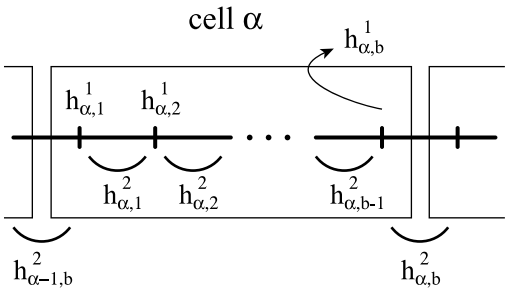

Figure 7.1: *The regrouping of the Hamiltonian terms: the intracell Hamiltonian contains all terms inside the rectangle and the intercell Hamiltonian those outside.*

α and $\alpha+1$ is given by $h^1_{\alpha,b}+h^2_{\alpha,b}$, the other terms are contained in the intracell Hamiltonians. As it should be, any intracell Hamiltonian has two ground states: the absorbing empty lattice and an active stationary state. These will again serve as effective cell vacancy and particle for the SRG procedure.

One can proceed in the same way as in Chapter 5, to proof that there is no proliferation of interactions. Since our regrouping lacks left-right symmetry, this result is however remarkable. And indeed, if one works out the proof, one notices that the self-enantiodromy property of the contact process is now explicitly needed to find this conservation of form. Consequently, this asymmetric regrouping cannot be used in, for example, the generalised contact process with two absorbing states.

We now give the analytical result for the SRG with cell length $b=2$. We denote the sites of the renormalised lattice by the index α, which is used for the cells of the original system. The renormalised values of the rates $\lambda_{\alpha,2}$ and $\mu_{\alpha,2}$ of the intercell Hamiltonian will be denoted as λ'_α and μ'_α. See Fig. 7.2. The SRG equations are then given by

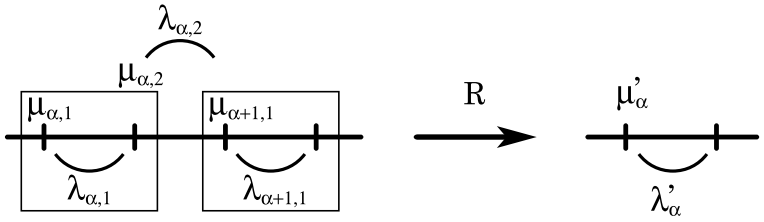

Figure 7.2: *SRG procedure for $b=2$. The intercell rates $\lambda_{\alpha,2}$ and $\mu_{\alpha,2}$ are renormalised to λ'_α and μ'_α.*

$$\begin{aligned} \lambda_{\alpha,2} &\xrightarrow{\mathcal{R}} \lambda'_\alpha = \lambda_{\alpha,2}\left(2\tfrac{\mu_{\alpha+1,1}}{\lambda_{\alpha+1,1}}+1\right)^{-1} \\ \mu_{\alpha,2} &\xrightarrow{\mathcal{R}} \mu'_\alpha = \mu_{\alpha,2}\left[1-\left(2\tfrac{\mu_{\alpha,1}}{\lambda_{\alpha,1}}+1\right)^{-2}\right] \end{aligned} \tag{7.13}$$

If we know the original distributions $P(\lambda)$ and $\Pi(\mu)$ we can use these equations to calculate the renormalised distributions and produce an RG flow in the parameter space of the control parameters A and R, which are the determined by P and Π. However, before we turn to this point, there are a few considerations that need to be made.

First, in the original system the rates were independent variables, does this still hold for the renormalised system? This point is the reason why we introduced the asymmetric regrouping of the Hamiltonian. In the resulting

equation (7.13) we see that the renormalisation of rate $\lambda_{\alpha,2}$ only depends on the rates in the cell to its right, while that of $\mu_{\alpha,2}$ only depends on the rates in the cell to its left. Since the original rates are independent, λ'_α will be not be correlated to μ'_α. The only correlations that occur after the SRG transformation, are those between λ'_α and $\mu'_{\alpha+1}$. However, when the cell size b of the SRG procedure becomes larger, these correlations will decrease. We will therefore make the approximation that the renormalised variables are again independent. When we drop the irrelevant indices we obtain the SRG equations

$$\begin{aligned} \lambda_i &\xrightarrow{\mathcal{R}} \lambda'_i = \lambda_i \left(2\tfrac{\mu_k}{\lambda_k}+1\right)^{-1} \\ \mu_i &\xrightarrow{\mathcal{R}} \mu'_i = \mu_i \left[1-\left(2\tfrac{\mu_l}{\lambda_l}+1\right)^{-2}\right] \end{aligned} \tag{7.14}$$

or in terms of the logarithmic rates Λ_i and M_i

$$\begin{aligned} \Lambda_i &\xrightarrow{\mathcal{R}} \Lambda'_i = \Lambda_i - \ln\left[2e^{M_k-\Lambda_k}+1\right] \\ M_i &\xrightarrow{\mathcal{R}} M'_i = M_i + \ln\left[1-\left(2e^{M_l-\Lambda_l}+1\right)^{-2}\right] \end{aligned} \tag{7.15}$$

where we used different indices for uncorrelated variables.

Secondly, there is the question whether the renormalised distributions P' and Π' are of the same form as P and Π. If we can find form-invariant distributions, we could iterate an analytical RG flow in the (A,R) space, which for small R values can be expected to be accurate.

7.3.2 Lognormal Distribution

We will now show that for small R-values, the SRG with cell size $b=2$ leaves lognormal distributions for λ_i and μ_i form invariant. Instead of working directly with λ_i and μ_i we will switch to the logarithmic rates Λ_i and M_i as defined in (7.10). If λ_i and μ_i are drawn from a lognormal distribution, Λ_i and M_i have a normal distribution. We therefore define Λ_i and M_i to be independently and identically distributed according to

$$\Lambda_i \sim N\left(\Lambda_0, \sigma_\Lambda^2\right) \tag{7.16}$$

$$M_i \sim N\left(M_0, \sigma_M^2\right). \tag{7.17}$$

Where $X \sim N(X_0, \sigma_X^2)$ means that X has a normal distribution with mean X_0 and variance σ_X^2, i.e. $X \sim \frac{1}{\sqrt{2\pi}\sigma_X} e^{-\frac{(X-X_0)^2}{2\sigma_X^2}}$. For this distribution the control parameters of the system are simply

$$\begin{aligned} A &= \Lambda_0 - M_0 \\ R &= \sigma_\Lambda^2 + \sigma_M^2. \end{aligned}$$

We now have to calculate the distribution of the renormalised rates defined by (7.15). Hereto we use the following two properties

$$\left\{\begin{array}{l} X \sim N(X_0, \sigma_X^2) \\ Y \sim N(Y_0, \sigma_Y^2) \end{array}\right. \qquad \begin{array}{c} X, Y \text{ indepedent} \\ \Longrightarrow \end{array} \qquad \{X + Y \sim N(X_0 + Y_0, \sigma_X^2 + \sigma_Y^2)$$

$$\left\{\begin{array}{l} X \sim N(X_0, \sigma_X^2) \\ Y = f(X) \quad \text{analytical} \\ \qquad\quad \text{monotonic} \end{array}\right. \qquad \begin{array}{c} \sigma_X << 1 \\ \Longrightarrow \end{array} \qquad \left\{\begin{array}{l} Y \sim N(Y_0, \sigma_Y^2) \\ Y_0 = f(X_0) \quad \sigma_Y = \sigma_X \, |f'(X_0)|. \end{array}\right.$$

For this last property one has to transform the distribution of X according to $f(X)$ and make an asymptotic expansion for very small σ_X. These two properties ensure that for $\sigma_\Lambda << 1$ and $\sigma_M << 1$ the renormalised stochastic variables Λ_i' and M_i' are again described by a normal distribution. The resulting RG equations for the control parameters A and R can be found by a simple calculation and are given by

$$\begin{array}{lcl} A = \Lambda_0 - M_0 & \stackrel{\mathcal{R}}{\to} & A - \ln\left[2e^{-A} + 1\right] - \ln\left[1 - \left(2e^{-A} + 1\right)^{-2}\right] \\ R = \sigma_\Lambda^2 + \sigma_M^2 & \stackrel{\mathcal{R}}{\to} & R\left\{1 + \left(\frac{2e^{-A}}{2e^{-A}+1}\right)^2 + \left[\frac{4e^{-A}\left(2e^{-A}+1\right)^{-3}}{1-(2e^{-A}+1)^{-2}}\right]^2\right\} \end{array} \tag{7.18}$$

which can be expected to be correct in the limit $R \to 0$.

Let us analyse these equations. First, we notice that $R = 0$ is an invariant line of the RG flow, corresponding to the homogeneous contact process. The fixed point on this line is given by ($R = 0$, $A_c = \ln\left(1 + \sqrt{5}\right) = 1.174...$). This value for A corresponds in the original rates to $\frac{\lambda}{\mu} = 3.236...$, which is the approximation of the homogeneous critical point $\frac{\lambda}{\mu} = 3.297...$ for cell size $b = 2$. Secondly, we notice that a disordered system $R > 0$, will by the SRG be mapped on a system with a larger R. This suggests that disorder is relevant in the contact process: the homogeneous fixed point is unstable for any amount of quenched disorder, and a cross-over will appear to a disorder fixed point. To make this statement quantitative we can linearise the RG flow in the homogeneous fixed point. This results in:

$$\mathcal{R}\begin{pmatrix} A_c + \delta A \\ \delta R \end{pmatrix} = \begin{pmatrix} A_c \\ 0 \end{pmatrix} + \begin{pmatrix} \frac{3(7+3\sqrt{5})}{11+5\sqrt{5}} & 0 \\ 0 & \frac{169+75\sqrt{5}}{123+55\sqrt{5}} \end{pmatrix} \begin{pmatrix} \delta A \\ \delta R \end{pmatrix}.$$

We find that both $(A - A_c)$ and R are relevant scaling variables and the RG eigenvalues are respectively $y_1 = 0.890...$ and $y_2 = 0.452....$ The former

eigenvalue is an approximation for the homogeneous exponent $\frac{1}{\nu_\perp} = 0.911...$ while the ratio of y_2/y_1 gives the cross-over exponent

$$\phi = \frac{y_2}{y_1} = 0.508....$$

This exponent makes it possible to estimate how small R needs to be in order to still observe the homogeneous critical behaviour. This becomes clear by using the scaling relation for the particle density: $\rho\left[(A - A_c), R\right] = b^{-\beta/\nu_\perp} \cdot \rho\left[b^{1/\nu_\perp}(A - A_c), b^{y_2}R\right]$ which implies $\rho\left[(A - A_c), R\right] = (A - A_c)^{-\beta} \cdot \rho\left[(A - A_c)^{-\phi}R\right]$. For R very small, the second factor in the scaling of ρ is essentially a constant and one observes the homogeneous exponent β. When R becomes larger the second factor in the scaling of ρ comes into play. A criterion for the value of R where this happens is given by the "cross-over point" $(A - A_c)^{-\phi}R = 1$.

In equilibrium statistical mechanics, the *Harris criterion* [96] relates the cross-over exponent of a disordered system to its spatial dimension and the exponent $\nu_\perp$, provided the disorder has only short-range correlations. For one-dimensional systems this relation is given by

$$\phi = 2 - \nu_\perp \quad \text{or} \quad y_2 = \frac{2}{\nu_\perp} - 1. \tag{7.19}$$

For the random contact process with uncorrelated disorder it predicts $y_2 = 0.823...$ $\phi = 0.903...$ while our renormalisation gave $y_2 = 0.452...$ $\phi = 0.508....$ In the derivation of the Harris criterion, typical equilibrium techniques are used [1], so it is unclear whether this relation should hold in general for non-equilibrium systems.[2] For the contact process however, we will see that the exponent ϕ obtained from the SRG does converge to the Harris value when the cell size b of the SRG goes to infinity. In the next subsection we will show this numerically, using a simpler distribution, and in the subsection thereafter we will give more general analytical arguments for it, based on the SRG.

Finally we used this lognormal distributions to get a first idea of the RG flow for strong disorder. For larger R values, the distributions do not remain lognormal, and we approximated the RG flow by "projecting" the renormalised distributions after each RG step on lognormal ones with a corresponding mean and variance. The resulting flow is plotted in Fig. 7.3a. Although the quantitative part of the flow cannot be trusted for large disorder, as we will explain later, it is interesting to take a closer look at this region. For simplicity however, we will use a simpler distribution that can still be handled analytically in this limit.

[2] For directed percolation there exist heuristic arguments, suggesting that the Harris criterion is valid [85].

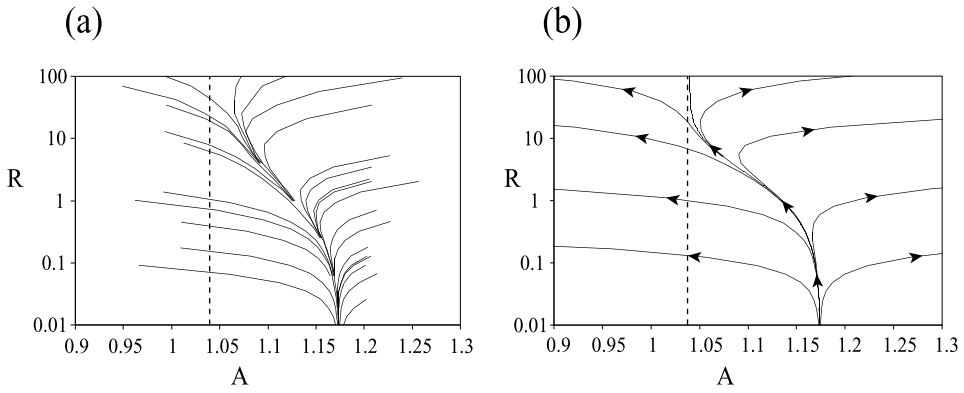

Figure 7.3: *The RG flows produced by the SRG with cell size $b = 2$ for the random contact process. The R-axis is put on a logarithmic scale. a) Lognormal distributions are used for λ_i and μ_i. The SRG is performed numerically. b) A binary distribution is used for λ_i. The SRG is performed analytically. In both plots, the vertical dotted line is located at $A = \ln\sqrt{8}$*

7.3.3 Binary Distribution

The advantage of a discrete distribution is that the averaging can be performed exactly. For small systems an analytical treatment is possible and for "medium size" systems a complete enumeration of the disorder-realisations is numerically manageable. To make this as simple as possible without losing the essential physics we take the rate μ_i equal to 1 for all sites and the rate λ_i binary distributed with equal probability:

$$\lambda_i \sim P(\lambda) = \frac{1}{2}\delta\left(\lambda - \lambda^+\right) + \frac{1}{2}\delta\left(\lambda - \lambda^-\right) \tag{7.20}$$

$$\mu_i \sim \Pi(\mu) = \delta(\mu - 1). \tag{7.21}$$

All λ_i are independent and we choose the convenient parametrisation $\lambda^{\pm} = e^{A \pm \sqrt{R}}$ from which we obtain

$$\Lambda_i = A \pm \sqrt{R} \qquad \text{and} \qquad M_i = 0 \tag{7.22}$$

where A and R are indeed the control parameters as defined by (7.11) and (7.12). When we perform an SRG transformation, the renormalised rates will not have a binary distribution. We approximate the RG flow by projecting these distributions on binary ones with the same mean and variance.

Let us start with the SRG for a cell size $b = 2$, given by (7.15). In this equation, only three independent $\lambda's$ are present. Consequently, a calculation

b	$\mathbf{y}_2$
5	0.7857683511483862
6	0.7864534810809475
7	0.7871762752097698
8	0.7878728119763543
9	0.7885234099706365
10	0.7891242396190991
11	0.7896772827398393
$b \to \infty$	$y_2 = 0.81(2)$ $\phi = 0.89(2)$
Harris	$y_2 = 0.823...$ $\phi = 0.903...$

Table 7.1: *Cross-over exponent found by SRG for the quenched random contact process with a binary distribution. The averaging was performed exactly. The result is compared with the values of the Harris criterion.*

of the renormalised A and R only involves $2^3 = 8$ possible realisations, all with equal probability. This can easily be done analytically and the resulting RG flow is drawn in Fig. 7.3b. In this flow we clearly find an attractive fixed point with an infinite R-value. To find the precise critical value of A we approximate the RG equations (7.15) to zeroth order in $e^{-|M_i - \Lambda_i|}$ for $R \to \infty$. In this limit the RG equation for A becomes

$$\mathcal{R}(A) = A + \left[A - \ln\sqrt{8}\right]. \tag{7.23}$$

We find that the infinite randomness fixed point is located at $A = \ln\sqrt{8}, R = \infty$. In the next section we will show that this value is exact. With Equation (7.23) we also have access to the critical exponent $\nu_\perp$.

$$\left.\frac{\partial \mathcal{R}(A)}{\partial A}\right|_{A=\ln\sqrt{8}} = 2 = b^{\nu_\perp},$$

from which we obtain $\nu_\perp = 1$. The same exponent was found for the divergence of the *typical,* but not the average correlation length in the RTIM model (cf introduction of this chapter). In the next section, which is about large disorder, we will give a possible explanation for this result.

To conclude this subsection we analyse again the RG flow around the homogeneous fixed point at $R = 0$. In the previous subsection we used a lognormal distribution for the rates and found a cross-over exponent $\phi = 0.508...$ for $b = 2$ while the Harris criterion predicted $\phi = 0.903....$ We want to know whether for increasing b the cross-over exponent converges to this value. Since for larger cell sizes the SRG cannot be performed analytically,

the lognormal distribution is not convenient to work with. Using the binary distribution this calculation can more easily be extended. When b is not too large, all the disorder realisations needed for the calculation of the average can be fully enumerated. With an exact numerical diagonalisation tool we performed the SRG for cell sizes up to $b = 11$, the result is presented in Table 7.1. After an extrapolation in b, the cross-over exponent is consistent with the Harris value. In the next subsection this result will be supported by an analytical argument based on the SRG.

7.3.4 The Harris Criterion

We will use the logarithmic rates Λ_i and M_i to analyse the SRG behaviour in the proximity of the homogeneous critical point. For simplicity of notation, we will take $M_i = 0$ without disorder ($\mu_i = 1$). This implies that the control parameter A for the activity of the system is given by $A = [\Lambda_i]_{\text{av}}$. If we write $\Lambda_i - A = \delta\Lambda_i$, we get that $\delta\Lambda_i$ is a stochastic variable with mean zero and a variance equal to that of Λ_i. Since the variance R of Λ_i is very small close to the homogeneous critical point, we arrive at

$$M_i = 0$$
$$\Lambda_i = A + \delta\Lambda_i \qquad \delta\Lambda_i \sim P(\Lambda_i - A) \qquad \begin{cases} [\delta\Lambda_i]_{\text{av}} = 0 \\ var(\delta\Lambda_i) = R << . \end{cases}$$

In the following derivation we will assume $\delta\Lambda_i$ to be independent. The function P is not explicitly used, and can be *any probability distribution.*

We will renormalise the system with a cell of length b as indicated in Fig. 7.4. In this calculation we will include possible correlations between the

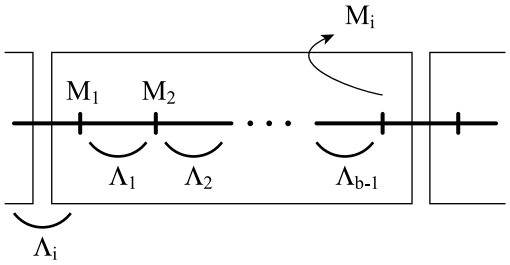

Figure 7.4: *Grouping of terms for the SRG procedure with cell size b.*

renormalised M_i and Λ_i. From the SRG we only use the aspect that it has

the form

$$\begin{aligned} M_i &\xrightarrow{\mathcal{R}} M_i + h_M\left(\Lambda_1, \ldots, \Lambda_{b-1}, M_1, \ldots, M_{b-1}\right) \\ \Lambda_i &\xrightarrow{\mathcal{R}} \Lambda_i + h_\Lambda\left(\Lambda_1, \ldots, \Lambda_{b-1}, M_1, \ldots, M_{b-1}\right) \end{aligned}$$

with h_M and h_Λ analytical functions. Since we took $M_i = 0$ we can leave them out of the derivation and if we denote $h = h_M + h_\Lambda$ an analytical function, the only needed SRG equation is given by

$$\Lambda_i \xrightarrow{\mathcal{R}} \Lambda_i + h\left(\vec{\Lambda}\right) \tag{7.24}$$

where we wrote $\vec{\Lambda} = (\Lambda_1, \ldots, \Lambda_{b-1})$.

We will now evaluate the RG flow in the space of the control parameters:

$$\begin{aligned} A = [\Lambda_i]_{\text{av}} &\xrightarrow{\mathcal{R}} [\Lambda_i]_{\text{av}} + \left[h\left(\vec{\Lambda}\right)\right]_{\text{av}} \\ R = var\left(\Lambda_i\right) &\xrightarrow{\mathcal{R}} var\left(\Lambda_i\right) + var\left(h\left(\vec{\Lambda}\right)\right). \end{aligned} \tag{7.25}$$

Since the values of the stochastic variable $\Lambda = A + \delta\Lambda$ have a small standard deviation $\sqrt{R}$ around their mean value A, we can expand the analytical function h to second order in $\sqrt{R}$ as

$$\begin{aligned} h\left(\vec{\Lambda}\right) &= h\left(\vec{A}\right) + \sum_{k=1}^{b-1} \frac{\partial h(\vec{A})}{\partial \Lambda_k}\, \delta\Lambda_k \\ &\quad + \sum_{k=1}^{b-1} \frac{\partial^2 h(\vec{A})}{\partial \Lambda_k^2}\, \delta\Lambda_k^2 + \sum_{k \neq l} \frac{\partial^2 h(\vec{A})}{\partial \Lambda_k \partial \Lambda_l}\, \delta\Lambda_k\, \delta\Lambda_l. \end{aligned}$$

Since $[\delta\Lambda_k]_{\text{av}} = 0$ and because of independence also $[\delta\Lambda_k\, \delta\Lambda_l]_{\text{av}} = R\delta_{k,l}$, we can directly compute $\left[h\left(\vec{\Lambda}\right)\right]_{\text{av}}$ and $var\left(h\left(\vec{\Lambda}\right)\right)$:

$$\begin{aligned} \left[h\left(\vec{\Lambda}\right)\right]_{\text{av}} &= h\left(\vec{A}\right) + R\sum_{k=1}^{b-1} \frac{\partial^2 h(\vec{A})}{\partial \Lambda_k^2} + O\left(R^{3/2}\right) \\ var\left(h\left(\vec{\Lambda}\right)\right) &= R\sum_{k=1}^{b-1} \left(\frac{\partial h(\vec{A})}{\partial \Lambda_k}\right)^2 + O\left(R^{3/2}\right). \end{aligned}$$

From this we get the SRG flow

$$\begin{aligned} A &\xrightarrow{\mathcal{R}} \mathcal{R}_A(A, R) = A + h\left(\vec{A}\right) + O(R) \\ R &\xrightarrow{\mathcal{R}} \mathcal{R}_R(A, R) = R\left[1 + \textstyle\sum_{k=1}^{b-1}\left(\frac{\partial h(\vec{A})}{\partial \Lambda_k}\right)^2\right] + O\left(R^{3/2}\right). \end{aligned} \tag{7.26}$$

Next we have to linearise this flow in the homogeneous critical point ($A = A_c, R = 0$). Since for $R = 0$ we clearly have $\frac{\partial \mathcal{R}_R}{\partial A} = 0$, the linearised operator is of the form $\begin{pmatrix} \frac{\partial \mathcal{R}_A}{\partial A} & \frac{\partial \mathcal{R}_A}{\partial R} \\ 0 & \frac{\partial \mathcal{R}_R}{\partial R} \end{pmatrix}_{R=0, A=A_c}$ and the eigenvalues are given by the diagonal elements, which can be related to the corresponding exponents:

$$b^{1/\nu_\perp} = \frac{\partial \mathcal{R}_A(0, A_c)}{\partial A} = 1 + \sum_{k=1}^{b-1} \frac{\partial h(\vec{A}_c)}{\partial \Lambda_k} \tag{7.27}$$

$$b^{y_2} = \frac{\partial \mathcal{R}_R(0, A_c)}{\partial R} = 1 + \sum_{k=1}^{b-1} \left(\frac{\partial h(\vec{A}_c)}{\partial \Lambda_k} \right)^2 . \tag{7.28}$$

For large b the first term 1 becomes irrelevant, and if we accept the following equality for cell size $b \to \infty$

$$\left(\sum_{k=1}^{b-1} \frac{\partial h(\vec{A}_c)}{\partial \Lambda_k} \right)^2 = b \sum_{k=1}^{b-1} \left(\frac{\partial h(\vec{A}_c)}{\partial \Lambda_k} \right)^2 \tag{7.29}$$

we finally arrive at $b^{2/\nu_\perp} = b^{y_2+1}$ or

$$\phi \doteq y_2 \nu_\perp = 2 - \nu_\perp . \tag{7.30}$$

This is exactly the Harris formula (7.19).

The crucial point is the validity of (7.29). This equation is correct if in the summation the main contribution comes from the terms in the bulk of the cell, which have essentially all the same value. Let us take a look at the meaning of $\frac{\partial h(\vec{A}_c)}{\partial \Lambda_k}$. This quantity is the effect of a change of rate Λ at site k on RG equation (7.24) evaluated at the critical point of the homogeneous contact process. These RG equations are constructed by projecting operators at the boundaries of the cell on ground states of the cell. This means that a change of rate Λ at site k can only effect the RG equations if it effects the boundary behaviour of the ground states of the cell. Since we are evaluating this quantity in the critical point, where correlations become infinite, we can expect the bulk terms to be relevant and equation (7.29) to be correct in the limit $b \to \infty$.

In conclusion, we can say that the contact process is unstable with respect to quenched disorder. If the rates are independently drawn from a probability distribution with non-zero variance, the critical behaviour is no longer governed by the homogeneous fixed point. When we applied the standard

renormalisation, this point turned out to be repulsive with a cross-over exponent that was found, both numerically and analytically, to be $\phi = 2 - \nu_\perp$ which is the same as predicted by the Harris criterion known from equilibrium systems.

7.4 Large Disorder

7.4.1 The Alternating Contact Process

In order to get some insight in the effect of disorder on the performance of the SRG, it is instructive to take a look at the alternating contact process. In this model we take the rate $\mu = 1$ for all sites, and the contamination rate is alternatively large (λ^+) and small (λ^-). If we apply the SRG with cell size 2 to this model, it is after one SRG step transformed into the homogeneous contact process. Since we know the critical point of the homogeneous contact process very accurately, we could use this technique to find the critical point of the alternating contact process. Consider the case

$$\lambda^\pm = e^{A \pm \sqrt{R}}$$

and let us examine the critical value of A that the SRG provides us in the extreme case $R \to \infty$.

There are two possible ways to group the Hamiltonian terms

a) Collect all terms with large λ^+ in the intracell Hamiltonians
b) Collect all terms with small λ^- in the intracell Hamiltonians.

For both approaches we can perform the SRG transformations (7.14). This results in the homogeneous contact process with activity $\frac{\lambda}{\mu}$, which in the limit $R \to \infty$ is given by:

$$\text{a) } \frac{\lambda}{\mu} = \lambda^- \frac{\lambda^+}{2+\lambda^+} \frac{(2+\lambda^+)^2}{4+4\lambda^+} \approx \frac{\lambda^+\lambda^-}{4} = \frac{e^{2A}}{4}$$

$$\text{b) } \frac{\lambda}{\mu} = \lambda^+ \frac{\lambda^-}{2+\lambda-} \frac{(2+\lambda^-)^2}{4+4\lambda^-} \approx \frac{\lambda^+\lambda^-}{2} = \frac{e^{2A}}{2}.$$

Since the critical point of the homogeneous process is $\lambda/\mu = 3.297...$, we obtain that the critical point of the alternating process is

$$\text{a) } A_c = \ln 2 + \ln \sqrt{3.297...} \qquad \text{b) } A_c = \ln \sqrt{2} + \ln \sqrt{3.297....}$$

Clearly, at least one of these results is incorrect!

The answer to this dilemma is given by yet another way to look at the SRG. In Chapter 4 we introduced the SRG first as an ad hoc procedure that

we later justified in a perturbation theory. A third point of view is that of an infinite-rate expansion. In subsection 2.3.4 this technique defined an *effective Hamiltonian* that rigorously describes the dynamics of a system *when one of the reaction rates becomes infinite*. This Hamiltonian is constructed by projecting the original Hamiltonian on the subspace spanned by the ground states of the infinite-rate reaction. The intuitive explanation was that the system always relaxes very quickly into the ground states of the infinite-rate reaction and the other reactions can only imply transitions from one of these ground states to the other. For the alternating contact process with $R \to \infty$, this construction coincides exactly with that of the SRG in case a). One can indeed proof that solution a) is mathematically exact.

This provides the solution to the problem. When grouping the Hamiltonian terms, the reactions with the *highest rate* should be included in the *intracell Hamiltonian*. In this light, one can understand why the SRG produced wrong results in the contact process with strong disorder. For this random case, some large rates will be in the intracell Hamiltonian, but equally well there will be large rates in the intercell Hamiltonian and the results cannot be trusted.

In performing the SRG on the contact process, we can now distinguish three scenarios. First, when the rates in the cells are of the same magnitude as those outside the cells, the SRG produces good results for the stationary behaviour of the model. This was found in the homogeneous case and we also expect the results for very small disorder to be correct. When the rates inside the cells are smaller, the result is poor. Finally, when the rates inside are much bigger, the SRG becomes exact, even for finite cell lengths!

Until now, we always performed a renormalisation on the whole lattice at once. If we consider the RG flow as a dynamics, this could be called parallel updating. For a disordered system this clearly is not the way to proceed. On the other hand, if we could somehow, in each SRG step concentrate the renormalisation on that site of the lattice where the rate is the largest, the result could be expected to be much better. This idea is in the spirit of the SDRG of Ma, Dasgupta and Hu [79], [80]. In the next subsection we develop such a "sequential SRG".

7.4.2 The Sequential SRG

Consider the contact process where the rates λ_i and μ_i can be site-dependent. We will try to perform a sequential or local SRG by taking a cell of two site as in Fig. 7.5. The Hamiltonian in the cell again has an active $|A,0\rangle$ and an absorbing $|\phi,0\rangle$ ground state. Any vector of the system which has on sites i and $i+1$ the form $|A,0\rangle$ or $|\phi,0\rangle$ is a ground state of the intracell Hamiltonian. We have to project the original Hamiltonian on the space $\mathcal{W}$ spanned by these

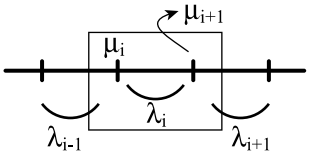

Figure 7.5: *Grouping of the Hamiltonian terms for a sequential SRG.*

vectors.

Denote h_i^1 the one-site Hamiltonian representing the reaction $A \to \phi$ on site i with rate μ_i, and h_i^2 the two-site Hamiltonian for the reaction $A\phi, \phi A \to AA$ on sites $i, i+1$ with rate $\lambda_i/2$. The only terms of the Hamiltonian that can be influenced by the projection on $\mathcal{W}$ are h_{i-1}^2, h_{i+1}^2 and h_{i+1}^1. The calculation is straightforward and the result is that these operators are (once more) of the same form and the renormalised rates are

$$\begin{array}{lcl} \lambda_{i-1} & \xrightarrow{\mathcal{R}} & \lambda_{i-1}\left(2\frac{\mu_i}{\lambda_i}+1\right)^{-1} \\ \lambda_{i+1} & \xrightarrow{\mathcal{R}} & \lambda_{i+1} \\ \mu_{i+1} & \xrightarrow{\mathcal{R}} & \mu_{i+1}\left[1-\left(2\frac{\mu_i}{\lambda_i}+1\right)^{-2}\right]. \end{array} \tag{7.31}$$

Again, the fact that we find conservation of form is a consequence of the self-enantiodromy property of the contact process.

The whole idea of this sequential SRG was to apply it on a site where one of the rates λ_i or μ_i is much larger than its neighbouring rates. We will denote this limit respectively by "$\lambda_i >>$" or "$\mu_i >>$". Besides the fact that the RG becomes accurate in this limit, we can also simplify the equations (7.31) since either $\frac{\mu_i}{\lambda_i} \to 0$ or $\frac{\mu_i}{\lambda_i} \to \infty$. We obtain:

$\lambda_i >>$	$\mu_i >>$
$\lambda_{i-1} \longrightarrow \lambda_{i-1}$	$\lambda_{i-1} \longrightarrow \frac{1}{2}\frac{\lambda_{i+1}\lambda_i}{\mu_i}$
$\mu_{i+1} \longrightarrow 4\frac{\mu_{i+1}\mu_i}{\lambda_i}$	$\mu_{i+1} \longrightarrow \mu_{i+1}$

(7.32)

The SRG equations are very simple and we expect them to be exact in the given limit. Moreover, in this limit the SRG creates no correlations between the reaction rates since only one rate is updated in each RG step.

To conclude, we consider the effect of this local renormalisation on observables. In the case of the parallel SRG we were able to determine the number of particles in the ground state by renormalising the corresponding observable operator E_i^{11}. This was straightforward since the renormalised operator was

the same on each lattice site and the lattice was homogeneously rescaled. In the sequential SRG these two points need reconsideration.

First, the sequential SRG implies that some parts of the lattice become rescaled more often than other parts. Suppose that after some renormalisation steps, we calculate the total number of particles in the ground state of the system. If we want to relate this quantity to the number of particles in the ground state of the original system, we have to keep track of how many times each site has been renormalised.

Secondly, the sequential SRG leads to site-dependent observables: when a local SRG is performed on sites $i, i+1$ only the observables acting on these sites are renormalised. This complication is however compensated by the fact that the sequential SRG is only applied to sites for which $\lambda_i >>$ or $\mu_i >>$, and a simplification can be carried through. In the case $\lambda_i \to \infty$ the ground states in the cell are $|AA\rangle$ and $|\phi\phi\rangle$ while for $\mu_i \to \infty$ they are $|\phi A\rangle$ and $|\phi\phi\rangle$. These extremely simple ground states imply that all observables (which are diagonal operators) are by the RG mapped onto themselves, except E_i^{11} which is for $\mu_i \to \infty$ mapped onto zero.

The need to store site-dependent rescaling and the fact that all observables are renormalised in a trivial way, can efficiently be combined in a rescaling of a weight function. The procedure starts by associating a weight $n_i = 1$ to each site. Every time the local SRG (7.32) is performed on sites $i, i+1$, this weight is updated. In the limit $\lambda_i >>$, these sites are almost always in the states AA or $\phi\phi$. When this is renormalised to one effective site with a new μ_i, this site behaves as an original one (all observables are mapped onto themselves), but it has a weight $n = n_i + n_{i+1}$. In the limit $\mu_i >>$, site i is almost always in state ϕ. This site does not contain any degrees of freedom and the renormalisation is essentially a decimation of site i (E_i^{11} is mapped onto zero). Hence, for this limit the update of the weight is $n = n_{i+1}$.

Concluding this subsection, we can say that the sequential SRG performed on a site where $\lambda_i >>$ or $\mu_i >>$, is given by equations (7.32) combined with respectively $n = n_i + n_{i+1}$ and $n = n_{i+1}$.

The same equations can be found using a perturbation calculation for the spectrum of the local Hamiltonian around a large rate. This was the technique used by Ma, Dasgupta and Hu when they introduced their SDRG [79], [80].

7.4.3 Exact Solution for Large Disorder

Consider the contact process with quenched disorder, for which the rates λ_i and μ_i are identically and independently distributed according to respectively $P(\lambda)$ and $\Pi(\mu)$. Following the SDRG technique, one puts the rates λ_i and μ_i in one series in descending order. The largest rate is denoted as Ω and sets the

time scale of the system. During the sequential renormalisation, the largest rates are consecutively replaced by new ones and the probability distributions $P(\lambda,\Omega)$ and $\Pi(\mu,\Omega)$ are subject to variation.

When the initial disorder is large enough, the equations (7.32) will produce on average a lower renormalised rate and Ω will decrease. This means that all rates are approaching zero under RG transformations and the control parameter for the randomness $R = var\left(\ln\frac{\lambda_i}{\mu_i}\right)$ is becoming infinite. At the infinite randomness fixed point (IRFP) one finds $\Omega \longrightarrow \Omega^* = 0$ and from the scaling behaviour of $P^*(\lambda,\Omega)$ and $\Pi^*(\mu,\Omega)$ the random critical exponents can be deduced.

With the renormalisation equations at hand, one can write down a set of integro-differential equations, which govern the evolution of the distributions $P(\lambda,\Omega)$ and $\Pi(\mu,\Omega)$ under successive RG transformations, i.e. as Ω is lowered. These techniques are standard in the SDRG method and the analytical solution is known for RG equations of the form

$\lambda_i >>$	$\mu_i >>$
$\mu_{i+1} \longrightarrow \kappa\frac{\mu_{i+1}\mu_i}{\lambda_i}$	$\lambda_{i-1} \longrightarrow \kappa\frac{\lambda_{i+1}\lambda_i}{\mu_i}$
$n = n_i + n_{i+1}$	$n = n_{i+1}.$

(7.33)

For $\kappa = 1$ these are the SDRG equations of the random transverse Ising model (RTIM) [81], [82] for $\kappa = 2/q$ of the random quantum Potts model [93], and they are also encountered in the random clock- and Ashkin-Teller model [95].

If we make in the quenched random contact process the transformation $\tilde{\lambda} = \lambda/\sqrt{8}$ the RG equations (7.32) become exactly those of (7.33) with $\kappa = \sqrt{2}$.

Hence, we can without further calculation adopt the results of the random quantum spin chains, which can be summarised as follows. For strong enough initial disorder, the critical behaviour of the quenched random contact process is governed by an IRFP. The location of the fixed point is exactly given by $[\ln\mu]_{\rm av} = \left[\ln\tilde{\lambda}\right]_{\rm av}$ or since $\tilde{\lambda} = \lambda/\sqrt{8}$:

$$R = var\left(\ln\frac{\lambda_i}{\mu_i}\right) = \infty \qquad A = [\ln\lambda]_{\rm av} - [\ln\mu]_{\rm av} = \ln\left(\sqrt{8}\right). \tag{7.34}$$

In the IRFP the critical exponents are exactly known as [81], [82]

$$\beta_b = \frac{3-\sqrt{5}}{2} \qquad \beta_s = 1 \qquad \nu_\perp = 2, \tag{7.35}$$

where β_b and β_s describe how the average stationary bulk and surface density grow as a function of $\left(A - \ln(\sqrt{8})\right)$. Finally, scaling at the IRFP is strongly

anisotropic, represented by $z = \infty$ or more precisely, the relation between the spatial correlation and the relaxation time is given by

$$\ln \tau \sim \sqrt{\xi}. \tag{7.36}$$

As far as we know, these are the first exactly determined critical exponents for a (non-trivial) phase transition out of an absorbing state.

Remark 8 When we used the parallel SRG, the RG equations were the same as for the SDRG (see (7.13) and (7.31)) Consequently we did recover the correct critical point (cf Fig. 7.3), but for the exponent $\nu_\perp$ we didn't find the correct value 2, but the typical value 1. This can now intuitively be understood. Since for strong random systems the physics is governed by rare events, one should concentrate on them to recover the correct behaviour. The SDRG does this by renormalising the large rates, which can be seen as rare events. The parallel SRG however, treats all events in the same way, and recovers the typical behaviour instead.

After this exact solution, the main question we are left with is how large the basin of attraction of the IRFP is. All systems that by renormalisation are driven to this IRFP have a critical behaviour that is exactly given by the results derived above. The SDRG equations (7.33) are correct when the disorder is infinite, but they are not exact for finite disorder, and can consequently not be used to rigorously determine the basin of attraction of the IRFP.

However, there is an argument, analogous to that in [95], that can be made. It is based on the fact that the system is attracted by the IRFP only if the largest rate Ω systematically decreases when performing the SDRG equations (7.33). The value of κ can play an important role in this matter. When κ is large, some RG-steps may *in*crease Ω. For weak enough disorder, this can happen so often that the SDRG does not work. For stronger, but still finite disorder, these "wrong" renormalisation steps become rare and the system flows into the IRFP. In [95] the SDRG had a parameter $\kappa > 1$, as in our model, and there is was found that, unlike in the RTIM ($\kappa = 1$), the basin of attraction is finite. For a disorder below a certain value, the system is not controlled by the IRFP but in a regime of "intermediate disorder" where the critical exponents were found to vary continuously with the strength of the disorder.

In the next section we present our results of a numerical study of the quenched random contact process. Since the results obtained from the SDRG involve several ill controlled approximations, such a numerical verification is necessary. Moreover, since we expect that the IRFP is only attractive for strong enough disorder, we hope to get insight from the numerics into the intermediate disorder regime for which no reliable results can be obtained from analytical RG approaches.

	Inactive	**Critical**	**Active**
ρ_s	$\sim e^{-bL}$	$\sim L^{-\beta_s/\nu_\perp}$	$\sim c + e^{-bL}$
Y_L	$\sim -bL$	$\sim -(1+\beta_s/\nu_\perp)$	$\sim -bL$

Table 7.2: *Behaviour of ρ_s and Y_L in the three regimes of the homogeneous contact process.*

7.5 DMRG and Intermediate Disorder

The numerical research that led to the results in this section was performed with the use of the binary distribution introduced in subsection 7.3.3: $\mu_i = 1$, $\lambda_i = e^{A \pm \sqrt{R}}$. With the DMRG algorithm we calculated the lowest gap in the spectrum of the Hamiltonian and the particle density in the active stationary state. In the former case we used open boundary conditions and projected out the trivial (absorbing) ground state in the same way as described in subsection 6.3.1. In the latter case we fixed a particle on site 1 of the system (forcing it to be active) and calculated the stationary bulk and surface particle density on respectively site $L/2$ and L.

7.5.1 Phase Diagram

In a first calculation we approximated the position of the critical point in the disorder regime $R \in [0, 2]$. Hereto we used the DMRG to calculate the surface and bulk density averaged over the disorder: $[\rho_s]_{\text{av}}$ and $[\rho_b]_{\text{av}}$. This was performed for system sizes up to $L = 14$, for which the averaging was done exactly. We found the surface density to converge faster as a function of L and we will concentrate on this quantity.

Let us start with the finite size analysis for the homogeneous case $R = 0$. As a function of L, the particle density will decay exponentially to zero in the inactive phase and exponentially to a positive constant c in the active phase. Exactly at the critical point the density decays algebraically to zero. This behaviour is summarised in Table 7.2. To determine the location of the critical point it is convenient to introduce the following quantity which can easily be evaluated numerically

$$Y_L = \frac{d \ln \frac{d\rho_s}{dL}}{d(\ln L)}. \tag{7.37}$$

As indicated in Table 7.2 this function goes to $-\infty$ for increasing system sizes, except at the critical point, where it remains finite. If we plot Y_L as a function of A for a fixed (and large enough) system size L, we expect this curve to have a maximum at the critical point.

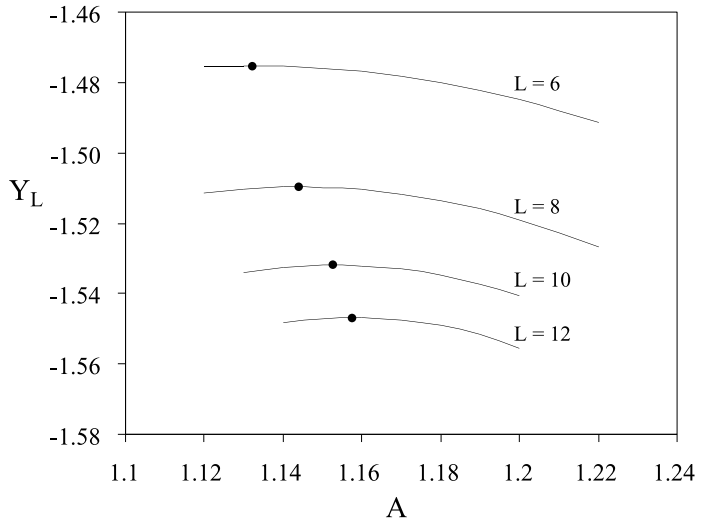

Figure 7.6: *Plot of Y_L as a function of A, for the binary distribution with disorder $R = 1$.*

This analysis can be repeated for the average density $[\rho_s]_{\text{av}}$ in the disordered case $R > 0$. The only difference is that we do not know that the decay in the inactive and active phase is exponentially. But as long as this decay is faster than that in the critical point (which is likely) the graphical argument to locate the critical point remains valid. In Fig. 7.6 the result is shown for $R = 1$. For every L the maximum of the corresponding curve produces an estimate for the critical value of A and the corresponding $-(1 + \beta_s/\nu_\perp)$. For the latter one the system sizes were to small to extrapolate $L \to \infty$. In the next subsection we will use a different technique to get access to the critical exponents. However, for the position of the critical line the limited data at hand was sufficient to make a reliable extrapolation. The resulting phase diagram is presented in Fig. 7.7(a), and it is compared with the critical curves we got from the parallel SRG presented earlier in the chapter. One can notice that for increasing L the SRG curves shift towards the DMRG result. Moreover, from Chapter 5 we know that the SRG-estimates for the homogeneous ($R = 0$) critical point converge to $A = \ln(3.297...) = 1.193...$ which corresponds to the value found by the DMRG for $R = 0$. To compare the shape of the different estimates for the critical line, it is therefore instructive to shift them as presented in Fig. 7.7(b). One notices that for this regime of

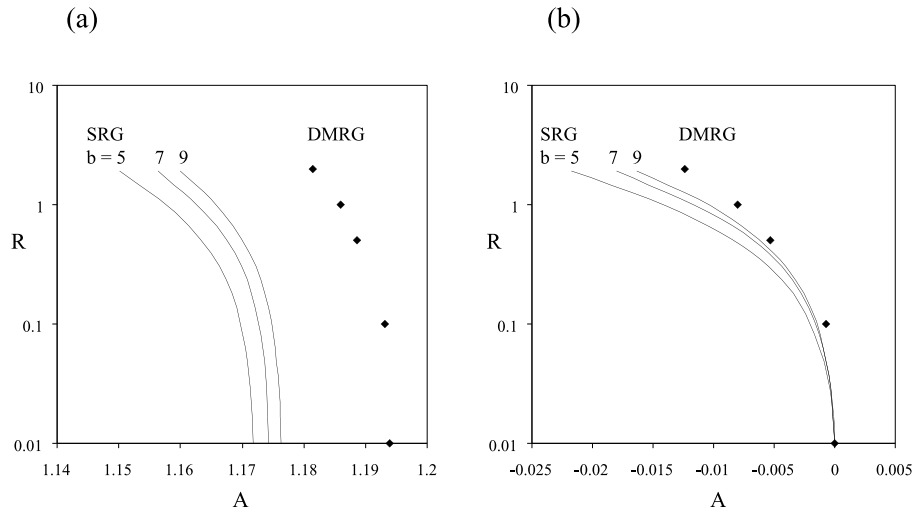

Figure 7.7: *(a) Phase diagram of the quenched random contact process with binary distribution. The full lines are the result of a (parallel) SRG calculation with cell sizes $b = 5, 7$ and 9. The diamonds are the result of the DMRG approach, for which the error is of the same order as the size of the symbols. Both are for $R \in [0, 2]$.*
(b) Same as in (a) but with A shifted over the value of the homogeneous critical point estimate.

randomness ($R \in [0, 2]$) the phase diagram of the parallel SRG and DMRG are in good agreement.

7.5.2 Critical Exponents

To determine the critical exponents we applied the DMRG to system sizes up to $L = 24$. For smaller sizes $L \leq 14$ we performed exact disorder averages, whereas for larger sizes we considered at least 10000 samples for each L. We again concentrated on the disorder region $R \in [0, 2]$ for which we know the phase diagram. For larger disorder we encountered numerical difficulties in the DMRG algorithm.

Consider first the average surface and bulk density $[\rho_s]_{\text{av}}$ and $[\rho_b]_{\text{av}}$. Take a fixed disorder value R, and denote the distance from the corresponding critical point A_c as $\Delta = (A - A_c)/A_c$. For small Δ the quantity $[\rho_s]_{\text{av}}$ obeys the finite size scaling

$$[\rho_s(L, \Delta)]_{\text{av}} = L^{-\beta_s/\nu_\perp} f\left(\Delta L^{1/\nu_\perp}\right) \tag{7.38}$$

and the same relation holds for $[\rho_b]_{\rm av}$ with β_b. From an optimal data collapse of the densities for a range of L and Δ, we can estimate the values of $\beta/\nu_\perp$ and $\nu_\perp$ for every fixed R. In Fig. 7.8 the collapse is presented for $R = 0.5$ with

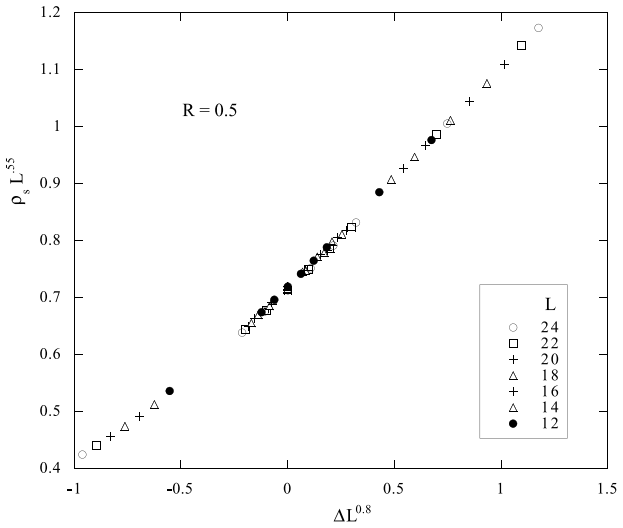

Figure 7.8: *Scaling plot of the surface particle density at* $R = 0.5$, $A_c = 1.19$ *with* $\beta_s/\nu_\perp = 0.55$ *and* $1/\nu_\perp = 0.8$.

the estimates $\beta_s/\nu_\perp = 0.55$ and $1/\nu_\perp = 0.8$. For varying disorder strength the estimated critical exponents $\beta_s/\nu_\perp$ and $\beta_b/\nu_\perp$ are shown in Fig. 7.9 in which one can observe two different regimes. For weak disorder, $R < R_c \approx 1.5$ we find a region in which the critical exponents vary continuously with R. For $R > R_c$ the exponents seem to be saturated at the values of the IRFP as given in (7.35). The exponent $\nu_\perp$ exhibits a similar behaviour. For $R = 0$ we recover the homogeneous value of $\nu_\perp = 1.096...$ which increases with increasing R, but at $R = 1.5$ we find $\nu_\perp = 1.7$ while the IRFP value is 2. Hence this exponent does not seem to saturate as fast as $\beta/\nu_\perp$. However, we should mention that the estimates for $\nu_\perp$ coming from the bulk and surface data differ a bit and the results are consequently less accurate. We are planning to take a closer look at this problem in the near future.

Nevertheless these results are similar to those found in a class of quantum spin chains where the parameter κ of the SDRG equations (7.33) is larger than one [95]. The basin of attraction of the IRFP does not cover the whole parameter space and there exists an intermediate disorder region where the critical exponents vary continuously with R.

To conclude the numeral aspect of this research we mention the results

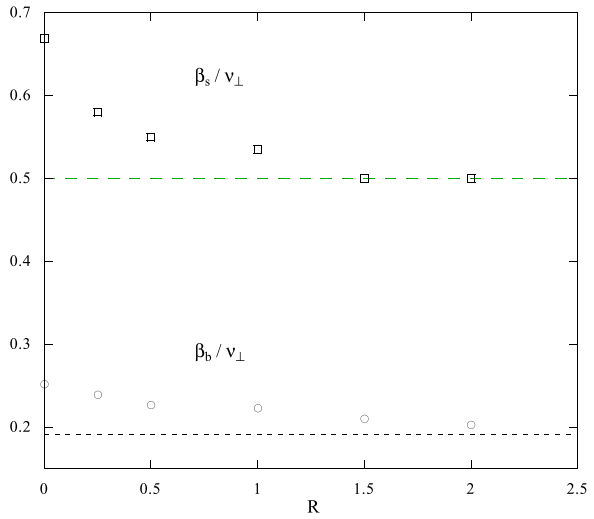

Figure 7.9: *Estimates of the exponents $\beta_s/\nu_\perp$ (squares) and $\beta_b/\nu_\perp$ (circles) from the collapse of the DMRG data. The broken lines indicate the values at the infinite randomness fixed point (IRFP). The errors are of the same order as the size of the symbols.*

of analysis of the lowest gap Γ of the Hamiltonian, which can be used to determine the dynamical exponent z. In the intermediate disorder regime we expect a traditional scaling, i.e. a finite z value. However, in a critical system that is dominated by the IRFP z is infinite and the gap distribution is given by [81], [82]

$$P(\ln \Gamma) = f\left(L^{-1/2} \ln \Gamma\right) L^{-1/2} \tag{7.39}$$

with f a scaling function. The scaling collapse in Fig. 7.10 indicates that at $R = 1.5$ the exponent z is determined by the IRFP, consistent with the results found for the exponents $\beta/\nu_\perp$. In the intermediate disorder regime $R < R_c$ the collapse is less pronounced, suggesting that z is finite, but we were not able to determine reliable estimates.

7.6 Conclusions

7.6.1 General Picture

Let us collect the results of this chapter and try to draw a general picture of the quenched random contact process. First, when the disorder is strong

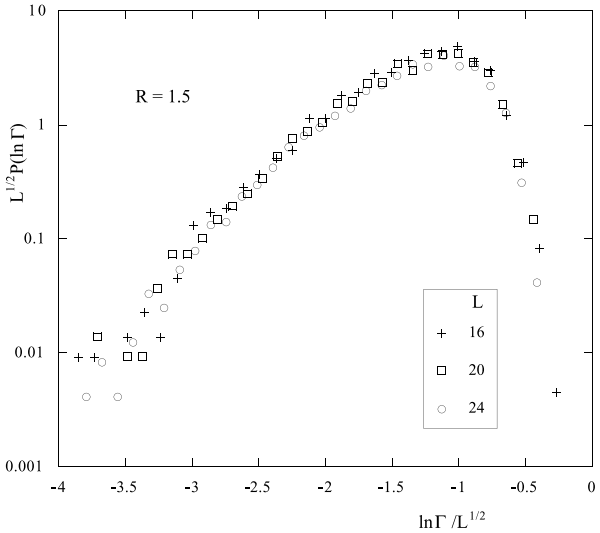

Figure 7.10: *Scaling collapse of the lowest gap* Γ *at* $R = 1.5$ *and* $A_c = 1.185$.

enough, the critical behaviour of the system is governed by the IRFP and the exact exponents can be derived with the SDRG:

$$\begin{aligned} \beta_b &= \frac{3-\sqrt{5}}{2} \qquad \beta_s = 1 \qquad \nu_\perp = 2, \\ z &= \infty \qquad \ln \tau \sim \sqrt{\xi}. \end{aligned}$$

This is the first example of an absorbing state phase transition for which such exact information becomes available. In RG terms the dominance of the IRFP is given by the fact that all systems with a disorder $R > R_c$ are by the RG flow driven to the fixed point at $A = \ln \sqrt{8}, R = \infty$.

Secondly, in the intermediate disorder regime $R < R_c$ our numerical DMRG results show that the critical exponents vary continuously with the disorder strength. In the RG picture this means that the phase boundary below R_c is a line of fixed points. However, here we arrive at a difficulty since we showed with the parallel SRG that the homogeneous fixed point is repulsive with respect to disorder. If we accept that a correct RG flow is analytical, the line of fixed points in the intermediate regime cannot extend to the homogeneous critical point, but has to be restricted to $[R_{c_1}, R_{c_2}]$ as shown in Fig. 7.11, which is the only analytical RG flow that is consistent with all the results. If this flow is correct there would be a region of small disorder $R \in]0, R_{c_2}]$ where the critical exponents are independent of R. Since the size of this region is not

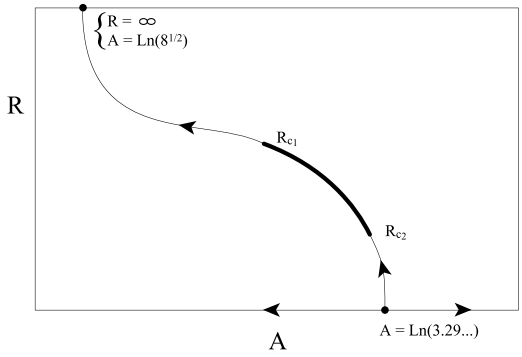

Figure 7.11: *Sketch of the RG flow that is consistent with all the data we found. The thick line represents the line of fixed points.*

known, a numerical verification could be difficult and with the current DMRG data we were not able to check its existence.

7.6.2 Prospectives

Since the critical stationary behaviour of this quenched random contact process in the intermediate disorder regime is still not clear, we plan to extend our research on it in the near future. A first approach can be the use of the DMRG in combination with a *continuous* distribution for the random rates. Up to now we used a discrete one, which is very accurate if a complete enumeration of the rate realisations is possible. However, when sampling is needed to approximate averages, a continuous distribution is likely to produce better results. A second way to probe the intermediate regime is by using the sequential SRG in its original form (7.31), i.e. before the approximation to (7.32) is made. These former RG equations are more accurate for intermediate disorder, but they can no longer be handled analytically and a numerical approach will be necessary.

Next there are several unstudied generalisations possible. First it would be interesting to check whether other one-dimensional models (e.g. belonging to the PC universality class) are described by the same IRFP when strong disorder is added upon their rates. This is wouldn't be surprising since we found that in the IRFP the disorder completely dominates the critical behaviour and the effect of non-hermiticity becomes irrelevant: the critical exponents are the same as those of the disordered hermitian RTIM model. A similar conjecture can be made for higher dimensional models. Since the RG equations of the random contact process are very similar to those of the RTIM model, it

is possible that in higher dimensions the model (and other stochastic models) renormalises like the RTIM of the corresponding dimensionality. Another point of further study is the investigation of random stochastic models in the off-critical region, i.e. in the Griffiths phases.

Appendix A

Notations and Abbreviations

A.1 Notations for quantum formalism

L	length of the lattice
A	presence of a particle
ϕ	absence of a particle
η	a configuration of the system
X	set of all configurations
$P_\eta(t)$	probability of finding system in η at time t
$r_{\eta\to\eta'}$	transition rate to go from η to η'
H	Hamiltonian, infinitesimal generator of the Markov process
$\lvert P(t)\rangle = \sum_\eta P_\eta(t) \lvert\eta\rangle$	state of the system
$\langle s\rvert = \sum_\eta \langle\eta\rvert$	normalisation vector
$\langle F\rangle = \langle s\rvert F \lvert P(t)\rangle$	expectation value of F
Γ_0 (or simply Γ)	lowest energy gap of H, being the real part of the eigenvalue with smallest non-zero real part
T^*	projection operator $\lim_{t\to\infty} e^{-Ht}$

Unless specified otherwise, we use

$\delta_{i,j}$ as the Kronecker delta

$$E^{00} = \begin{bmatrix} 1 & 0 \\ 0 & 0 \end{bmatrix}, E^{11} = \begin{bmatrix} 0 & 0 \\ 0 & 1 \end{bmatrix}, E^{01} = \begin{bmatrix} 0 & 1 \\ 0 & 0 \end{bmatrix}, E^{10} = \begin{bmatrix} 0 & 0 \\ 1 & 0 \end{bmatrix}$$

or more general $\left(E^{ab}\right)_{ij} = \delta_{a,i}\delta_{b,j}$

$\mathbf{1}$ as the identity operator

$E_n^{ab} = \bigotimes_{i=1}^{n-1} \mathbf{1} \otimes E^{ab} \otimes \bigotimes_{i=n+1}^{L} \mathbf{1}$

A.2 Abbreviations for models and techniques

ASEP :	asymmetric exclusion process
BARW :	branching and annihilating random walks
DMRG :	density matrix renormalisation group
DP :	directed percolation (universality class)
IRFP :	infinite randomness fixed point
PC :	parity conserving (universality class)
RG :	renormalisation group
RTIM :	random transverse field Ising model
SDRG :	strong disorder renormalisation group
SRG :	standard renormalisation group
SVD :	singular value decomposition

Appendix B

Proof of the Density Matrix Theorem

In this appendix a proof of the theorem in subsection 6.2.2 is given. It is an algebraic exercise based on the proof in the original paper [12].

B.1 Theorem

Let the dimension of the configuration space of the system block and the environment respectively be given as n_1 and n_2. Furthermore, denote the two sets of orthonormal basis vectors of the system block and the environment respectively as $|i\rangle, i = 1, \ldots, n_1$ and $|j\rangle, j = 1, \ldots, n_2$ and the target state of the superblock as $|\psi\rangle$. Take $m \in \mathbb{N}$ with $m < n_1$ and denote any vector of the system block as $|u\rangle$.

If one wants to minimise

$$S = \left| |\psi\rangle - \sum_{\alpha=1}^{m} \sum_{j=1}^{n_2} a_{\alpha,j} |u^\alpha\rangle |j\rangle \right|^2 \tag{B.1}$$

by varying over all $a_{\alpha,j}$ and $|u^\alpha\rangle$ subject to $\langle u^\beta | u^\alpha\rangle = \delta_{\beta,\alpha}$, the solution for the vectors $|u^\alpha\rangle$ is given by the following procedure.

Take $|\psi\rangle \langle\psi|$ the density matrix of the target state on the superblock and construct the reduced density matrix on the system block

$$\rho_{ii'} = \sum_{j=1}^{n_2} \langle i| \langle j| \quad |\psi\rangle \langle\psi| \quad |i'\rangle |j\rangle . \tag{B.2}$$

ρ is an hermitian operator with n_1 real eigenvalues. The m eigenvectors of ρ with largest eigenvalue are the vectors $|u^\alpha\rangle$ in the solution of the minimisation problem.

B.2 Reformulation

Fix m and denote $\left|\tilde{\psi}\right\rangle = \sum_{\alpha=1}^{m}\sum_{j=1}^{n_2} a_{\alpha,j}\,|u^\alpha\rangle\,|j\rangle$. We wish to minimise

$$S = \left||\psi\rangle - \left|\tilde{\psi}\right\rangle\right|^2 \tag{B.3}$$

by varying over all $a_{\alpha,j}$ and $|u^\alpha\rangle$ subject to $\langle u^\beta\,|u^\alpha\rangle = \delta_{\beta,\alpha}$. We first rewrite $\left|\tilde{\psi}\right\rangle = \sum_{\alpha=1}^{m}|u^\alpha\rangle\left(\sum_{j=1}^{n_2} a_{\alpha,j}\,|j\rangle\right)$ by defining $a_\alpha = \sqrt{\sum_{j=1}^{n_2} a_{\alpha,j}^2}$ and the normalised vectors $|v^\alpha\rangle = \left(\sum_{j=1}^{n_2} a_{\alpha,j}\,|j\rangle\right)/a_a$ to give

$$\left|\tilde{\psi}\right\rangle = \sum_{\alpha=1}^{m} a_\alpha\,|u^\alpha\rangle\,|v^\alpha\rangle\,. \tag{B.4}$$

The original problem is now transformed in a minimisation of

$$S = \sum_{i,j}\left|\psi_{i,j} - \sum_{\alpha=1}^{m} a_\alpha\,\langle i\,|u^\alpha\rangle\,\langle j\,|v^\alpha\rangle\right|^2 \tag{B.5}$$

over $a_\alpha, |u^\alpha\rangle$ and $|v^\alpha\rangle$. Before we solve this minimisation, we reformulate the problem in a matrix form. Since one can write $|\psi\rangle = \sum_{i=1}^{n_1}\sum_{j=1}^{n_2}\psi_{i,j}\,|i\rangle\,|j\rangle$ we interpret this vector as a matrix, defining

$$\psi = \sum_{i=1}^{n_1}\sum_{j=1}^{n_2}\psi_{i,j}\,|i\rangle\,\langle j|\,, \tag{B.6}$$

a $n_1 \times n_2$ matrix. We used "$\langle\ \ |$" as the dual vector of "$|\ \ \rangle$". If we interpret $\left|\tilde{\psi}\right\rangle$ as a matrix on the same space, this can be written in the form

$$\tilde{\psi} = \sum_{\alpha=1}^{m} a_\alpha\,|u^\alpha\rangle\,\langle v^\alpha|\,. \tag{B.7}$$

Finally we define the distance between two matrices of the same form as

$$S\,(A,B) = \sum_{i,j}|\langle i|\,A\,|j\rangle - \langle i|\,B\,|j\rangle|^2\,. \tag{B.8}$$

The original problem is now reformulated as the minimisation of the distance between matrix ψ and $\tilde{\psi}$ over $a_\alpha, |u^\alpha\rangle$ and $|v^\alpha\rangle$.

The solution to this is provided by the singular value decomposition of ψ.

B.3 Singular Value Decomposition

The singular value decomposition (SVD) is a generalised form of the better known diagonalisation. Let M be a square, complex-valued, hermitian matrix. The familiar theorem of diagonalisation tells us that M can be rewritten as

$$M = UDU^* = \sum_\alpha d_\alpha \left|U_\alpha\right\rangle \left\langle U_\alpha\right| \tag{B.9}$$

where D is a diagonal matrix with diagonal elements d_α, U is a unitary matrix with columns $|U_\alpha\rangle$ and * is complex conjugate of the transposed. This decomposition is unique up to a simultaneous permutation of d_α and $|U_\alpha\rangle$ and up to the formation of linear combinations of $|U_\alpha\rangle$ whose corresponding elements d_i are equal. The SVD is similar and tells us the following.

Let ψ be a rectangular matrix of the form

$$\psi \in \mathbb{C}^{n_1} \times \mathbb{C}^{n_2} \tag{B.10}$$

and assume $n_2 \geq n_1$. This can be decomposed as

$$\psi = UDV^* = \sum_{\alpha=1}^{n_1} d_\alpha \left|U_\alpha\right\rangle \left\langle V_\alpha\right| \tag{B.11}$$

where U is a unitary $n_1 \times n_1$ matrix with columns $|U_\alpha\rangle$, D is a diagonal matrix with diagonal elements d_α and V is a rectangular $n_1 \times n_2$ matrix with orthonormal columns $|V_\alpha\rangle$. This decomposition is unique in the same way as the diagonalisation of an hermitian matrix is.[1]

B.4 Solution of Minimisation

We want to approximate ψ by a matrix of the form $\tilde{\psi} = \sum_{\alpha=1}^{m} a_\alpha \left|u_\alpha\right\rangle \left\langle v_\alpha\right|$, with respect to the distance measure (B.8) and $m < n_1$. Using the SVD (B.11) of ψ it is a simple exercise to find that the best approximation is given by taking for a_α the m largest-magnitude elements d_α and for $\left|u_\alpha\right\rangle \left\langle v_\alpha\right|$ the corresponding $\left|U_\alpha\right\rangle \left\langle V_\alpha\right|$. This solves the minimisation problem and tells us how to calculate the wanted vectors $|u^\alpha\rangle$. To finish the proof, we again use

[1] If ψ is square then it is invertible if and only if all d_α are non-zero. The d_α are called the singular values of ψ, giving the name to the decomposition.

matrix form of ψ and the SVD to rewrite the reduced density matrix ρ:

$$\begin{aligned}\rho_{ii'} &= \sum_{j=1}^{n_2} \langle i| \langle j| \quad |\psi\rangle \langle \psi| \quad |i'\rangle |j\rangle = \sum_{j=1}^{n_2} \langle i| UDV^* |j\rangle \langle i'| UDV^* |j\rangle^* \\ &= \sum_{j=1}^{n_2} \langle i| UDV^* |j\rangle \langle j| VD^*U^* |i'\rangle\end{aligned}$$

or in matrix form

$$\rho = UDD^*U^*. \tag{B.12}$$

Denote $w_\alpha = |d_\alpha|^2$. We find that indeed the solution vectors $|u^\alpha\rangle$ are eigenvectors of the reduced density matrix and the eigenvectors of ρ with largest eigenvalue w_α are the columns of U with the largest-magnitude singular value $|d_\alpha|^2$ of the SVD.

As a final point we could estimate the error made. If we order the eigenvalues: $w_1 \geq w_2 \geq \ldots$ and define the error as the distance between $\tilde{\psi}$ and ψ:

$$\varepsilon = S(\psi, \tilde{\psi}) = \sum_{\alpha=m+1}^{n_1} |d_\alpha|^2 = \sum_{\alpha=m+1}^{n_1} w_\alpha, \tag{B.13}$$

we find a result consistent with (6.12).

Bibliography

[1] J. Cardy, *Scaling and Renormalization in Statistical Physics*, Cambridge University Press, Cambridge, 1996.

[2] N. V. Kampen, *Stochastic Processes in Physics and Chemistry*, North-Holland, Amsterdam, 1981.

[3] J. Murray, *Mathematical Biology*, Springer, Berlin, 1989.

[4] *Nonequilibrium Statistical Mechanics in One Dimension*, edited by V. Privman, Cambridge University Press, Cambridge, 1997.

[5] R. Kroon and R. Sprik, *Nonequilibrium Statistical Mechanics in One Dimension*, edited by V. Privman, Cambridge University Press, Cambridge, 1997.

[6] S. Redner, *Nonequilibrium Statistical Mechanics in One Dimension*, edited by V. Privman, Cambridge University Press, Cambridge, 1997.

[7] A. A. Lushnikov *Phys. Lett. A* **120**, p. 135, 1987.

[8] M. Henkel, E. Orlandini, and J. Santos *Annals of Physics* **259**, p. 163, 1997.

[9] L. Gwa and H. Spohn *Phys. Rev. A* **46**, p. 844, 1992.

[10] G. Schütz and E. Domany *J. Stat. Phys.* **72**, p. 277, 1993.

[11] B. Derrida, M. Evans, V. Hakim, and V. Pasquier *J. Phys. A* **26**, p. 1493, 1993.

[12] S. White *Phys. Rev. Lett.* **69**, p. 2863, 1992.

[13] S. White *Phys. Rev. B* **48**, p. 10 345, 1993.

[14] M. Kaulke and I. Peschel *Eur. Phys. J. B* **5**, p. 727, 1998.

[15] E. Carlon, M. Henkel, and U. Schollwöck *Eur. Phys. J. B* **12**, p. 99, 1999.

[16] B. Lee *J. Phys. A: Math. Gen.* **27**, p. 2633, 1994.

[17] P. Lee and J. Cardy *J. Stat. Phys.* **80**, p. 971, 1995.

[18] J. Cardy and U. Täuber *Phys. Rev. Lett.* **77**, p. 4780, 1996.

[19] J. Cardy and U. Täuber *J. Stat. Phys.* **90**, p. 1, 1998.

[20] W. Kinzel, *Percolation Structures and Processes*, edited by G. Deutsher, R. Zallen, and J. Adler, Hilger-Bristol, 1983.

[21] T. Harris *Ann. Prob.* **2**, p. 969, 1974.

[22] H. Janssen *Z. Physik B* **42**, p. 151, 1981.

[23] P. Grassberger *Z. Physik B* **47**, p. 365, 1982.

[24] P. Grassberger *J. Stat. Phys.* **79**, p. 13, 1995.

[25] M. Doi *J. Phys. A: Math. Gen.* **9**, p. 1479, 1976.

[26] L. Peliti *J. Physique* **46**, p. 1469, 1984.

[27] M. Barma, M. Grynbergh, and R. Stinchcombe *Phys. Rev. Lett.* **70**, p. 1033, 1993.

[28] F. Alcaraz, M. Droz, M. Henkel, and V. Rittenberg *Ann. Phys.* **230**, p. 250, 1994.

[29] G. M. Schütz *J. Stat. Phys.* **79**, p. 234, 1995.

[30] G. M. Schütz, *Phase Transitions and Critical Phenomena*, edited by C. Domb and J. L. Lebowitz, Academic, London, 2000.

[31] T. Liggett, *Interacting Particle Systems*, Springer, Berlin, 1985.

[32] T. Liggett, *Stochastic Interacting Systems*, Springer, Berlin, 1999.

[33] R. Glauber *J. Math. Phys.* **4**, p. 294, 1963.

[34] H. Janssen *Z. Physik B* **42**, p. 151, 1981.

[35] I. Gradshteyn and I. Ryzhik, *Table of Integrals, Series, and Products*, Academic Press, Inc., New York, 1980.

[36] S. Strogatz, *Nonlinear Dynamics and Chaos*, Addison-Wesley, Reading, 1994.

[37] S. Obukhov *Physica A* **101**, p. 145, 1980.

[38] R. Durrett, *Lecture Notes on Particle Systems and Percolation*, Wadsworth and Brooks/Cole, Pacific Grove, CA, 1988.

[39] C. Bezuidenhout and G. Grimmitt *Ann. Probab.* **18**, p. 1462, 1990.

[40] P. Grassberger and A. de la Torre *Ann. Phys.* **122**, p. 373, 1979.

[41] J. Marro and R. Dickman, *Nonequilibrium Phase Transitions in Lattice Models*, Cambridge University Press, Cambridge, 1999.

[42] B. Widom *J. Chem. Phys.* **43**, p. 3898, 1963.

[43] L. Kadanoff *Physics* **2**, p. 263, 1966.

[44] K. Wilson *Phys. Rev. B* **4**, p. 3174, 1971.

[45] K. Wilson and J. Kogut *Phys. Rep. C* **12**, p. 75, 1974.

[46] M. Fisher and M. Barber *Phys. Rev. Lett.* **28**, p. 1516, 1972.

[47] I. Jensen and R. Dickman *J. Stat. Phys.* **71**, p. 89, 1993.

[48] I. Jensen *J. Phys. A* **29**, p. 7013, 1996.

[49] J. Hooyberghs and C. Vanderzande *J. Phys. A: Math. Gen.* **33**, p. 907, 1999.

[50] S. Drell, M. Weinstein, and S. Yankielowicz *Phys. Rev. D.* **14**, p. 487, 1976.

[51] P. Pfeuty, R. Jullien, and K. Penson, *Real Space Renormalization*, edited by Th. Burkhardt and J.M.J. Van Leeuwen, Springer, Berlin, 1982.

[52] A. Stella, C. Vanderzande, and R. Dekeyser *Phys. Rev. B* **27**, p. 1812, 1983.

[53] K. Krebs, M. Pfanmüller, B. Wehefritz, and H. Hinrichsen *J. Stat. Phys.* **78**, p. 1429, 1995.

[54] J. Hooyberghs and C. Vanderzande *Phys. Rev. E* **63**(41109), 2001.

[55] H. Hinrichsen *Phys. Rev. E* **55**, p. 219, 1997.

[56] G. Golub and C. V. Loan, *Matrix Computations*, Johns Hopkins University Press, Baltimore, 3 ed., 1996.

[57] J. Essam, A. Guttmann, I. Jensen, and D. Tanlakishani *J. Phys. A* **29**, p. 1619, 1996.

[58] J. de Mendonça *J. Phys. A* **32**, p. L467, 1999.

[59] I. Jensen *Phys. Rev. Lett.* **77**, p. 4988, 1996.

[60] I. Jensen *J. Phys. A* **32**, p. 5233, 1999.

[61] R. Burlisch and J. Stoer *Numer. Math.* **6**, p. 413, 1964.

[62] M. Henkel and G. M. Schütz *J. Phys. A* **21**, p. 2617, 1988.

[63] H. Hinrichsen *Braz. J. Phys.* **30**, p. 69, 2000.

[64] P. Grassberger, F. Krause, and T. V. der Twer *J. Phys. A* **17**, pp. L105 – L109, 1984.

[65] D. Zhong and D. B. Avraham *Phys. Lett. A* **209**, pp. 333–337, 1995.

[66] I. Jensen *Phys. Rev. E* **47**, p. 1, 1993.

[67] I. Jensen *Phys. Rev. Lett.* **70**, p. 1465, 1993.

[68] N. Menyhárd *J. Phys. A* **27**, p. 6139, 1994.

[69] N. Inui, A. Y. Tretyakov, and H. Takayasu *J. Phys. A* **28**, p. 145, 1995.

[70] E. Carlon, M. Henkel, and U. Schollwöck *Phys. Rev. E* **63**, p. 036101, 2001.

[71] H. Hinrichsen *Phys. Rev. E* **63**, p. 065103, 2001.

[72] I. Jensen *Phys. Rev. E* **50**, p. 3623, 1994.

[73] J. Hooyberghs, E. Carlon, and C. Vanderzande *Phys. Rev. E* **64**, p. 036124, 2001.

[74] *Density-Matrix Renormalisation: A New Numerical Method in Physics*, edited by I. Peschel, X. Wang, M. Kaulke, K. Hallberg, Springer, New York, 1998.

[75] M. Droz, J. K. L. D. Silva, A. Malaspinas, and J. Yeomans *J. Phys. A* **19**, p. 2671, 1986.

[76] B. Derrida, V. Hakim, and V. Pasquier *J. Stat. Phys.* **85**, p. 763, 1996.

[77] S. Kwon, J. Lee, and H. Park *Phys. Rev. Lett.* **85**, p. 1682, 2000.

[78] G. Odor *Phys. Rev. E* **63**, p. 021 113, 2000.

[79] S. Ma, C. Dasgupta, and C. Hu *Phys. Rev. Lett.* **43**, p. 1434, 1979.

[80] C. Dasgupta and S. Ma *Phys. Rev. B* **22**, p. 1305, 1980.

[81] D. Fisher *Phys. Rev. Lett.* **69**, p. 534, 1992.

[82] D. Fisher *Phys. Rev. B* **51**, p. 6411, 1995.

[83] J. Hooyberghs, F. Iglói, and C. Vanderzande *Send to Phys. Rev. Lett., a preprint can be found at arXiv:cond.mat/0203610* .

[84] M. Bramson, R. Durret, and R. Schonmann *Ann. Prob.* **19**, p. 960, 1991.

[85] A. Noest *Phys. Rev. Lett.* **57**, p. 90, 1986.

[86] A. Moreira and R. Dickmann *Phys. Rev. E* **54**, p. R3090, 1996.

[87] R. Cafiero, A. Gabrielli, and M. Muñoz *Phys. Rev. E* **57**, p. 5060, 1998.

[88] I. Webman, D. Ben-Avraham, A. Cohen, and S. Havlin *Phil. Mag. B* **77**, p. 1401, 1998.

[89] S. Sachdev, *Quantum Phase Transitions*, Cambridge University Press, Cambridge, 1999.

[90] R. Griffiths *Phys. Rev. Lett.* **23**, p. 17, 1969.

[91] B. McCoy *Phys. Rev. Lett.* **23**, p. 383, 1969.

[92] B. McCoy and T. Wu *Phys. Rev.* **179**, p. 1968, 1969.

[93] T. Senthil and S. Majumdar *Phys. Rev. Lett.* **76**, p. 3001, 1996.

[94] F. Iglói, R. Juhász, and P. Lajkó *Phys. Rev. Lett.* **86**, p. 1343, 2001.

[95] E. Carlon, P. Lajkó, and F. Iglói *Phys. Rev. Lett.* **87**, p. 277201, 2001.

[96] A. B. Harris *J. Phys. C* **7**, p. 1671, 1974.